INVESTIGATING THE FUNCTIONAL RESPONSE OF A SUBSURFACE BIOFILM COMMUNITY TO XENOBIOTIC STRESS

By

Rachelle Renee Rhodes

Thesis submitted to the Faculty of the Virginia Polytechnic Institute and State University in partial fulfillment of the requirements for the degree of

MASTERS OF SCIENCE

In

Environmental Engineering

Dr. Nancy G. Love, Chair

Dr. John T. Novak

Dr. Madeline Schreiber

May 12, 2004

Blacksburg, Virginia

Keywords: Biofilm, GGKE, potassium, functional response

INVESTIGATING THE FUNCTIONAL RESPONSE OF A SUBSURFACE BIOFILM COMMUNITY TO XENOBIOTIC STRESS

Rachelle R. Rhodes

ABSTRACT

Biologically-mediated subsurface remediation by biofilm communities is a poorly understood process that is spatially and temporally dynamic. Two microbial responses, catabolism and the stress response glutathione-gated potassium efflux (GGKE), to benzene, pentachlorophenol (PCP), or Cd exposure were studied in up-flow sand columns to examine the contribution of each response to the overall functional response of a subsurface biofilm. Benzene was catabolized in the aerobic zone, and did not activate the GGKE response, and exhibited the highest biomass concentrations of all columns. PCP was not catabolized during this study, but was found to elicit two responses, oxidative phosphorylation uncoupling and GGKE, that appeared to be concentration dependent. Oxidative uncoupling was the controlling metabolic response up to 10 mg/L PCP, while the GGKE stress response was activated near 20 mg/L PCP. PCP column biomass did not show long-term biomass detachment, although immediate detachment occurred during initial GGKE activation. Cd column biomass activated the GGKE response as perturbing Cd concentrations increased. Extracellular polymeric substance (EPS)-Cd complexation was a possible detoxification mechanism, as biomass concentrations did not decrease with increasing Cd concentration, and increased as Cd concentrations decreased. Results of this study suggested that the increased exposure of electrophilic contaminants to sand column biomass did not cause biomass detachment.

ACKNOWLEDGEMENTS

I would like to acknowledge the U.S. EPA Midwest Hazardous Substance Center (grant #R-82877001) and the Waste Policy Institute for funding this research.

I would to thank my advisory committee, Dr. John Novak and Dr. Madeline Schreiber, for their assistance and support throughout this research. I would especially like to thank my research and major advisor, Dr. Nancy Love, for her guidance, encouragement, and support. The skills she has taught me will go far beyond my time as a graduate student, and will benefit me throughout my career.

I would also like to thank my unofficial co-advisor at the University of Cincinnati, Dr. Bishop, for providing collaborative information and guidance. In addition, his masters' student, Denise Gillam, deserves accolades for her effort in helping design, trouble-shoot, and maintain the sand columns.

I would also like to thank other students advised by Dr. Love, Joy Muller, Rick Kelly, Ines Henriques, and Katherine Linares, for all of their help in answering questions as I acclimated to laboratory research.

I would like to thank two indispensable department staff members: Julie Petruska and Jody Smiley. Julie's knowledge of laboratory techniques and general know-how is greatly appreciated, specifically during the design and building of the flowcells used in this work. Jody's knowledge of analytical chemistry helped me master numerous analysis techniques, with countless hours spent in the analytical lab discussing these items.

Finally, the unending support and encouragement of my family and husband, Ben, was what has helped me keep my eye on the original goal - thank you is not enough.

PREFACE

This full thesis version layout was designed to provide all of the data obtained from preparatory and sand column experimentation. This research, performed at Virginia Tech, is complementary to research performed at the University of Cincinnati under the same proposal. The reader will find all results data contained in chapter 5, which is subdivided into five sections. Four of these five sections contain sub-sections which report the results of individual columns, a sub-section for comparison purposes, and a sub-section devoted to referencing the results in terms of the hypothesis.

TABLE OF CONTENTS

LIST OF TABLES

LIST OF FIGURES

List of Abbreviations

AA: atomic adsorption
ATP: adenosine triphosphate
BCA: bicinchoninic acid
BOFS: biogenic organic feed solution
BSA: bovine serum albumin
Cd: cadmium
CDNB: chlorodinitrobenzene
CFU: colony forming units
CO_2: carbon dioxide
COD: chemical oxygen demand
df: degrees of freedom
DGGE: denaturing gradient gel electrophoresis
DNA: deoxyribonucleic acid
DO: dissolved oxygen
DOC: dissolved organic carbon
ECD: electron capture detector
EPS: extracellular polymeric substances
F: flowcell port (followed by a loc. #)
FID: flame ionization detector
GC: gas chromatograph
GGKE: glutathione-gated potassium efflux
GSH: glutathione
GSSG: glutathione disulfide
H^+: hydrogen ion, proton
HPC: heterotrophic plate count
HRT: hydraulic retention time
HRT_{calc}: calculated hydraulic residence time
HRT_{mean}: mean hydraulic residence time (experimental)
K^+: potassium
L: liquid port (followed by a loc. #)
MCL: maximum contaminant level
MMO: methane monooxygenase
NEM: *N*-ethylmaleimide
O_2: oxygen
ORC: oxygen-release compounds
OUR: oxygen uptake rate
P: pump
PAG: poly alkyl glycerol
PCP: pentachlorophenol
PCP^-: anionic PCP from
PCP^0: neutral PCP from
SBR: sequencing batch reactor
SC: sand column
SEAM3D: Sequential Electron Acceptor Model – 3 Dimensional
-SH: sulfhydryl group
t: time
TCE: trichloroethylene
t_{obs}: t-test observation
TOC: total organic carbon
UC: University of Cincinnati
UFA: unsaturated fatty acid
UST: underground storage tank
UV-VIS: ultraviolet visual
VS: volatile solids
VT: Virginia Tech
WW: wastewater
WWTP: wastewater treatment plant
$\alpha_{0.025}$: 95% confidence interval critical value
Δ: change in

Chapter 1: Executive Summary

Subsurface contamination by xenobiotic chemicals is a ubiquitous problem and can pose a grave public heath risk. A specific class of xenobiotic chemicals, electrophiles, may have deleterious effects on subsurface microbial communities. Biologically-mediated in-situ treatment has been increasingly used as a treatment strategy. However, there are many mechanisms controlling remediation that are not well understood.

Biologically-mediated subsurface remediation is mediated by bacterial communities through a variety of mechanisms, including catabolism and microbial stress responses. Catabolism involves the enzyme-mediated breakdown of a compound to yield energy for bacterial growth and cell maintenance. Stress responses are activated within bacteria to internally detoxify the chemical and protect cellular components, such as DNA. Electrophilic compounds, or electron-loving chemicals, are chemicals that react with electron donors by accepting bonding electrons, and have been found to elicit a specific protective stress response called glutathione-gated potassium efflux (GGKE). GGKE activation results in potassium (K^+) efflux from the cell, and has been shown to cause deflocculation of bacterial assemblages in activated sludge systems (Bott and Love, 2002). Deflocculation results in unintentional biomass loss in activated sludge systems and adversely impacts treatment ability. Likewise, detrimental effects, such as biomass detachment from soil, may occur in saturated subsurface zones contaminated with electrophiles if potassium efflux occurs.

For this research, it was hypothesized that temporal changes in the concentration of different xenobiotic stressors to subsurface environments will influence K^+ efflux and

catabolism responses by biofilms differently, resulting in unique community functional responses. This hypothesis was tested by exposing biomass in up-flow sand columns to one of three contaminants: (1) benzene, a biodegradable hydrocarbon; (2) pentachlorophenol (PCP), a biodegradable electrophilic chlorinated hydrocarbon; and (3) cadmium (Cd), a non-biodegradable electrophilic metal.

Several experiments were designed to address the research objectives: (1) determine the biodegradative fate of benzene and PCP; (2) determine the long-term biomass response to xenobiotic exposure, specifically K^+ efflux induced biomass detachment; (3) determine the sand associated biomass characteristics; and (4) determine the contaminant-acclimated biomass response to short-term contaminant perturbation. These objectives were experimentally performed using four up-flow sand columns that contained a mixed community of enriched soil bacteria, enriched mixed liquor, and a pure PCP degrading culture. The columns were fed a base amount of readily biodegradable organic chemicals supplemented with benzene, PCP, Cd, or no contaminant (control). Additional sacrificial biofilms were grown in lateral flowcells and provided with the same conditions as the up-flow sand columns. The biodegradative fate of benzene and PCP in the sand columns was determined by pore water sampling and gas chromatograph analysis. The long-term (phase I) biomass response to xenobiotic influx was determined by measuring the pH fluctuation, oxygen uptake, organic carbon removal, planktonic bacterial concentration, and K^+ efflux over time. The biochemical composition of the sand-associated biomass was monitored spatially and temporally by determining total biomass concentrations, extracellular polymeric substance (EPS) concentrations, and community adaptation (experiments conducted by Irina Chakraborty)

within the four lateral flowcells along the length of the column, and within the sand columns on the last day of experimentation. Finally, the short-term (phase II) biomass response to xenobiotic influx was monitored by perturbing each column with a targeted 25 mg/L contaminant feed to determine the pre-perturbation base-line response, the initial response, the 30 minute response, and post-perturbation response through monitoring of planktonic bacteria, dissolved organic carbon, K^+, and contaminant concentrations along the length of the column. Effluent dissolved oxygen (DO) was also monitored to assess catabolism and functional responses of GGKE activation (K^+ efflux and biomass detachment).

Biodegradable and/or electrophilic characteristics of each contaminant were expected to provide information on the bacterial functional response with respect to GGKE activation. Benzene was expected to be catabolized without activation of the GGKE response. Cd was expected to activate the GGKE response, and cause biomass detachment from sand. PCP was expected be catabolized, allowing PCP to be detoxified, making GGKE activation and biomass detachment unnecessary.

Experimental results indicate that benzene was biodegraded aerobically without activating the GGKE response. PCP was not biodegraded in the PCP column, despite having included a known PCP degrader in the original inoculum. Results suggest that two metabolic responses may have been activated in the presence of PCP: oxidative phosphorylation uncoupling and GGKE. Oxidative phosphorylation uncoupling, observed as increased oxygen uptake, increased in intensity as PCP concentrations increased to 10 mg/L, with GGKE activation occurring at PCP concentrations near 20 mg/L. The higher PCP concentration was only applied as a perturbation and enhanced

the ability to detect GGKE activation, which is an acute stress response that resulted in biomass detachment only during initial stages of activation. The effect of a biodegradable electrophile, such as PCP, on GGKE activation could not be determined due to the lack of PCP biodegradation in the PCP column. Cadmium appears to have activated the GGKE response, resulting in biomass detachment during acute tests, but did not exhibit chronic biomass loss due to possible complexation with EPS.

The results of this study have implications for understanding the functional response of subsurface bacterial communities in response to the xenobiotics benzene, PCP, and Cd. The use of benzene as a model biodegradable xenobiotic was shown. PCP did not prove to be a model biodegradable electrophile. However, the functional response by PCP column biomass provided information concerning competitive metabolic processes. Cd proved to be a model non-biodegradable electrophile.

Chapter 2: Literature Review

2.1 Subsurface Contamination

Subsurface contamination by xenobiotics, chemical substances foreign to living organisms, is a ubiquitous problem throughout the world. In the United States, various laws, including the Comprehensive Environmental Response Compensation, and Liability Act, referred to as Superfund, and the Superfund Amendments and Reauthorization Act, have been enacted requiring remediation of contaminated areas to reduce the dangers associated with health impacting substances.

Remediation options are assessed based on the location, mobility, and chemical nature of the contaminant. General remediation strategies include physical removal and treatment, contaminant stabilization, or insitu treatment by chemical or biological means. Biologically-mediated insitu treatment has been increasingly used by the USEPA to treat hydrocarbon contaminated sites, but is used to some degree without a complete understanding the mechanisms occurring during remediation. Microbial biofilms predominantly perform biologically-mediated restoration, and are highly complex systems.

2.2 Subsurface Microbial Systems

Biofilms are complex assemblages of living and dead bacteria, cell debris, and extracellular polymeric substances (EPS) attached to solid surfaces (Costerton, 1995; Bishop *et al.*, 1995). The growth rate, metabolic activity, and species competition determine the biofilm structure, and in turn, the biofilm structure and bulk liquid flow velocity in the outside environment affects the mass transfer mechanisms into the biofilm

(Bishop *et al*., 1995; van Loosdrecht *et al.*, 1995; de Beer and Schramm, 1999). Zhang and Bishop (1994a) reported that an increase in substrate loading rate, feed solution velocity, and biofilm roughness individually decreased the mass transfer resistance of DO into the biofilm. Biofilm morphology changes as mass transfer conditions change (Paulsen *et al.* 1997). Paulsen *et al.* (1997) observed the formation of interconnecting biofilm strands between sand grains, or bioweb structures, while flooding the biofilm with water or an oil-water mixture.

Biofilm structures are highly stratified with regard to bacterial community, biofilm density, metabolic activity, and porosity (exocellular volumetric fraction of water) (Bishop *et al*., 1994; Zhang and Bishop, 1994a, b, c). Zhang and Bishop (1994b and 1994c) found that biofilms contained 82-89% and 83-86% active bacteria in the top layer, and 5-11% and 57-63% active bacteria in the bottom layers in biofilms greater and less than 500 μm thick, respectively. The redox potential within the biofilm changes as the biofilm depth increases, with aerobic oxidation occurring in the shallow top portion, and anoxic oxidation occurring in the deeper portions of the biofilm (Yu and Bishop, 1998; Bishop and Yu, 1999). Bishop and Yu (1999) report that the stratification of aerobic/sulfate- reducing and aerobic/nitrifying biofilms were well defined, suggesting that redox potential could determine microbial stratification over time. Zhang and Bishop (1994b) reported stratification of porosity, measuring the average mean pore radius within the top layer of biofilm to be 2.3 μm, which decreased by 85% in the bottom layers.

Heterogeneity of cell density in biofilms promotes interactions within the biofilm that may influence biofilm community development (James *et al.*, 1995). There are

several types of bacterial interactions within biofilms that have negative, positive, and no effect on bacterial populations, shaping the bacterial community structure. These interactions include: neutralism, or no effect upon either organism; competition, where organisms compete for substrate; ammensalism, where one organism produces compounds that are inhibitory to another second organism; commensalism, where only one out of the two organisms benefit without ill effects on the second; and protocooperation, where both organisms benefit (James *et al.*, 1995). The results of these interactions produce spatially non-uniform biofilms, as seen by Zhang *et al.* (1995a) when comparing three types of biofilms: heterotrophic; heterotrophic-autotrophic; and nitrifying. Zhang *et al.* (1995a) found that heterotrophs out-compete nitrifiers for substrates in the heterotrophic and heterotrophic-autotrophic biofilms, and heterotrophs co-exist in the pure nitrification system of nitrifying biofilms. Zhang *et al.* (1994d) determined that biofilm growth models inadequately described community development when only the primary substrate was accounted for, noting that metabolic products and addition of metabolic compounds can support metabolically active microbial groups. Zhang and Bishop (1994b) found that facultative bacteria increased between 10 to 1000 fold from the top to bottom layers of biofilms, and heterotrophs outnumbered autotrophs in all biofilms sampled. Similar to biofilms, suspended growth systems also undergo community adaptation while acclimating to environmental change from a wastewater treatment plant to a laboratory sequencing batch reactor. In laboratory-scale activated sludge reactors, Kaewpipat and Grady (2002) used denaturing gradient gel electrophoresis (DGGE) to determine that two identically operated sequencing batch reactors (SBRs) had different microbial populations 58 days after separation. The

different SBR bacterial communities were subsequently mixing and separated again, but after 112 days of separation the communities showed strong similarity, indicating that a stabilization period prior to splitting reactors to parallel systems is necessary to ensure biologically-based similarity in results.

2.3 Xenobiotic Impact on Subsurface Biofilms

The addition of toxic xenobiotic chemicals to a subsurface environment requires the microbial community to adapt, and impacts both individual and group level organisms. Adaptation, defined as the modification of an organism or its parts that allow the organism to survive and grow in its environment, can occur through group microbial structure function changes and individual gene expression. The biofilm microbial structure, defined as the microbial stratification within EPS, and function, defined as the ability of the biofilm to catabolize a given substrate, are strongly influenced by genetic expression and exchange of plasmids between bacteria (Karthikeyan *et al.*, 1999).

Microbial structure-function responses include bacterial stratification within biofilms, clustering, web-like biofilm protrusions, and EPS production. Zhang *et al.* (1995b) report that biofilms became highly stratified in aerobic/anaerobic zones as a result of concurrent DO diffusion and biological uptake in the top biofilm layer, which allowed degradation of azo dyes by anaerobic cleavage of the azo bond in the bottom layer and subsequent aerobic degradation of the by-products in the top layer. Karthikeyan *et al.* (1999) observed closely associated growth of bacteria within the biofilm, allowing similar metabolic trait development due to more effective sharing of resources, information, and genetic material between organisms. Biowebs, web-like

protrusions consisting of active biomass, were seen between sand grains in a biofilm system degrading toluene, compared with relatively uniform *P. aeruginosa* biofilms using a glucose substrate (Ebihara and Bishop, 1999). Kreft and Wimpenny (2001) observed that EPS production can have a detrimental effect on the growth rates of bacteria producing EPS, which requires additional energy, but the presence of EPS may stimulate growth of non-EPS producers as EPS is used as substrate.

Microbial adaptation to xenobiotic influx has been found to rely on cometabolism, or metabolism of a compound by existing enzymes that does not yield energy for the bacteria, plasmid transfer between adjacent bacteria within the biofilm, and mutation. Rivas and Arvin (2000) report that a low thiophene to benzene ratio allows cometabolism of thiophene by a biofilm. Alvarez-Cohen *et al.* (1992) report fortuitous biodegradation of TCE via the enzyme such methane monooxygenase (MMO) by type II methanotrophs. Similarly, Speitel and Segar (1995) report TCE cometabolism in biofilms by the methanotroph *M. trichosporium* OB3b. Plasmids, extra-chromosomal genetic material unessential for growth (Madigan *et al.*, 2003), are transferred between bacteria in close proximity. Sharp *et al.* (1998) found that TCE degrative plasmid, TOC_{31c}, was conserved within the biofilm, but at a lower concentration than found with planktonic bacterial growth, and that the reduction in plasmid production may be due to metabolic demand competition with EPS production in biofilms.

2.4 Bacterial Stress Responses

There are several types of general stress responses including: bacterial sporulation, stationary phase long-term survival, adaptive mutation, and cell-cell

communication. Bacterial sporulation is a stress response triggered by nutrient limitation, allowing the formation of an endospore that is resistant to heat, desiccation, or organic solvents (Sonenshein, 2000; Setlow, 2000). Stationary phase metabolism allow bacteria to become more adept in exploiting scarce nutrients and cell lysis products in starvation conditions (Finkel *et al.*, 2000). Adaptive mutation was once thought to be a random occurrence, but bacteria may use several methods to conserve adaptive mutations over deadly mutations. These methods include the production of variant DNA copies while maintaining a DNA master copy; retention of mutation during stationary phase due to energetic inability for DNA; and the existence of a minority of bacteria experience high rates of mutation Roche and Foster (2000). This bacterial minority experience mutations that cause immediate death, or genetic advancement (Rosche and Foster, 2000). Cell-cell communication, through the use of oligopeptides in gram positive bacteria, and homoserine lactones in gram negative bacteria, allows population density information to be monitored and may signal sporulation, toxin release for competitive inhibition, and conjugational ability for sharing of genetic material (Winans and Zhu, 2000).

Bacteria have also developed specific responses to environmental stresses such as heat shock, cold shock, osmoregulation, acid stress, metalloregulation systems, and oxidative stress. Heat shock stress responses allow bacteria to cope with damage to proteins by producing proteins that mediate protein repair, folding, and degradation (Yura *et al.*, 2000). The cold shock stress response, detected by a transient increase in DNA supercoiling, activates an increase in the proportion of unsaturated fatty acids (UFA) in the membrane lipids, therefore making the UFA-phospholipid membrane more flexible,

allowing cold temperature acclimation for continued growth (Phadtare *et al.*, 2000). Osmoregulation is an active process within microorganisms, requiring a balanced turgor pressure, the pressure difference between the internal and external membrane and cell wall, which must be maintained throughout growth by means of cation and anion management (Bremer and Krämer, 2000). Acid stress can have negative effects on biochemical reactions and macromolecular structures, and is regulated through the use of potassium-proton pump activation that result in alkalinization of the cytoplasm in an acidic environments, and sodium-proton pump activation that results in acidification of the cytoplasm in alkaline environments (Foster, 2000). Metal stress responses are controlled by metal sensing transcription factors that ultimately result in efflux of the offending metal from the cell (Outten *et al.*, 2000). Oxidative stress from superoxide, hydrogen peroxide, or hydroxyl radicals, which can lead to DNA, protein, and membrane damage, is regulated by *soxR* and *oxyR* regulons that activate gene expression for peroxide deactivating enzymes (Storz and Zheng, 2000).

These stress responses are environmentally relevant to the subsurface as they affect bacterial communities on a seasonal basis. Cold shock may occur in the winter causing freezing and thawing conditions in the soil. As summer heats up the soil, osmotic changes may occur as drying increases ionic strength in soil moisture. Stationary phase will also allow the bacteria to remain viable as nutrients decrease, which may be followed by sporulation to circumvent death by starvation. Acid stress and metalloregulation may be coordinated stress responses as environmental acidification solubilizes metals, increasing ease of transport and making them toxically bioavailable.

2.5 Glutathione-gated Potassium Efflux

A specific oxidative stress response called the glutathione-gated potassium efflux (GGKE) that has been known to occur in wastewater treatment systems (Bott and Love, 2002) involves a compound called glutathione (GSH). Glutathione, a tripeptide, is responsible for the majority of the low-molecular weight fraction of thiol, or sulphydryl group (-SH) within bacteria cells (Apontoweil and Berends, 1975). Glutathione is a sacrificial compound produced by many gram negative, aerobic bacteria (Fahey *et al.*, 1978) to conjugate with electrophilic contaminants, resulting in detoxification of the electrophile.

Glutathione conjugation with electrophilic compounds occurs in the cytoplasm, forming glutathione-electrophile complexes, or glutathione adducts (Ness *et al.*, 1997; Ferguson *et al.*, 1997). Electrophiles will preferentially complex with the reactive sulphydryl group on glutathione (Elmore *et al.*, 1990). The glutathione adduct formation activates two potassium-proton (K^+/H^+) antiports, called K^+ efflux channels; KefB and KefC, which are the cell membrane-contained proteins found in *Escherichia coli* (Elmore *et al.*, 1990; Ferguson *et al.*, 1997). The particular mode of activation of KefB and KefC by glutathione adducts has yet to be determined, but is suspected to result from either negative attachment feedback from loss of glutathione at the glutathione-binding site, or detection of glutathione adduct formation (Elmore *et al.*, 1990; Munro *et al.*, 1991; Ferguson *et al.*, 1996). Activation of the KefB and KefC K^+/H^+ antiports causes potassium (K^+) efflux from the cell and proton (H^+) influx into the cytoplasm (Ferguson *et al.*, 1997). The efflux of K^+ is performed concurrently with H^+ influx, so that osmotic pressure is maintained (Meury *et al.*, 1985). Research has also found that KefB

activation is a result of uncontrolled production of methylglyoxal, an internally produced electrophilic metabolite of glycolysis (Ferguson *et al*., 1993), with KefC activation by influx of external electrophiles, such as chlorodinitrobenzene (CDNB), *N*-ethylmaleimide (NEM) (Ferguson *et al.*, 1997).

There are multiple effects of the influx of H^+ into the cytoplasm, which provides DNA, protein, and lipid protection (Ferguson *et al*., 1997; Booth, 1999). The decrease in cytoplasmic pH from H^+ influx activates existing repair mechanisms such as a DNA binding repair protein, Dps (Ferguson, 1999; Ferguson *et al*., 2000). The decrease in pH directly affects the conformation of important macromolecules; permitting supercoiling of DNA, and protonation of protein binding sites (Thomas and Booth, 1992). DNA and protein conformational changes prevent oxidation of reactive sites by the electrophile. Finally, destructive alkylation of DNA bases is prevented (Oktyabrsky *et al.*, 1993).

K^+ efflux resulting from GGKE activation has been observed after electrophile addition in engineered systems. Bott and Love (2002) determined a source-cause-effect relationship between electrophilic shock and deflocculation in lab-scale sequencing batch reactors (SBRs). The introduction of electrophiles, such as CDNB, NEM, Cd, and PCP, to SBRs were shown to activate GGKE, releasing K^+ into the bulk liquid, physiologically increasing the monovalent to divalent cation ratio, and causing deflocculation (Bott and Love, 2002). Prior to the work performed by Bott and Love (2000), Higgins and Novak (1997) determined that an increase of the monovalent to divalent cation ratio to 2:1 hindered settling and dewatering properties in laboratory scale activated sludge reactors. This physical/chemical cause showed that cohesive divalent cations were replaced with monovalent cations within floc structures (Higgins and Novak, 1997). The cation bridge

model explains that floc structure is weakened when divalent cations are replaced by monovalent cations at negatively charged sites on biopolymers (Higgins and Novak, 1997).

Timely activation of the K^+/H^+ antiports to influx H^+ and release K^+ after exposure to electrophiles is crucial to bacterial survival (Ferguson *et al.*, 1997). Potassium efflux times vary with respect to the bacterial culture, and may be associated with the toxicity and concentration of the compound activating the GGKE response (Ferguson *et al.*, 1997). Meury *et al.* (1980) observed a 90% loss of intracellular K^+ 25 to 35 minutes after addition of NEM to *E. coli* K 12. Ferguson *et al.* (1993) measured a 70% loss of K^+ from *E. coli* within 20 minutes of methylglyoxal addition, and showed an order of magnitude fewer cells than the control. Bott and Love (2002) determined the K^+ efflux time to be less than 15 minutes in activated sludge exposed to NEM, with insignificant K^+ contribution due to cell lysis, indicating minimal cell death.

GGKE activation results in deflocculation due to K^+ efflux in engineered biological reactor systems (Bott and Love, 2002) and may have serious implications for a similar disturbance in subsurface environments. Biomass detachment from aquifer sediments could result from GGKE activation, allowing stressed bacteria mobility away from the contamination. This situation could have deleterious effects on natural restoration processes by prolonging microbial adaptation and perpetuating toxicity. In addition, a loss of biomass would decrease the pool of available microorganisms, effectively decreasing the biodegradation ability.

2.6 Oxidative Phosphorylation Uncoupling

Oxidative phosphorylation is the production of ATP via the proton motive force, which is generated by membrane-mediated charge separation by the electron transport chain (Madigan *et al.*, 1997). The electron transport chain, a series of oxidation-reduction reactions in the cell membrane, results in H^+ ion concentration increases in the periplasm outside the cell membrane (Madigan *et al.,* 1997). The ionized form of PCP (PCP^-) is able to dissipate the proton gradient by picking up periplasmic protons (PCP^0) and shuttling them across the membrane into the cytoplasm or outside the cell (Figure 2.1; Escher *et al.*, 1996; Escher *et al.*, 1999; Madigan *et al,* 1997). Oxidative phosphorylation uncoupling force bacteria to reestablish the proton motive force, which results in increased O_2 uptake when O_2 is available as the terminal electron acceptor (Hickman and Novak, 1984; Escher *et al.*, 1999).

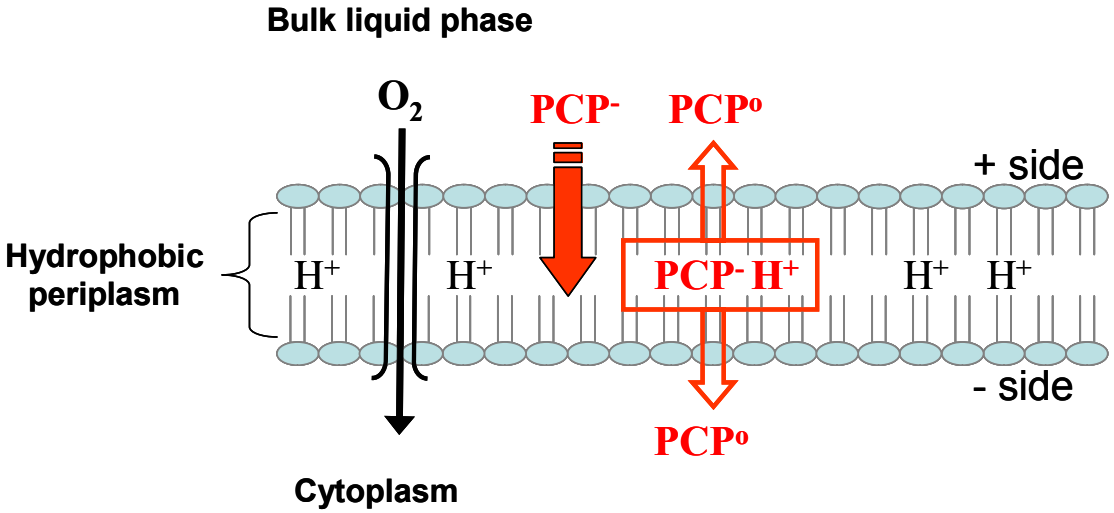

Figure 2.1. Schematic of oxidative phosphorylation uncoupling showing the diffusion of PCP^- into the periplasm and shuttling of uncharged PCP (PCP^o) into cytoplasm or out of the cell. Adapted from Escher *et al.* (1999).

2.7 Contaminants

Contaminants were chosen for this study based on biodegradability, electrophilicity, and environmental relevance. Biodegradability may allow detoxification of an electrophilic compound, allowing comparisons between non-biodegradable electrophile and non-electrophilic biodegradable compounds. In addition, environmental relevance of each chemical will allow results to have practical importance.

2.7.1 Benzene

Benzene, C_6H_6, is highly soluble up to 1.8 g/L at 25˚C (EPA, 2004) in water, having a log k_{ow} of 2.13 (Zytner, 1994), and is extremely volatile, having a Henry's law coefficient of 0.0053 atm-cu m/mole (EPA, 2004). Health risks from acute benzene exposure include: central nervous system effects, immune system depression, and bone marrow toxicity leading to aplastic anemia (EPA, 2004). Benzene has a maximum contaminant level (MCL) of 0.005 mg/L in drinking water, and has a safe short-term exposure level of 0.2 mg/L for a child consuming 1 L of water per day (EPA, 2004).

Benzene is commonly found in a mixture with toluene, ethylbenzene, and xylenes (BTEX), which are the main components of petroleum products (Stuart *et al.*, 1991). Leaking underground storage tanks (USTs) are a common source of benzene contamination into the groundwater and subsurface environment (Zytner, 1994). Groundwater sources used for drinking water supplies can be easily contaminated, resulting in public heath risks (Zytner, 1994), as benzene is considered a carcinogen.

Benzene is easily aerobically degraded (Zhang and Bouwer, 1997; Yerushalmi and Guiot, 1998). Benzene can also be anaerobically degraded with sulfate as the

electron acceptor by San Diego Bay sediment bacteria (Lovley *et al*., 1995), by marine sediment enrichment cultures (Phelps *et al*., 1996), and by a petroleum contaminated aquifer bacterial community amended with sulfate (Anderson and Lovley, 2000). Anderson *et al.* (1998) found that a *Geobacteraceae* bacterial community anaerobically degraded benzene using Fe (III) as a terminal electron acceptor. Wilson *et al.* (1986) found that benzene was mineralized in methanogenic conditions. Ma and Love (2001) found benzene to be recalcitrant under anaerobic conditions when nitrate was available as an electron acceptor, but degradable under micro-aerobic conditions by activated sludge.

2.7.2 Pentachlorophenol

Pentachlorophenol (PCP, C_6HCl_5O) is an electrophilic weak acid with a pK_a of 4.35 (Arcand *et al.*, 1995), and is slightly soluble in water (10 - 20 mg/kg water) at pH 7 (Arcand *et al.*, 1995). An electrophile is an "electron-loving" compound that bonds with a nucleophile, or reaction partner, by accepting both bonding electrons (IUPAC, 1997). PCP is present in two forms in water: neutral (PCP^0), or anionic (PCP^-) (Arcand *et al.*, 1995), with 99.4% of PCP in the anionic form at pH 7 (Rutgers *et al.*, 1998). The solubility of PCP greatly increases as pH increases due to its low pK_a, a solution pH of 9.46 allows dissolution of >10 g/L PCP (Arcand *et al.*, 1995). PCP is also has a high tendency to sorb to soils and biomass, with a log k_{ow} of 5.01 (Hickman and Novak, 1984).

PCP is used as an insecticide, fungicide and herbicide in the preservation of wood (Bellin *et al.*, 1990; Arcand *et al.*, 1995). PCP poses a significant health hazard, causing reproductive effects and damage to the liver and kidneys from chronic exposure, with some evidence showing potential for cancer (EPA, 2004). PCP has a MCL of 0.001

mg/L in drinking water, and has a safe short-term exposure level of 1.0 mg/L for a child consuming 1 L of water per day, or 0.3 mg/L for up to 7 years (EPA, 2004).

PCP is an anthropogenic, synthesized xenobiotic and does not occur naturally in the environment, although it has been found to be biodegradable under some conditions. Rutgers *et al.* (1998) found that the bacterial *Sphingomonas* strain P5 could degrade PCP, but was more inhibited at low pH values. Hickman and Novak (1984) allowed activated sludge to acclimate to PCP, resulting in an unsustained PCP removal of 95%. Melin *et al.* (1997) report that a feed concentration of 2.5 mg/L PCP was degraded to less than 2 μg/L in a fluidized-bed reactor, although PCP was shown to inhibit the biomass above 1.1 mg/L.

2.7.3 Cadmium

Cadmium (Cd) is a divalent cationic heavy metal with an aqueous solubility of 1.2 x 10^6 mg/L at neutral pH and 25˚C. Cadmium is as electrophilic metal, is extremely motile, and is not assimilated by any organism for biological processes (Renella *et al.*, 2004). Cadmium has a MCL of 0.005 mg/L in drinking water, with a one to ten day exposure of 0.04 mg/L, or 0.005 mg/L for up to 7 years of exposure (EPA, 2004). Acute cadmium exposure may result in nausea, vomiting, diarrhea, muscle cramps, salivation, sensory disturbances, liver injury, convulsions, shock, and renal failure, with possible chronic exposure resulting in kidney, liver, bone, and blood damage (EPA, 2004).

Cadmium contamination of soils has been associated with mining, coal smelting, and application of biosolids (dewatered sewage sludges) (Renella *et al.*, 2004). Atmospheric deposition increases Cd concentrations on the soil, and is a result of incineration, metal smelting, and open-hearth fires (Yost, 1979; Wong *et al.*, 1980).

Cadmium is considered to be one of the most toxic metals, due to toxic bioaccumulation without any known biological use (Wong *et al.*, 1980).

Literature Cited:

Alvarez-Cohen, L. P. L. McCarty, E. Boulygina, R. S. Hanson, G.A. Brusseau, and H. C. Tsien. 1992. Characterization of a methane-utilizing bacterium from a bacterial consortium that rapidly degrades thrichloroethylene and chloroform. Applied and Environmental Microbiology. **58**(6):1886-1893.

Anderson, R. T., J. N. Rooney-Varga, C. V. Gaw, and D. R. Lovely. 1998. Anaerobic benzene oxidation in the Fe (III) reduction zone of petroleum-contaminated aquifers. Environmental Science and Technology. **32**(9):1222-1229.

Anderson, R. T. and D. R. Lovley. 2000. Anaerobic bioremediation of benzene under sulfate-reducing conditions in a petroleum-contaminated aquifer. Environmental Science and Technology. **34**:2261-2266.

Apontoweil, P. and W. Berends. 1975. Glutathione biosynthesis in *Escherichia coli* K 12 properties of the enzymes and regulation. Biochemica et Biophysica. **399**:1-9.

Arcand, Y., J. Hawari, and S. R. Guiot. 1995. Solubility of pentachlorophenol in aqueous solutions: The pH effect. Water Research. **29**(1):131-136.

Bellin, C. A., G. A. O'Conner, Y. Jin. 1990. Sorption and degradation of pentachlorophenol in sludge-amended soils. Journal of Environmental Quality. **19**:603-608.

Bishop, P. L., T. C. Zhang, and Y-C. Fu. 1995. Effects of biofilm structure, microbial distributions and mass transport on biodegradation processes. Water Science and Technology. **31**(1):143-152.

Bishop, P. L., and T. Yu. 1999. A microelectrode study of redox potential change in biofilms. Water Science and Technology. **39**(7):179-185.

Booth, I. R. 1999. The regulation of intracellular pH in bacteria, p. 19-37. *In* Bacterial responses to pH. Novartis Foundation Symposium 221. John Wiley & Sons, Chichester, England.

Bott, C. B., and N. G. Love. 2002. Investigating a mechanistic cause for activated-sludge deflocculation in response to shock loads of toxic electrophilic chemicals. Water Environment Research. **74**(3):306-315.

Bremer, E., and R. Krämer. 2000. Coping with osmotic challenges: Osmoregulation through accumulation and release of compatible solutes in bacteria, p.79-97. *In* G. Storz, and R. Hengge-Aronis (ed.), Bacterial stress response. ASM Press, Washington, DC.

Costerton, J. W. Overview of microbial biofilms. 1995. Journal of Industrial Microbiology. **15**:137-140.

De Beer, D. and A. Schramm. 1999. Microenvironments and mass transfer phenomena in biofilms studied with microsensors. Water Science and Technology. **39**(7):173-178.

Ebihara, T., and P. L. Bishop. 1999. Biofilm structural forms utilized in bioremediation of organic compounds. Water Science and Technology. **39**(7):203-210.

Elmore, M. J., A. J. Lamb, G. Y. Ritchie, R. M. Douglas, A. Munro, A. Gajewska, and I. R. Booth. 1990. Activation of potassium efflux from *Escherichia coli* by glutathione metabolites. Molecular Microbiology. **4**(3):405-412.

Environmental Protection Agency (EPA). 2004. Technical Fact Sheet [Online] http://www.epa.gov.

Escher, B. I., M. Snozzi, and R. P. Schwarzenbach. 1996. Uptake, speciation, and uncoupling activity of substituted phenols in energy transducing membranes. Environmental Science and Technology. **30**(10):3071-3079.

Escher, B. I., R. Hunziker, and R. P. Schwarzenbach. 1999. Kinetic model to describe the intrinsic uncoupling activity of substituted phenols in energy transducing membranes. Environmental Science and Technology. **33**(4):560-570.

Fahey, R. C., W. C. Brown, W. B. Adams, and M. B. Worsham. 1978. Occurrence of glutathione in bacteria. Journal of Bacteriology. **133**(3):1126-1129.

Ferguson, G. P. A. W. Munro, R. M. Douglas, D. McLaggan, and I. R. Booth. 1993. Activation of potassium channels during metabolite detoxification in *Escherichia coli*. Molecular Microbiology. **9**(6):1297-1303.

Ferguson, G. P., A. D. Chacko, C. Lee, and I. R. Booth. 1996. The activity of the high-affinity K^+ uptake system Kdp sensitizes cells of *Escherichia coli* to methylglyoxal. Journal of Bacteriology. **178**(13):3957-3961.

Ferguson, G. P., Y. Nikolaev, D. McLaggan, M. Maclean, and I. R. Booth. 1997. Survival during exposure to the electrophilic reagent *N*-ethylmaleimide in *Escherichia coli*: Role of KefB and KefC potassium channels. Journal of Bacteriology. **179**(4):1007-1012.

Ferguson, G. P. 1999. Protective mechanisms against toxic electrophiles in *Escherichia coli.* Trends in Microbiology. **7**(6):242-247.

Ferguson, G. P., J. R. Battista, A. T. Lee, and I. R. Booth. 2000. Protection of the DNA during the exposure of *Escherichia coli* cells to a toxic metabolite: the role of the KefB and KefC potassium channels. Molecular Microbiology. **35**(1):113-122.

Finkel, S. E., E. R. Zinser, and R. Kolter. 2000. Long-term survival end evolution in the stationary phase, p. 231-238. *In* G. Storz, and R. Hengge-Aronis (ed.), Bacterial stress response. ASM Press, Washington, DC.

Foster, J. W. 2000. Microbial responses to acid stress, p. 99-115. *In* G. Storz, and R. Hengge-Aronis (ed.), Bacterial stress response. ASM Press, Washington, DC.

Hickman, G. T., and J. T. Novak. 1984. Acclimation of activated sludge to pentachlorophenol. Journal of the Water Pollution Control Federation. **56**(4):364-368.

Higgins, M. J., and J. T. Novak. 1997. The effect of cations on the settling and dewatering properties of activated sludge: Laboratory results. Water Environment Research. **69**(2):215-224.

International Union of Pure and Applied Chemistry (IUPAC). 1997. "Electrophile". *In* A. D. McNaught, and A. Wilkinson (ed.), IUPAC Compendium of Chemical Terminology. [Online] http://www.iupac.org/publications/compendium/index.html.

James, G. A., L. Beaudette, and J. W. Costerton. 1995. Interspecies bacterial interactions in biofilms. Journal of Industrial Microbiology. **15**(4):257-262.

Kaewpipat, K. and C. P. L. Grady Jr. 2002. Population dynamics in laboratory-scale activated sludge reactors. Water Science and Technology.**46**(1-2):19-27.

Karthikeyan, S., G. M. Wolfaardt, D. R. Korber, and D. E. Caldwell. 1999. Functional and structural responses of a degradative microbial community to substrates with varying degrees of complexity in chemical structure. Microbial Ecology. **38**:215-224.

Kreft, J.-U., and J. W. T. Wimpenny. 2001. Effect of EPS on biofilm structure and function as revealed by an individual-based model of biofilm growth. Water Science and Technology. **43**(6):135-141.

Lovley, D. R., J. D. Coates, J. C. Woodward, and E. J. P. Phillips. 1995. Benzene oxidation coupled to sulfate reduction. Applied and Environmental Microbiology. **61**(3):953-958.

Ma, G. and N. G. Love. 2001. Creating anoxic and microaerobic conditions in sequencing batch reactors treating volatile BTX compounds. Water Science and Technology. **43**(3):275-282.

Madigan, M. T., J. M. Martinko, and J. Parker. 2003. Brock Biology of Microorganisms, 10th ed. Pearson Education, Inc., Upper Saddle River, NJ.

Melin, E. S., J. F. Ferguson, and J. A Puhukka. 1997. Pentachlorophenol biodegradation kinetics of an oligotrophic fluidized-bed enrichment culture. Applied Microbiology and Biotechnology. **47**:675-682.

Meury, J., A. Robin, and P. Monnier-Champeix. 1985. Turgor-controlled K^+ fluxes and their pathways in *Escherichia coli*. European Journal of Biochemistry. **151**:613-619.

Meury, J., S. Lebail, and A. Kepes. 1980. Opening of potassium channels in *Escherichia coli* membranes by thiol reagents and recovery of potassium tightness. European Journal of Biochemistry. **113**:33-38.

Munro, A. W., G. Y. Ritchie, A. J. Lamb, R. M. Douglas, and I. R. Booth. 1991. The cloning and DNA sequence of the gene for the glutathione-regulated potassium-efflux system KefC of *Escherichia coli*. Molecular Microbiology. **5**(3):607-616.

Ness, L. S., G. P. Ferguson, Y. Nikolaev, and I. R. Booth. 1997. Survival of *Escherichia coli* cells exposed to iodoacetate and chlorodinitrobenzene is independent of the glutathione-gated K^+ efflux system KefB and KefC. Applied and Environmental Microbiology. **63**(10):4083-4086.

Oktyabrsky, O. N., N. V. Golyasnaya, G. V. Smirnova, V. A. Demakov, N. Kh. Posokhina, and T. A. Kholstova. 1993. Acidification of *Escherichia coli* and *Salmonella typhimurium* cytoplasm reduces the mutagenic effect of *N*-methyl-*N'*-nitrosoguanidine. Mutation Research. **293**(3):197-204.

Outten, F. W., C. E. Outten, and T. V. O'Halloran. 2000. Metalloregulatory systems ad the interface between bacterial metal homeostasis and resistance, p. 145-157. *In* G. Storz, and R. Hengge-Aronis (ed.), Bacterial stress response. ASM Press, Washington, DC.

Paulsen, J. E., E. Oppen, and R. Bakke. 1997. Biofilm morphology in porous media, a study with microscopic and image techniques. Water Science and Technology. **36**(1):1-9.

Phadtare, S., K. Yamanaka, and M. Inouye. 2000. The cold shock response, p.33-45. *In* G. Storz, and R. Hengge-Aronis (ed.), Bacterial stress response. ASM Press, Washington, DC.

Phelps, C. D., J. Kazumi, and L. Y. Young. 1996. Anaerobic degradation of benzene in BTX mixtures dependent on sulfate reduction. FEMS Microbiology Letters. **145**:433-437.

Renella, G., M. Mench, D. van der Lelie, G. Pietramellara, J. Ascher, M. T. Ceccherini, L. Landi, and P. Nannipieri. Hydrolase activity, microbial biomass and community structure in long-term Cd-contaminated soils. Soil Biology & Biochemistry. **36**:443-451.

Rivas, I. M., and E. Arvin. 2000. Biodegradation of thiophene by cometabolism in a biofilm system. Water Science and Technology. **41**(4-5):461-468.

Roche, W. A., and P. L. Foster. 2000. Mutation under stress: Adaptive mutation in *Escherichia coli*, p. 239-248. *In* G. Storz, and R. Hengge-Aronis (ed.), Bacterial stress response. ASM Press, Washington, DC.

Rutgers, M., S. van Bommel, A. M. Breure, J. G. van Andel, and W. A. Duetz. 1998. Effect of pH on the toxicity and biodegradation of pentachlorophenol by *Sphingomonas* sp. strain P5 in nutristat culture. Environmental Toxicology and Chemistry. **17**(5):792-797.

Setlow, P. 2000. Resistance of bacterial spores, p. 217-230. The heat shock response: Regulation and function, p. 3-18. *In* G. Storz, and R. Hengge-Aronis (ed.), Bacterial stress response. ASM Press, Washington, DC.

Sharp, R. R., J. D. Bryers, and W. G. Jones. 1998. Activity and stability of a recombinant plasmid-borne TCE degradative pathway in biofilm cultures. Biotechnology and Bioengineering. **59**(3):318-327.

Sonenshein, A. 2000. Bacterial sporulation: A response to environmental signals, p. 199-215. *In* G. Storz, and R. Hengge-Aronis (ed.), Bacterial stress response. ASM Press, Washington, DC.

Speitel, G. E., and A. L. Segar. 1995. Cometabolism in biofilm reactors. Water Science & Technology. **31**(1):215-225.

Storz, G., and M. Zheng. 2000. Oxidative stress, p.47-59. *In* G. Storz, and R. Hengge-Aronis (ed.), Bacterial stress response. ASM Press, Washington, DC.

Stuart, B. J., G. F. Bowlen, and D. S. Kosson. 1991. Competitive sorption of benzene, toluene, and the xylenes onto soil. Environmental Progress. **10**(2):104-109.

Thomas, A. D., I. R. Booth. 1992. The regulation of expression of the porin gene *ompC* by acid pH. Journal of General Microbiology. **138**(9-10):1829-1835.

van Loosdrecht, M. C. M., D. Eikelboom, A. Gjaltema, A. Mulder, L. Tijhuis, and J. J. Heijnen. 1995. Biofilm Structures. Water Science and Technology. **32**(8):35-43.

Wilson, B. H., G. B. Smith, and J. F. Rees. Biotransformations of selected alkylbenzenes and halogenated aliphatic hydrocarbons in methanogenic aquifer material: A microcosm study. Environmental Science and Technology. **20**(10):997-1002.

Winans, S, and J. Zhu. 2000. Roles of cell-cell communication in confronting the limitations and opportunities of high population densities, p. 261-272. *In* G. Storz, and R. Hengge-Aronis (ed.), Bacterial stress response. ASM Press, Washington, DC.

Wong, P. T. S, C. I. Mayfield, Y. K. Chau. 1980. Cadmium toxicity in phytoplankton and microorganisms, p.571-585. *In* J. O. Nriagu (ed.), Cadmium in the Environment. John Wiley & Sons, New York City, NY.

Yerushalmi, L., and S. R. Guiot. 1998. Kinetics of biodegradation of gasoline and its hydrocarbon constituents. Applied Microbiology and Biotechnology. **49**(4):375-481.

Yost, K. J. 1979. Some aspects of the environmental flow of cadmium in the United States, p 181-206. *In* J. H. Mennear (ed.), Cadmium Toxicity. Marcel Dekker, Inc, New York City, NY.

Yu, T. and P. L. Bishop. 1998. Stratification of microbial metabolic processes and redox potential change in an aerobic biofilm studied using microelectrodes. Water Science and Technology. **37**(4-5):195-198.

Yura, T, M. Kanemori, and M. T. Morita. 2000. The heat shock response: Regulation and function, p. 3-17. *In* G. Storz, and R. Hengge-Aronis (ed.), Bacterial stress response. ASM Press, Washington, DC.

Zhang, T. C. and P. L. Bishop. 1994a. Experimental determination of the dissolved oxygen boundary layer and mass transfer resistance near the fluid-biofilm interface. Water Science and Technology. **30**(11):47-58.

Zhang, T. C. and P. L. Bishop. 1994b. Structure, activity and composition of biofilms. Water Science and Technology. **29**(7):335-344.

Zhang, T. C. and P. L. Bishop. 1994c. Density, porosity, and pore structure of biofilms. Water Research. **28**(11):2267-2277.

Zhang, T. C., Y. C. Fu, and P. L. Bishop. 1994d. Competition in biofilms. Water Science and Technology. **29**(10-11):263-270.

Zhang, T. C. Y. C. Fu, and P. L. Bishop. 1995. Competition for substrate and space in biofilms. Water Environment Research. **67**(6):992-1003.

Zhang, T. C., Y. C. Fu, P. L. Bishop, M. Kupferle, S. Fitzgerald, H. H. Jiang, and C. Harmer. 1995b. Transport and biodegradation of toxic organics in biofilms. Journal of Hazardous Materials. **41**:267-285.

Zhang, W-X. E. Bouwer. 1997. Biodegradation of benzene, toluene and naphthalene in soil-water slurry microcosms. Biodegradation. **8**:167-175.

Zytner, R. G. 1994. Sorption of benzene, toluene, ethylbenzene, and xylenes to various media. Journal of Hazardous Materials. **38**:113-126.

Chapter 3: Hypothesis and Research Objectives

The central hypothesis of this study is that temporal changes in the concentration of different xenobiotic stressors to subsurface environments will influence GGKE and catabolism responses by biofilms differently, inducing distinguishable community functional responses.

For this research, the protective GGKE stress response was tested using a matrix of contaminants that were biodegradable and/or electrophilic (Table 3.1). Biodegradability was expected to prevent GGKE activation, while non-biodegradable electrophilic stress was expected to activate the GGKE system, causing biomass detachment.

Table 3.1. Matrix of contaminant characteristics

Contaminant	Biodegradable?	GGKE Activating?
Benzene	Y	N
PCP	Y	Y
Cd	N	Y

The objectives of this research were to: (1) determine the biodegradative fate of target contaminants in the sand columns; (2) determine the long-term (phase I) biomass response to xenobiotic influx; (3) monitor sand-associated biomass biochemical composition and profiles over time; and (4) monitor the short-term (phase II) biomass response to xenobiotic influx. Each objective is discussed in detail next.

Prior to experimentation, four up-flow sand columns were established to maintain microbial communities fed with benzene, PCP, cadmium, or no contaminant. Additional sacrificial biofilms were grown in lateral flowcells and provided with the same conditions as the up-flow sand columns. A mixed bacterial consortium from uncontaminated soil, mixed liquor from a wastewater treatment plant with industrial input, and a PCP degrading culture were used to provide a diverse microbial community. The sand columns were pre-established prior to contaminant loading to allow the bacterial community to stabilize on a synthetic wastewater comprised of a biogenic feed solution and mineral salts slurry.

Objective 1

The biodegradative fate of two contaminants, benzene and PCP, was evaluated by monitoring the pore liquid phase over time. Analysis of benzene and PCP via gas chromatography was used to determine the degree of biodegradation. The data obtained through regular pore water sampling were used to ascertain the location of biodegradation, and the environmental contribution to biodegradation.

Objective 2

The long-term biomass response to xenobiotic influx was determined by measuring pH, effluent dissolved oxygen (DO), total organic carbon (TOC), or dissolved organic carbon (DOC), heterotrophic plate counts (HPC), and potassium (K^+). These measurements provided a profile of the system conditions over time. Effluent DO provided information on the aerobic status of the columns. HPC measurements provided

information on bacterial release over time. GGKE activation was monitored by changes in K^+ concentrations and TOC/DOC were monitored to determine the release of organic compounds over time.

Sand-associated biochemical parameters were monitored to ascertain the EPS composition within the biofilm and bacterial response to contaminant influx. Sand samples were sacrificed from the lateral flowcells at regular intervals as contaminant concentrations were increased and decreased to determine changes in total biomass, extracellular polymeric substances (EPS), and community adaptation. Volatile solids analysis determined total biomass concentrations over time. Changes in EPS over time were determined by carbohydrate and protein analysis. Community adaptation to xenobiotic influx were determined by Irina Chakraborty using denaturing gradient gel electrophoresis (DGGE).

Objective 3

The final sand column experiment provided the short-term response to xenobiotic perturbation. Samples of K^+, HPC, effluent DO, DOC, and the contaminant concentrations were measured. Multiple profile sets of these samples were taken to determine a baseline, initial, 30 minute, and post-perturbation response. These samples provided a short-term analysis of biochemical interactions during xenobiotic perturbation with a target concentration of 25 mg/L.

Chapter 4: Materials and Methods
4.1 Cultures and Media

The inoculum for the sand column experiments included a blend of soil bacteria enriched from an uncontaminated Frederick soil (3/4 mi. south of intersection of Rt 727 and Rt 698, Bridgewater, VA), mixed liquor from a domestic wastewater treatment plant with a heavy industrial flow (Muddy Creek WWTP, Cincinnati, OH), and the pure culture *Sphingobium chlorophenolicum* (ATCC 33790).

Five hundred milliliters of sterile soil extract liquid (Zuberer, 1994) from the top three soil horizons (A_p, Bt_1, Bt_2) of the uncontaminated Frederick soil was shaken with 500 g of the original non-sterile soil (A_p, Bt_1, Bt_2 horizons) for 18 days. Sterile soil extract was produced by autoclaving 500 g of Frederick soil and 500 mL of distilled water for 1 hour, adding 0.25 g $CaCO_3$, and repeatedly filtering the suspension through Whatman 934-AH, 55 mm diameter filters (Fisher Scientific, Fair Lawn, NJ) until clear. The soil extract was autoclaved for 30 minutes, at 120^{o}C and 121psi, and stored at 4˚C until used. Supernatant from the shaken soil was enriched in 0.1 X M9 media (Table 4.1) with 20 mg/L biogenic organic feed solution (BOFS) (Table 4.2) as chemical oxygen demand (COD) and was serially transferred to sterile 0.1 X M9 media with 20 mg/L COD every two days.

Table 4.1. 0.1 X M9 media used during soil bacteria growth experiments, and benzene and PCP batch degradation experiments.

Stock Name	Stock Concentration (g/L)	Initial Concentration in Batch (mg/L)
	10 X M9	*0.1 X M9*
NaH_2PO_4	30	300
Na_2HPO_4	60	600
NH_4Cl	10	100
NaCl	5	50
Individual Stocks		
$CaCl_2$ Stock	14.7	0.65
$MgSO_4 * 7H_2O$ Stock	246.5	11
Trace Metals Stock		
Nitrilotriacetic Acid	1.0	1.0
K_2HPO_4	2.09	2.1
$ZnCl_2$	0.03	0.030
$MnSO_4 *H_2O$	0.09	0.090
$CuCl_2 * 2H_2O$	0.01	0.010
$Na_2MoO_4*2H_2O$	0.01	0.010
$CoCl_2*6H_2O$	0.03	0.030
H_3BO_3	0.003	0.0030
$FeCl_3$	0.35	0.35

Table 4.2. BOFS stock and 20 mg/L BOFS batch experiment feed.

Stock	Component Conc. in Stock	20 mg/L BOFS in Batch Experiments
Protein Stock	*g/L*	*mg/L as COD*
Beef Extract	25.6	1.9
Phytone	13.6	1.0
Bacto-casitone	13.6	1.0
Yeast Extract	41.6	3.0
Sugar Stock	*g/L*	*mg/L as COD*
Fructose	15.6	1.1
Galactose	15.6	1.1
Glucose	15.6	1.1
Organic Acids Stock	*mL/L*	*mg/L as COD*
Glacial Acetic Acid[c]	98	8.0
Glycerol[d]	14	1.5

The enriched soil culture was grown and mailed overnight at room-temperature to the University of Cincinnati (UC), where it was serially cultured in 0.1 X M9 media with 20 mg/L BOFS as COD. *S. chlorophenolicum* was revived and grown in pure culture at UC according to ATCC instructions. The ATCC suggested media (1231 Trichlorophenol medium) consisted of one half-strength Tripticase soy broth supplemented with 100 mg/L 2,4,6-trichlorophenol.

The same volume of enriched soil culture and enriched mixed liquor culture (Muddy Creek WWTP, Cincinnati, OH) were blended with sand having an effective porosity of 0.44 (ELE- Soiltest, Loveland, CO). The inoculum and sand mixture were placed in four up-flow sand columns at UC and run for 16 weeks on buffered nutrient solution (Gillam, 2003). Following the 16 week bacterial community stabilization

period, the inoculum and sand mixture was removed from all four sand columns, mixed, and inoculated with *S. chlorophenolicum*. The inoculated sand was split into two aliquots: one aliquot was mailed by UPS to Virginia Tech (VT), and one remained at the UC in the same conditions as the VT packaged sand. The sand was in transit for 3.5 days. All columns and flowcell channels were filled with inoculated sand from UC.

Soil columns were fed a combined input of an HCl-acidified working stock of 55 or 14 mg/L BOFS as COD with 0.01 M phosphate buffer Sand Column (SC) media, pH 8.0 $\pm$0.2 (Table 4.3) to yield an influent simulated groundwater with a final concentration of 2 mg/L or 0.5 mg/L BOFS as COD (Table 4.4), respectively. A special Tris-HCl buffer (Table 4.5) was substituted for the 0.01 M phosphate buffer in the SC medium applied to the Cd column for the final Cd perturbation experiment to avoid precipitation problems encountered with high Cd concentrations (25 mg/L Cd). The individual and trace metals solutions were still applied during this Cd perturbation experiment.

Table 4.3. Sand column (SC) media stock solution and influent concentrations.

Stock Name	Stock Concentration (g/L)	Final Influent Concentration (mg/L)
1.0 M Phosphate Sand Column (SC) Salts Stock		
NaH_2PO_4	6.5	65
Na_2HPO_4	135	1350
NH_4Cl	10	100
NaCl	5	50
Individual Stocks		
$CaCl_2$ Stock	14.7	0.65
$MgSO_4 * 7H_2O$ Stock	246.5	11
KH_2PO_4 Stock	33.41	3.3
Trace Metals Stock		
Nitrilotriacetic Acid	1.0	1.0
K_2HPO_4	1.74	1.7
$ZnCl_2$	0.005	0.0050
$MnSO_4 *H_2O$	0.004	0.0040
$CuCl_2 * 2H_2O$	0.001	0.0010
$Na_2MoO_4*2H_2O$	0.00015	0.00015
$CoCl_2*6H_2O$	0.00002	0.000020
H_3BO_3	0.03	0.030
$FeCl_3$	0.07	0.070

Table 4.4 BOFS Stock and Column Feed Stock

Stock	Component Conc. in Stock	Stock Solutions for Target BOFS Concentration in Column Influent	
		2 mg/L Target[a]	0.5 mg/L Target[b]
Protein Stock	*g/L*	*mg/L as COD*	
Beef Extract	25.6	5.17	1.29
Phytone	13.6	2.75	0.68
Bacto-casitone	13.6	2.75	0.68
Yeast Extract	41.6	8.40	2.09
Sugar Stock	*g/L*	*mg/L as COD*	
Fructose	15.6	3.15	0.78
Galactose	15.6	3.15	0.78
Glucose	15.6	3.15	0.78
Organic Acids Stock	*mL/L*	*mg/L as COD*	
Glacial Acetic Acid[c]	98	22.24	5.53
Glycerol[d]	14	4.31	1.07

[a] 2 mg/L BOFS target in column required a 55 mg/L BOFS as COD feed solution.
[b] 0.5 mg/L BOFS target in column required a 14 mg/L BOFS as COD feed solution.
[c] Density = 1.05 g/mL glacial acetic acid, COD = 1.07g/ g glacial acetic acid
[d] Density = 1.25 g/mL glycerol, COD = 1.22 g/g glycerol

Table 4.5. 0.01 M Tris-HCl buffer used in place of 0.01 M phosphate SC salts stock during final Cd perturbation experiment.

Stock	Stock Concentration (g/L)	Final Influent Concentration (mg/L)
1.0 M Tris-HCl Buffer		
Tris	29.10	291
Tris- HCl	119.74	1197
NH_4Cl	10.0	100
NaCl	5.0	50
Phosphorus Stock		
Na_2HPO_4	46.8	5.2

The SC media was supplemented with the three contaminants at a range of concentrations as provided in Figure 4.1, and Table 4.6. Benzene was added to 9 L of sterile SC media by injecting benzene under the liquid surface using a six inch long leur-lok needle (Hamilton, Reno, NV) and gas-tight syringe (Hamilton, Reno, NV) the evening before a bottle was to be used. This protocol ensured benzene dissolution before the media was used. To dissolve PCP in SC media bottles, the initial pH of the media was increased to pH 11 using 50% w/w NaOH (Fisher Scientific, Fair Lawn, NJ), then a known mass of PCP was added and allowed to mix for two hours or until PCP was completely dissolved. Afterwards, the pH was decreased to the original solution pH (7.8 $\pm$ 0.1) using 35% w/w HCl (Fisher Scientific, Fair Lawn, NJ) and a standardized pH probe. Finally, a pre-weighed amount of cadmium was predissolved as $CdCl_2$ (Fisher Scientific, Fair Lawn, NJ) to 8.5 L distilled water while stirring prior to SC media salt addition. Then, the stock slurry was added to the 9 L SC media. This approach minimized precipitate formation in the media solution. All media bottles were closed with Viton- (Pelseal Technologies, Newton, PA) coated rubber stoppers (Fisher Scientific, Fair Lawn, NJ) to decrease sorption losses to rubber.

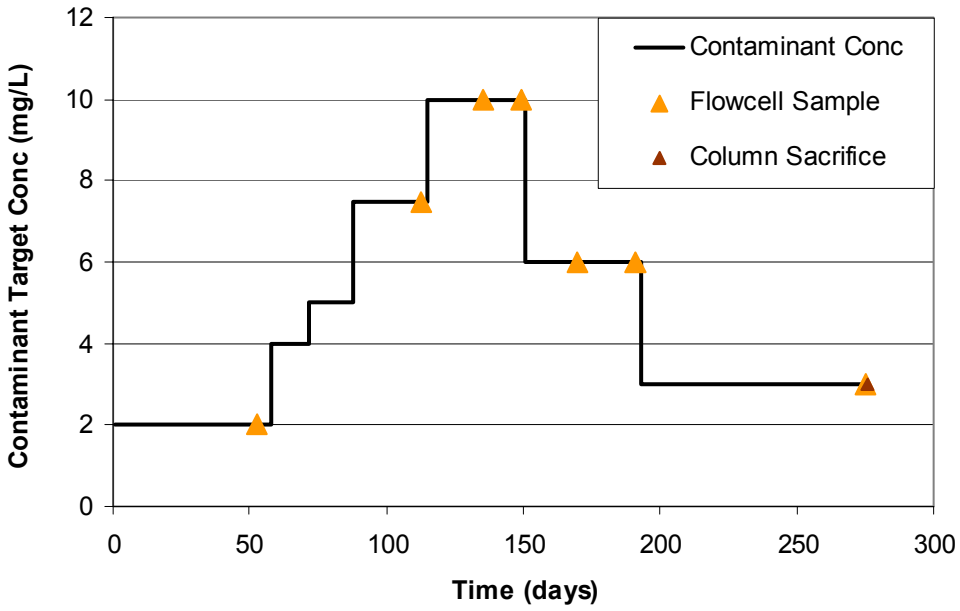

Figure 4.1. Sand column contaminant concentrations and sand sampling days.

Table 4.6. Contaminant concentrations and the periods they were applied.

Contaminant Concentration	Start Time (day)	End Time (day)
2	1	58
4	58	72
5	72	88
7.5	88	115
10	115	151
6	151	193
3	193	276

4.2 Contaminant Biodegradation Experiments

The enriched soil culture was used in benzene and PCP degradation experiments. The benzene degradation experiment was performed in a closed system using 20 mL EPA vials with Teflon coated septa in phenolic closures (Fisher Scientific, Fair Lawn, NJ). Five hundred milliliters of M9 media for the experiment was prepared in two stages.

Sterile M9 media with 20 mg/L BOFS as COD was spiked with 3.5 mg/L benzene the evening before experimentation to ensure benzene dissolution. Secondly, the M9 solution was super-saturated with at least 18 mg/L DO by adding H_2O_2 and catalase in appropriate amounts (Appendix A, Table A.1) to provide adequate oxygen for benzene and BOFS degradation. The experimental vials were seeded prior to filling with M9 media containing 20 mg/L BOFS as COD, 3.5 mg/L benzene, and supersaturated with O_2 (>18 mg/L dissolved oxygen (DO). Each set was comprised of duplicate control vials and triplicate experimental vials containing 20 µL enriched soil culture and filled with the M9 media solution. Seven sets were sacrificed during the four-day experiment. One control vial was filled before and after each triplicate experimental set. Samples were sacrificed every 24 hours until the DO was found to decrease, then samples were sacrificed approximately every 10 hours, for a total of 7 time based sacrifices. Benzene and DO was sampled from each vial. Benzene was analyzed using the method described in section 4.4, with a 7:1 extraction ratio of sample: hexane. DO was measured using a YSI Model 58 DO meter (YSI Inc., Yellow Springs, OH).

PCP degradability experiments were performed using the enriched soil bacteria, and enriched mixed liquor (Blacksburg-VPI Sanitation Authority, Blacksburg, VA). These cultures were used to seed sterilized 250 mL Erlenmeyer flasks closed with a sterile sponge and containing 200 mL of 0.1 X M9 media with 20 mg/L BOFS as COD and 2 mg/L PCP. An abiotic control was prepared with all ingredients but without inocula. Mixed liquor was enriched prior to experiments by transferring 100 µL of well-stirred mixed liquor to 0.1X M9 media with 20 mg/L BOFS as COD. Flasks were continually mixed on an orbital shaker, and samples were removed 3 times per week for 8

weeks. All flasks were amended with 20 mg/L BOFS as COD three times the first two weeks, twice on weeks 3 and 4, and once per week during weeks 5 through 8. PCP samples were processed according to the method described in section 4.4.

4.3 Column Set-up and Operation

Four glass columns (Custom Glassblowing of Louisville, Inc, Louisville, KY) having a total length of 40 cm and an inner diameter of 3.8 cm were operated in an up flow mode (Figure 4.2). The sand zone of each column was 30 cm in length, and each end cap was 5 cm in length, excluding the length of the barbed glass portion for the tubing connection. Each column contained 7 liquid ports, 4 flowcell tee ports, and had end caps integrated with a 40 mm diameter coarse frit (filter particles >40 to 60 nm). However, on day 155, all influent end caps were replaced with fritless end caps to reduce backpressure problems due to growth on the frits. Four flowcells were attached along the length of each column, and contained a nylon (GE Polymershapes, Huntersville, NC) manifold that was machined to include an internal weir that equalized the liquid head as it entered seven sand filled channels made of Teflon tubing (GE Polymershapes, Huntersville, NC) (Figure 4.3). The flowcell manifold was closed with a 1/16 in. thick Viton gasket (MSC Industrial Direct Co., Jonestown, PA) under a 1/4 in. thick nylon sheet (GE Polymershapes, Huntersville, NC). The flowcell effluent collection system was comprised of polypropylene T-connectors (Cole Parmer Instrument Co., Chicago, IL) and vinyl tubing (Fisher Scientific, Fair Lawn, NJ).

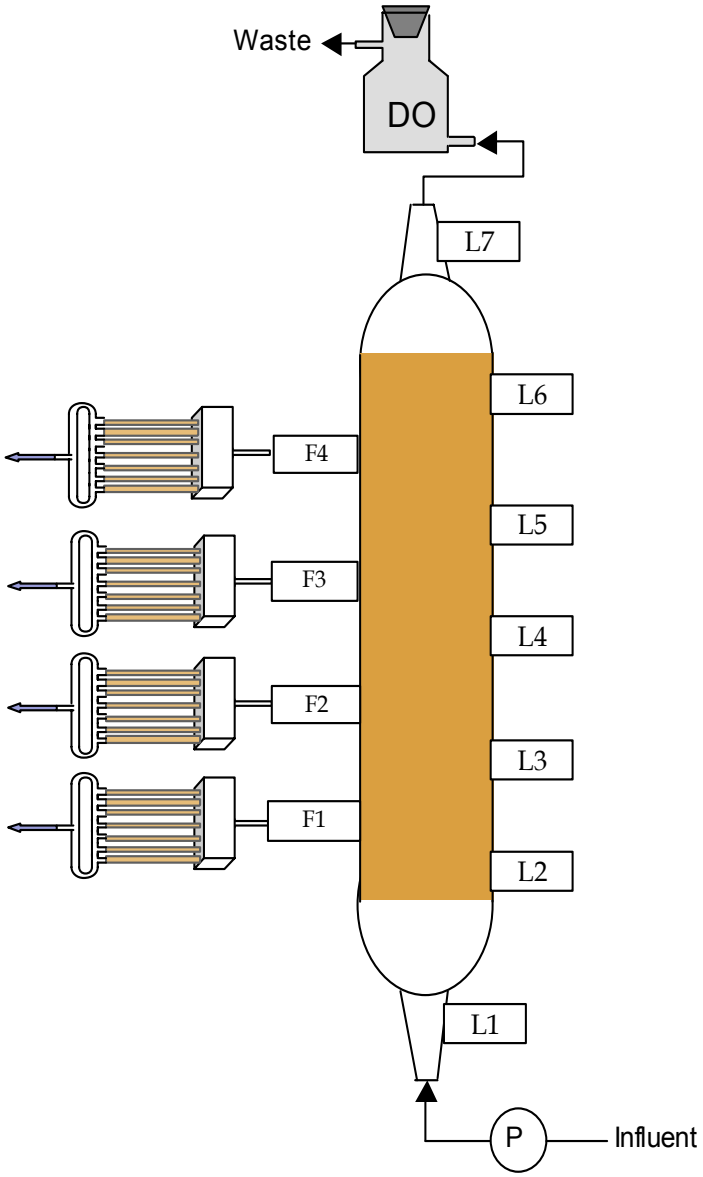

Figure 4.2. Soil column setup showing liquid ports (L1-7), flowcell ports (F1-4), and effluent dissolved oxygen (DO) bottle. P = pump.

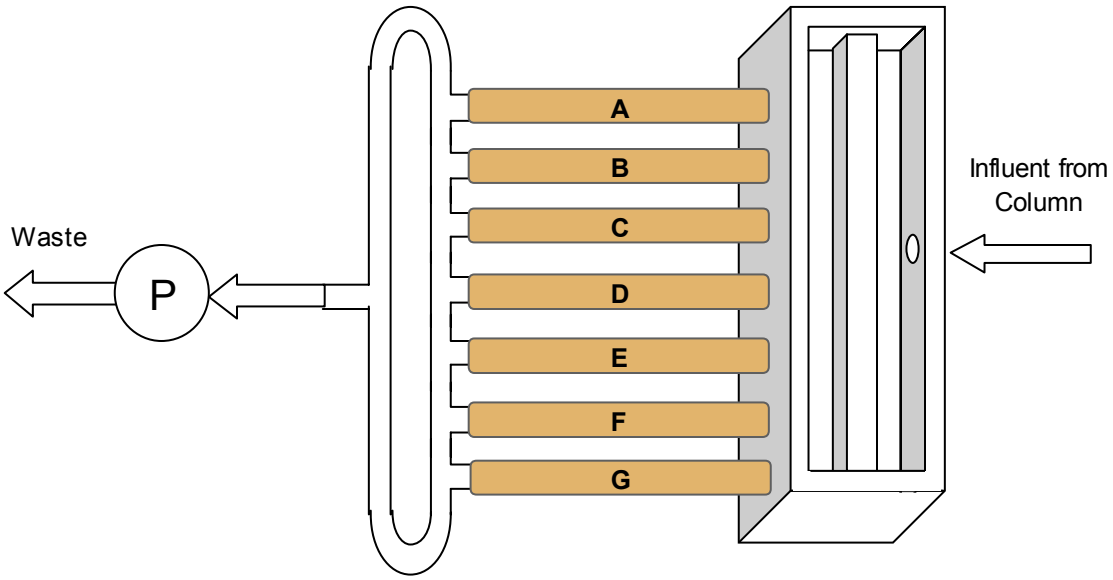

Figure 4.3. 7-Channel flowcell allows for equalized flow through each channel. Liquid head equalization chamber is shown without cover.

Four columns containing the sand-inoculum were operated at room temperature (23˚C) and included a control and three contaminant-fed units receiving benzene, PCP, or cadmium. Flow distribution for individual flowcells was within 20% for all 7 channels (Appendix A, Table A.2). Appendix A, Figure A.1 shows a full schematic of all components of the system.

Positive air pressure was gently applied to two types of media bottles (Corning, Acton, MA; Kimble Glass Co., Vineland, NJ) used during sand column experimentation in order to supply dissolved oxygen to all columns. The positive pressure also helped keep benzene in solution as the SC media volume was reduced in the bottle. This strategy did not sustain measurable DO in the effluent of several columns. Therefore, pure oxygen was used to pressurize all media bottles instead of air starting on day 225 to increase the dissolved oxygen (DO) levels in the effluent from the soil columns. Two peristaltic pumps (Cole Parmer Instrument Co., Chicago, IL) were used to apply the two

media sources to the influent of the columns. One pump equipped with four L/S 13 pump heads (Cole Parmer Instrument Co., Chicago, IL) was used to add BOFS feed at 0.1 mL/min, and a second pump equipped with four L/S 14 pump heads was used to add SC media at 2.7 mL/min. Individual flowcell effluent flow rates were maintained at 0.5 mL/min using a peristaltic pump (Cole Parmer Instrument Co., Chicago, IL) equipped with an 8-channel Ismatec cartridge (Cole Parmer Instrument Co., Chicago, IL). Flow was initiated to the columns on February 4, 2003 (day 1). All chemical flows were pumped through chemical-resistant and O_2 diffusion-limiting Viton tubing (Cole Parmer Instrument Co., Chicago, IL).

Two experimental phases, phase I and phase II, were conducted over the course of 9-months. Phase I was a long-term experimental phase that ran for 7-months where increasing, constant, and decreasing concentrations of each contaminant were applied to the three experimental sand columns. Columns were sampled and monitored according to the schedule provided in Table 4.7. Samples were removed as effluent samples from liquid ports L6 and L7. All effluent contaminant samples were removed from port L7 to determine the final contaminant concentration leaving the reactor, whereas effluent K^+, TOC and DOC samples were removed from liquid port L6 to determine final sand-associated concentrations for each. DO could only be sampled from the final column effluent during normal column operation due to the column configuration. Flowcell sand samples were removed periodically during this phase, as indicated in Figure 4.1 and Table 4.8.

Table 4.7. Phase I experiment sampling regime

Times per week	All Ports (L1 - 7)	Influent and Effluent[a,b]	Effluent
1	Benzene, Cd, PCP, K, TOC	HPC[b], K[a], TOC[a]	DO[c]
2		pH[b], Benzene[b], PCP[b], Cd[b]	

[a]Effluent samples were removed from L6.
[b]Effluent samples were removed from L7.
[c]Sampled after L7 in effluent DO bottle.

Table 4.8. Flowcell and column sacrifice days during sand column experiment.

Flowcell Channel (a-g)	Sand Sacrifice Time (day)
a	53
b	113
c	135
d	149
e	170
f	191
g	275
Column	276

Phase II was a short-term perturbation phase that encompassed the final 2-months of the experiment. Individual perturbation experiments involved adding shock loads of contaminant at a target concentration of 25 mg/L contaminant. The shock load contaminant was added as a step input for approximately 2 hours by replacing the SC media feed containing a target contaminant concentration of 3 mg/L with a 25 mg/L contaminant SC media feed. The target contaminant concentration was returned to a contaminant target concentration of 3 mg/L after each perturbation experiment. Tables 4.9 and 4.10 describe the perturbation contaminant and sampling plan, which occurred

over 7 hours per perturbed column. Sample times were decided based on the expected hydraulic residence time (HRT_{calc}). Flowcells were not connected during perturbation experiments.

The time of sample removal for each set was designed to coincide with pre-perturbation conditions (set A), initial biofilm response to perturbation (set B), biofilm response 30 minutes after perturbation onset (set C), and post perturbation response (sets D and E). Sample set E was not sampled during perturbation experiments performed on days 218, 220, and 227 because columns were not expected to contain perturbing contaminant concentrations in set D, but was added to perturbation experiments performed on days 233, 238, 241, 270 based on results from the previous perturbation experiments. Table 4.11 shows the specific perturbation days and corresponding SC media bottle gas pressure type.

Table 4.9. Perturbation experiment sampling regime for benzene and PCP columns.

Liquid Port	Approximate Sample Time (hr)											
	Set A		Contam. Spike Bottle Added	*Set B*		*Set C*		Contam. Spike Bottle Removed	*Set D*		*Set E*	
	HPC, DOC, K	Contam.		HPC, DOC, K	Contam.	HPC, DOC, K	Contam.		HPC, DOC, K	Contam.	HPC, DOC, K	Contam.
1	-1.00	-1.07	0.00	0.67	0.73	1.17	1.23	2.67	3.17	3.23	5.00	5.07
2	-0.83	-0.90		0.83	0.90	1.50	1.57		3.33	3.40	5.17	5.23
3	-0.67	-0.73		1.00	1.07	1.83	1.90		3.50	3.57	5.33	5.40
4	-0.50	-0.57		1.33	1.40	2.17	2.23		3.67	3.73	5.50	5.57
5	-0.33	-0.40		1.67	1.73	2.33	2.40		3.83	3.90	5.67	5.73
6	-0.17	-0.23		2.00	2.07	2.50	2.57		4.00	4.07	5.83	5.90

Table 4.10. Cadmium perturbation experiment sampling regime.

Liquid Port	Approximate Sample Time (hr)						
	HPC, DOC, K, Cd						
	Set A	Contam. Spike Bottle Added	*Set B*	*Set C*	Contam. Spike Bottle Removed	*Set D*	*Set E*
1	-1.00	0.00	0.67	1.17	2.67	3.17	5.00
2	-0.83		0.83	1.50		3.33	5.17
3	-0.67		1.00	1.83		3.50	5.33
4	-0.50		1.33	2.17		3.67	5.50
5	-0.33		1.67	2.33		3.83	5.67
6	-0.17		2.00	2.50		4.00	5.83

Table 4.11. Perturbation experiment days for each column and type of positive air pressure over SC media bottles.

Column	**Time of Perturbation Experiment (day)**		
Positive Pressure Type	*Air*	*Oxygen*	
Benzene	*N/A*	227	241
PCP	218	233	
Cd	220	238	270

Oxygen uptake rate (OUR) experiments to determine inhibition of benzene, PCP and Cd were performed on enriched port L2 bacteria from each of the three contaminant loaded columns while in mid to late exponential phase of growth. One mL of pore liquid from port L2 was removed and mixed, and 100 μL of the sample was cultured in 100 mL of R2A broth (Fisher Scientific, Fair Lawn, NJ). A growth curve was determined for each enriched port L2 culture by taking optical density (transmittance readings) in a Spectronic 20 over time. The growth curve information for each bacterial culture was used to determine the mid exponential phase absorbance readings prior to starting OUR experiments. While mixing, DO was measured using an Accumet Research dual channel meter (Fisher Scientific, Fair Lawn, NJ) and a 07-08-99 Thermo Orion DO probe

(Thermo Electron Corp., Houston, TX), and acquisitioned using LabView (National Instruments, Austin, TX) software. Enriched column bacteria cultures were diluted to allow a complete DO removal time of at least 10 minutes. Pre-made benzene solutions were added to 300 mL BOD bottles containing the enriched aerated benzene culture to obtain a targeted final concentration of 0 (control), 50, 100, 250, and 400 mg/L benzene. Targeted PCP concentrations of 0 (control), 10, 20 and 50 mg/L were tested with the enriched PCP column bacterial culture. Targeted Cd concentrations of 0 (control), 5, 10, 25, and 50 mg/L were tested with the enriched Cd column bacterial culture. OUR data were compiled and regressed against time to obtain the trend line slope for each chemical concentration. The slope values were normalized by the control OUR to determine the inhibition of each contaminant on the respective enriched column bacteria.

4.4 Liquid Phase Sampling and Analytical Methods

Benzene samples were taken from column liquid sample ports using a gas tight syringe, and immediately transferred to Teflon capped vials containing 99.9% hexane (Fisher Scientific, Fairlawn, NJ). Samples were then placed on a rotary mixer for 2 hours and extracted in a ratio of 7-parts sample to 1-part hexane during the Phase I experiment (Ma and Love, 2001), and extracted in a ratio of 1-part sample to 1-part hexane during the Phase II experiments. The change in extraction ratio was made to decrease the sample volume requirements from the column, allowing a minimum flow rate of 0.5 ml/min at the column effluent during repeated sampling. After extraction, samples were centrifuged for 20 minutes at 1300 x g, after which the hexane layer was transferred to 2 ml Teflon-lined crimp top autosampler vials containing 200 µL inserts. The vials were

crimped and stored at 4°C until analyzed. Benzene was analyzed on a Hewlett Packard 5890 gas chromatograph (GC), equipped with a flame ionization detector (FID), and a poly alkyl glycerol (PAG) column (Supelco, Bellefonte, PA) having a length of 30 m, 0.25 mm i.d., and film thickness of 0.25 μm. A 5 m guard column and split injection ratio of 1:30 were used. The initial column temperature was 70°C for 6 minutes, then ramped to a final temperature of 100°C in 1 minute, and held at 100°C for 3 minutes. The injection port and FID temperatures were 250°C and 260°C, respectively. The carrier gas, helium, was used at a pressure of 15 psi and flow rate 1.46 ml/min. A benzene stock for standards was prepared once in hexane by calculating the difference in mass of hexane before and after benzene addition (0.0468 g benzene) and using the density to determine the stock concentration as 936 mg/L benzene. Benzene analytical standards were prepared by transferring a specific volume of stock to volumetric flasks containing hexane using gas tight syringes (Hamilton, Reno, NV). The lowest standard concentration was 0.93 mg/L benzene. All standards and samples were injected twice and the average of the two injections is reported.

PCP samples were analyzed using a derivatization process described by Langwalt et al. (1998) and Mäkinen et al. (1993), followed by gas chromatography. PCP standards were made by dissolving PCP in SC media at pH 11 with NaOH, then reducing the pH to 7.8 with HCl. Standards and samples were derivatized by adding 25 μL acetic anhydride per mL sample, vortex mixing vigorously, and allowing the blend to sit for 1 hour. Hexane was then added for a dilution extraction of 1-part sample to 4-parts hexane for phase I samples and standards, and extracted in a ratio of 1-part sample to 10-parts hexane to accommodate high PCP concentrations during the phase II experiments. The

lowest standard concentration was 0.12 mg/L PCP. PCP was analyzed using a Hewlett Packard 5890 gas chromatograph (GC), equipped with a Electron Capture Detector (ECD), and a SPB-1701 column (Supelco, Bellefonte, PA), having a length of 30 m, i.d. of 0.25 mm and film thickness of 0.25 μm. The initial column temperature was 60 ºC for 1 minute, then ramped to 220ºC in 7 minutes, then held at 220°C for 8.0 minutes. The injection port and ECD temperatures were 225°C and 350°C, respectively. The carrier gas, helium, was used at a flow rate of 1.3 ml/min. The make-up gas, nitrogen, was used at a flow rate of 60 mL/min. All standards and samples were injected twice and the average of the two injections is reported.

Cadmium samples were collected using a 10 mL BD syringe with a 23 gauge needle (Fisher Scientific, Fairlawn, NJ). Samples were acidified with concentrated nitric acid, then a 1 mL aliquot was diluted with nanopure water in volumetric flasks to a final volume of 10 mL for phase I samples, and a final volume of 25 mL to accommodate high Cd concentrations used during the phase II experiment. All cadmium samples were analyzed in triplicate. Cadmium was analyzed using a flame atomic adsorption spectrophotometer (AA) Perkin Elmer 5100. The acetylene gas pressure was set at 13 psi, air flow was set between 40 and 60 psi, wavelength was set to 228.8 nm, and slit width was 0.7 nm. Standards were made with a Cd reference solution (Fisher Scientific, Fair Lawn, NJ) in SC media. The Cd analysis detection limit was 0.002 mg/L (APHA, 1998).

Unfiltered potassium samples were collected during phase I, while phase II samples were filtered with 0.2 μm nylon filters (Fisher Scientific, Fair Lawn, NJ). All K^+ samples were acidified with one drop of concentrated nitric acid, then diluted 1-part

sample to 5-parts 1.27 g/L cesium chloride (CsCl) solution to eliminate sodium interference during analysis. Potassium was analyzed using a flame AA Perkin Elmer 5100 with acetylene flow set at 13 psi, air flow set between 40 and 60 psi, wavelength set to 766.5 nm, and slit width at 0.4 nm. Potassium standards were made with K reference solution (Fisher Scientific, Fair Lawn, NJ) in SC media with 1.27 g/L CsCl (Alpha Aesar, Ward Hill, MA). Samples were analyzed in triplicate.

Unfiltered total organic carbon (TOC) samples were collected during phase I, while dissolved organic carbon (DOC) samples were collected during phase II. DOC samples were filtered using a 0.2 μm nylon filter (Fisher Scientific, Fair Lawn, NJ). All organic carbon samples were acidified with 85% phosphoric acid and stored at 4°C until analyzed. Analysis was performed according to method 5310 C in Standard Methods (APHA, 1998) by persulfate-ultraviolet oxidation using a DC-80 Dohrman Carbon Analyzer. Samples were analyzed in triplicate.

Dissolved oxygen (DO) was measured once per week from the effluent of all columns during phase I using an Accumet Research dual channel meter (Fisher Scientific, Fair Lawn, NJ) and a Thermo Orion model 97-08-99 DO probe (Thermo Electron Corp., Houston, TX). Flowcells remained connected with flow moving through them while the measurement was taken. DO was measured throughout the phase II experiment using LabView DO acquisition software (National Instruments, Austin, TX). Specially blown glass 95 mL bottles were used. These bottles allowed the liquid from the column effluent to enter through an opening in the bottom of the bottle and exit near the top of the stopper-capped bottle (Virginia Tech Chemistry Department Glass Shop, Blacksburg, VA) so that no headspace existed in the bottle. The bottles were filled brim-

full, and then capped for 2 hours prior to DO measurement to remove external oxygen interference.

pH was measured twice per week from the influent and effluent ports using colorpHast 6.5 – 10.0 range pH strips (Fisher Scientific, Fair Lawn, NJ) due to liquid volume constraints. pH was measured at the same time as TOC and K^+ samples were collected. The pH was measured by adding three drops of sample to the pH sensitive paper on the strip, and then comparing the strip to the color-coding index to determine the pH value.

Samples were removed for heterotrophic plate counts (HPC) from the influent and effluent liquid ports using a sterile BD needle (Fisher Scientific, Franklin Lakes, NJ) and sterile 1 mL BD syringe (Fisher Scientific, Franklin Lakes, NJ). HPCs were performed according to method 9215 in Standard Methods (APHA, 1998) using R2A agar (Difco, Sparks, MD) plates. Dilutions were made in SC media without BOFS and plated in triplicate.

4.5 Attached Biofilm Sampling and Analytical Methods

Flowcell channels were sacrificed at least twice during each phase of the experiment. The individual flowcell channels were emptied into sterile petri plates (Fisher Scientific, Fair Lawn, NJ) and mixed with a sterile spatula. Column sand was emptied into sterile aluminum pans and sectioned off in 6 to 7 cm increments for influent, four corresponding flowcell, and effluent sections, resulting in 6 sample sources from each column. These sections were transferred into pre-labeled sterile glass beakers (Fisher Scientific, Fair Lawn, NJ) with a sterile spoon, and mixed with a sterile spatula.

A total of 5 analyses were performed on sand channel and column samples. These analyses included microbial community analysis, proteins, carbohydrates, and volatile solids (VS). Additionally, glutathione samples (1.5 $\pm$ 0.1 g) were collected in duplicate into sterile microcentrifuge tubes and stored at –50°C. Glutathione analysis has yet to be conducted. Microbial community analysis samples of 1.00 $\pm$ 0.01 g were measured in triplicate into sterile bead beater tubes (Fisher Scientific, Fair Lawn, NJ), and stored at –50˚C until analyzed using denaturing gradient gel electrophoresis (DGGE) and community profile analysis (conducted by Irina Chakraborty).

Total (TS) and volatile solids (VS) samples from flowcell channels (2.0 $\pm$ 1.0 g) and column sand (10.7 $\pm$ 2.4 g) were measured in duplicate into pre-burned and pre-weighed aluminum pans (Fisher Scientific, Fair Lawn, NJ) and stored in 4°C, and analyzed within 24 hours. All TS and VS samples were processed within 24 hours of the start of flowcell and column sacrifices. Total and volatile solids samples were processed according to methods 2540 B and 2540 E, respectively, in Standard Methods (APHA, 1998) by drying sand at 100°C for 1 hour, then heating sand to 500°C for 20 minutes. Each heating step was followed by cooling the sand samples in a desiccator at room temperature, and weighing in a Mettler H10 scale (Fisher Scientific, Fair Lawn, NJ) accurate to three decimal places. Samples were analyzed in duplicate and are reported as volatile solids mass per mass dry sand

Protein samples of 0.5 $\pm$ 0.1g wet sand were measured in duplicate into sterile 1.5 ml polypropylene microcentrifuge tubes (Fisher Scientific, Fair Lawn, NJ) and stored at –50°C until analyzed. Total proteins were determined using the bicinchoninic acid (BCA) protein assay (Pierce, Rockford, IL) method from Smith et al. (1995), modified

with an initial base digestion step (Herbert, et al., 1971; Love, 1994). Sand samples were removed from the –50°C freezer, and 1 ml of 1 N NaOH was added to each sample, causing the sample to thaw, followed by vigorous vortexing for 20 seconds. Samples were then heated to 100°C for 5 minutes in a wet heat block, allowed to cool to room temperature, then vigorously vortexed again. Fifty microliters of liquid was transferred to 1.5 ml polypropylene microcentrifuge tubes containing the BCA working reagent (prepared according to manufacturers instructions), and were incubated at 37°C for 30 minutes. Special 1 N NaOH-based bovine serum albumin (BSA) standards were made using a 19.65 g/L BSA working stock in 1 N NaOH. The BSA working stock was made by weighing 1.0443 g of a 20 g/dL BSA (Sigma Diagnostics, St. Louis, MO) stock into 1 N NaOH. The density of the 20 g/L BSA stock was calculated to be 1.063 ± 0.004 g/cm^3 by determining the mass difference of removal of 0.5 mL of 20 g/dL BSA was from a vial, then dividing by 0.5 mL. This procedure was performed 5 times using both 20 g/L BSA stock and nanopure water, so that a correction factor could be applied to the 20 g/dL stock based on the experimental density of nanopure water. The density of the 20 g/dL BSA stock was used to determine the working stock concentration. One mL of each standard was added to a 1.5 mL polypropylene microcentrifuge tube containing $0.5 \pm$ 0.1g sand, then heated to 100°C for 5 minutes in a wet heat block, allowed to cool to room temperature, then vigorously vortexed for 20 seconds. Fifty microliters of the heated standards were transferred to 1.5 ml polypropylene microcentrifuge tubes containing the BCA working reagent. After color development, standards and samples were transferred to separate 1.5 ml disposable polystyrene cuvettes, and analyzed in a Beckman DU 640 UV-VIS spectrophotometer (Beckman Coulter, Fullerton, CA) at 562

nm. Protein concentrations were calculated per mass dry sand, and were determined by calculating the percent dry sand for each volatile solids. The percent dry sand was applied to each protein sand mass sample. Duplicate sand samples were measured in triplicate, and the average of the duplicate samples is reported.

Carbohydrate samples of 0.5 $\pm$ 0.1g wet sand were measured in duplicate into separate 7 ml acid-washed Pyrex glass tubes (Fisher Scientific, Fairlawn, NJ), and were analyzed within 12 hours of the start of channel and column sacrifice. Carbohydrate concentrations were determined using a phenol method described by Daniels et al. (1994) and modified for use with sand samples by Zhang (1999). Sand samples were diluted with 1.0 ml of nanopure water, and then vigorously vortexed for 5 seconds. Standards were made using a 100.2 mg/L glucose working stock. One milliliter of each standard was added to separate 7 ml acid-washed Pyrex glass tubes. Standards and samples were processed by adding 1.0 ml of phenol and 5.0 ml concentrated sulfuric acid, with each addition followed by vigorous vortexing for 5 seconds. Standards and samples were allowed to react for 10 minutes, then placed in a 25°C water bath for 15 minutes. Carbohydrate concentrations were calculated per mass dry sand, which were determined by calculating the percent dry sand for individual volatile solids samples. The carbohydrate mass was divided by the dry sand mass to obtain the carbohydrate concentration. Samples were analyzed in a Spectronic 20 (Bausch & Lomb, Philadelphia, PA) at 488 nm. Samples were taken in duplicate.

4.6 Tracer Studies

Tracer studies were performed on all columns to ascertain the flow regime. Tracer studies were performed in duplicate without flowcells connected, and once with flowcells connected. Tracer studies were performed on the benzene and PCP columns on days 271 and 272. Cadmium and control tracer studies were performed on days 273 and 274. Twenty milliliters of the tracer salt, 1 N NaCl, was injected into liquid port L1 starting at time zero using a 23 gauge needle (Fisher Scientific, Fair Lawn, NJ) and 30 ml BD syringe (Fisher Scientific, Fair Lawn, NJ). The 20 mL of 1N NaCl was injected during the first 40 to 85 seconds of the experiment. The NaCl tracer was measured directly at the column effluent using a YSI 3403 conductivity probe (Yellow Springs Instrument Co., Yellow Springs. OH) and YSI Model 32 Conductance Meter (Yellow Springs Instrument Co., Yellow Springs. OH). The conductivity probe had a cell constant (K) of 1.0 cm^{-1}; therefore, the solution conductance (mmhos) equals the conductivity (mmhos/cm). Individual tracer studies were deemed concluded when the final conductivity was $\pm$ 0.1 mmhos/cm from the original conductivity reading.

The tracer study conductivity data were converted to determine the E-curve and experimental mean HRT (HRT_{mean}). The baseline conductivity was removed to show the pulse-input-affecting effluent conductivity. The conductivity data were then converted to a NaCl concentration using a conversion equation (Equation 4.1). The conversion equation is the trend line fitted to a graph of NaCl concentration values versus conductance ($0.001 \leq c_i \leq 7864.7$). The NaCl concentration data were then used to generate a concentration versus time graph. The area under the curve of the concentration versus time was found by integrating trend line equations fitted to each

graph, and was used to calculate E (Equation 4.2). The E-curve consists of E versus time (Hart and Hom, 1996) and theoretically had an area under the curve equal to 1 , and was then used to find the mean HRT (Equation 4.3).

$$c_i = \frac{(x_i - 0.0345)}{0.0018} \tag{4.1}$$

c_i = NaCl concentration (mg/L)
x_i = Conductance (mMhos)

$$E = \frac{c_i}{\sum c_i \Delta t_i} \tag{4.2}$$

Δt_i = change in time (hr)
$\Sigma\, c_i\, \Delta t_i$ = Area under the curve

$$HRT_{mean} = \frac{\sum t_i c_i \Delta t_i}{\sum c_i \Delta t_i} \tag{4.3}$$

HRT_{mean} = the mean hydraulic residence time
t_i = time (hr)

Literature Cited:

American Public Health Association (APHA), American Water Works Association, and Water Environment Federation 1998. Standard Methods for the Examination of Water and Wastewater. 20th Edition. United Book Press, Inc. Baltimore, MD.

Daniels, L., Hanson, R. S., and J. A. Phillips. 1994. Chemical analysis. In P. Gerhardt, R.G.E. Murray, W.A. Wood, and N.R. Krieg (ed.), Methods for General and Molecular Bacteriology. American Society for Microbiology. Washington, D.C.

Gillam, D. 2003. Adaptation of subsurface microbial biofilm communities in response to chemical stressors. MS thesis. University of Cincinnati, Cincinnati, OH.

Hart, F. L., V. Hom. 1996. Reactor Dynamics - Wastewater Disinfection, ch. 4. In WEF, OEM Wastewater Disinfection Manual. Water Environment Federation,

Herbert, D, Phipps, P. J., Strange, R. E. 1971. Chemical analysis of microbial cells, p 209-344. In J.R. Norris, and D.W. Ribbons (ed.), Methods in Microbiology, vol 5B. Academic Press, London, England.

Langwaldt, J. H., M. K. Mannisto, R. Wichmann, and J. A. Puhakka. 1998. Simulation of in situ subsurface biodegradation of polychlorophenols in air-lift percolators. Applied Microbiology and Biotechnology. **49:** 663 – 668.

Ma, G., and N. G. Love. 2001 Creating anoxic and microaerobic conditions in sequencing batch reactors treating volatile BTX compounds. Water Science and Technology **43**:275-282.

Mäkinen, P. M., T. J. Theno, J. F. Ferguson, J. E. Ongerth, and J. A. Puhakka, 1994. Chlorophenol toxicity removal and monitoring in aerobic treatment: Recovery from process upsets. Environmental Science and Technology **27:**1434–1439.

Love, N.G. 1994. The impact of growth in a dual substrate limited environment in the stability and expression of the TOL Plasmid. Ph.D. dissertation. Clemson University, Clemson, SC.

Smith, P.K., R. I. Krohn, G. T. Hermanson, A. K. Mallia, F. H. Gartner, M. D. Provenzano, E. K. Fujimoto, N. M. Goeke, B. J. Olson, and D. C. Klenk. 1985. Measurement of protein using bicinchoninic acid. Analytical Biochemistry **150:**76–85.

Zhang, X. 1999. Biofilm extracellular polymeric substances – Methodology development, spatial distribution and property investigation. Ph.D. dissertation. University of Cincinnati, Cincinnati, Ohio.

Zuberer, David A. (1994). Recovery and enumeration of viable bacteria, p 119-144. In J. M. Bigham, S. H. Michelson, R. W. Weaver, S. Angle, P. Bottomley, D. Bezdicek, S. Smith, A. Tabatabai, A. Wollum, Methods of Soil Analysis Part 2: Microbial and biochemical properties. Eds. Soil Science Society of America, Inc., Wisconsin.

Chapter 5: Results
5.1 Biodegradation Experiments

5.1.1 Benzene Biodegradation Experiment

Soil bacteria cultured from an uncontaminated Frederick soil were found to aerobically degrade benzene during a closed batch experiment (Figure 5.1). Benzene was degraded in the seeded samples within 72 hours of inoculation. The DO concentration decreased to 5.8 mg/L in abiotic control batches and 1.6 mg/L in the seeded batches, indicating bacterial growth in all vials. The decrease in DO seen in all samples after 60 hours is likely due to bacterially-contaminated air contacting the sterile vials while using a chemical fume hood as the vials were filled with benzene-spiked M9 media containing 20 mg/L BOFS as COD.

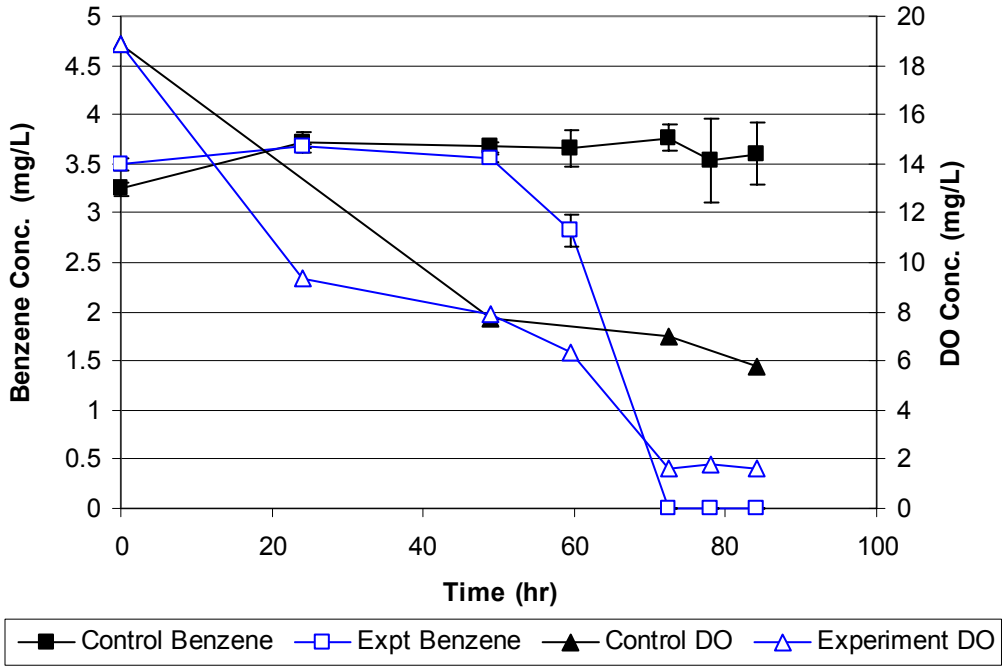

Figure 5.1. Benzene and DO concentrations during the benzene degradation experiment, where error bars show the range of benzene concentration from duplicate unseeded samples and standard deviations for the triplicate seeded samples over time; some error bars are within the symbol size. DO measurements are single measurements.

Stoichiometric calculations (Appendix B, Table B.1) showed that a total of 20.75 mg/L O_2 was required for complete degradation of 3.5 mg/L benzene and 20 mg/L BOFS as COD, assuming a biomass yield of 0.5 mg $COD_{biomass}$/mg $COD_{substrate}$. The control vials showed a decrease in oxygen, which was likely due to degradation of the 20 mg/L BOFS addition due to contamination, and not due to loss of benzene. Benzene degradation experiment data are provided in Appendix B-Table B.2.

5.1.2 PCP Biodegradation Experiment

PCP concentration data during a 2-month batch PCP degradation experiment prior to sand column experimentation did not definitively demonstrate that PCP biodegradation occurred. The PCP concentration in the uninoculated control flask was measured to be between the concentration found in the soil and wastewater (WW) bacteria inoculated flasks (Figure 5.2). PCP samples from the batch degradation experiment were stored, and groups of 27 or more samples were analyzed on four separate days. Figure 5.2 shows an increase and decrease in PCP concentrations, but these changes in concentration are due to PCP analysis problems. The fluctuation in PCP concentrations was due to small differences in the N_2 flow rate through the ECD during each separate analysis batch, and an unexplained decrease of 5.0 mg/L in the GC-ECD detection range. Nevertheless, when compared to the abiotic control, no difference could be discerned in the seeded flasks. PCP biodegradation experiment data are provided in Appendix B-Table B.3.

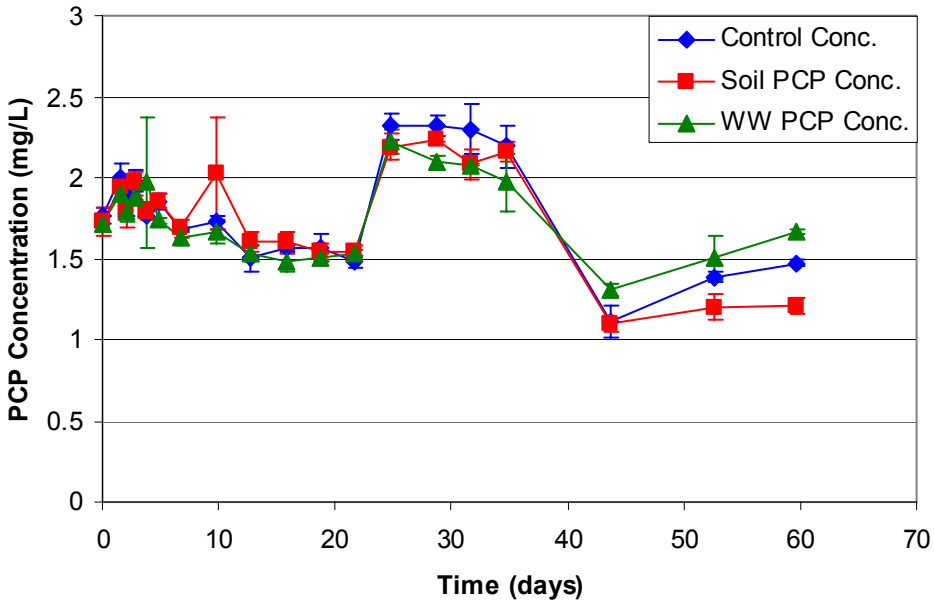

Figure 5.2. PCP degradation experiment using soil and wastewater bacteria. Error bars indicate the standard deviation of triplicate samples; some error bars within the symbol size.

5.1.3 Relevance of Data

The use of benzene as a model biodegradable contaminant was shown through batch biodegradation experimentation; however, PCP was not shown to be a model biodegradable contaminant during batch experimentation with enriched soil or mixed liquor cultures. The decision to use the enriched soil bacterial culture as a component in the sand column inoculum was made because the culture did have the capacity to biodegrade benzene. In addition, the PCP biodegradation experiment data led to the decision to add a known PCP degrading pure culture, *S. chlorophenolicum*, to the sand column inoculum. The addition of *S. chlorophenolicum* to the sand column inoculum after the 16 week community stabilization period, which was performed without contaminant addition, decreased the likelihood of competitive losses of the pure culture within the bacterial community.

5.2 Phase I – Liquid Samples

Phase I experimentation was designed to determine the long-term biofilm response to xenobiotic stress. The chemical concentration was increased, held steady, and decreased for 115, 36, and 125 days, respectively. Target chemical concentrations were increased on days 58, 72, 88, and 115, and were decreased on days 151, and 193 (Figure 4.1).

Results from the control, benzene, PCP, and Cd columns are presented individually. These sections are followed by a comparison section (5.2.5) comparing the percent contaminant removed, effluent DO, and effluent HPC concentrations. The last sub-section in 5.2 provides information on the relevance of phase I data.

5.2.1 Control Column

The influent and effluent of the control column were sampled for benzene, PCP, and cadmium at the same time that sampling was conducted on the benzene, PCP and cadmium-fed columns. Throughout phase I experimentation, no benzene, PCP, or cadmium was found in the control column. It is therefore assumed that no chemical cross-contamination occurred between other columns. Control column contaminant concentration data are contained in respective contaminant column Appendices-D, E, and F-Tables D.1, E.1, and F.1.

Effluent DO data indicate that biofilm stabilization occurred 78 days into the phase I experiment. The compiled effluent DO data varied between days 1 through 78 with concentrations that ranged from 4.7 to 0.1 mg/L. Dissolved oxygen measurements ranged from 0.1 to 0.3 mg/L from day 85 to 205 (Figure 5.3A). The air tank was

replaced with an oxygen tank on day 225, causing the effluent DO to increase to 1.0 mg/L. DO data are located in Appendix C-Table C.2.

Control TOC and DOC data indicate that organic carbon was consumed in the control column over the course of the phase I experiment. Control column TOC data show that the influent concentration was typically greater than the effluent, except on days 15, 141, 176, 184, 204, and 266 (Figure 5.3B). A comparison of these specific days to the experiment log showed that only one day of high effluent TOC may be explained by a change to normal column function. Day 184 data showed that the influent and effluent TOC values were 1.96 and 9.2 mg/L, respectively. The control column ran dry on day 183 due to a break in the SC media glass tubing in the media bottle, and was refilled the evening of day 183. The loss of media in the column may have caused the biofilm abrasion from the sand into solution, therefore resulting in higher effluent TOC reading. Additionally, two of the three DOC readings show high effluent DOC. This may be due to improper filter rinsing. TOC/DOC data are located in Appendix C-Table C.4.

Potassium analysis showed great variation in the control column throughout phase I experimentation. The influent and effluent concentrations fluctuated (Figure 5.4), possibly due to the large dilution of potassium stock (0.9 mL into 9L) that occurred when preparing SC media bottles. The increase in influent K^+ (denoted in Figure 5.4 by arrow) was made to ensure adequate K^+ was available throughout the column after K^+ analysis showed some effluent K^+ values were less than 0.1 mg/L. Normalized K^+ values ($K^+_{effluent}/K^+_{influent}$) showed a deviation from 1.0 when K^+ release or uptake occurred (Figure 5.5A). A large release of K^+, defined by the effluent containing 1.5 times the influent K^+ concentration, is seen on days 12, 64, 88, 115, 134, 179, and 190. No

correlations with column maintenance or system change were found to explain K^+ releases on these specific days. Increases in effluent K^+ concentrations over influent concentrations are most likely due to the sampling procedure as samples were unfiltered and acidified. Without filtration, planktonic bacterial cells were lysed as the sample was acidified, resulting in an increase in K^+ concentration. The K^+ sampling procedure complications affected all columns. K^+ concentration fluctuation throughout phase I experimentation is likely due to the batch preparation method of all media bottles. K^+ data are provided in Appendix C-Table C.1.

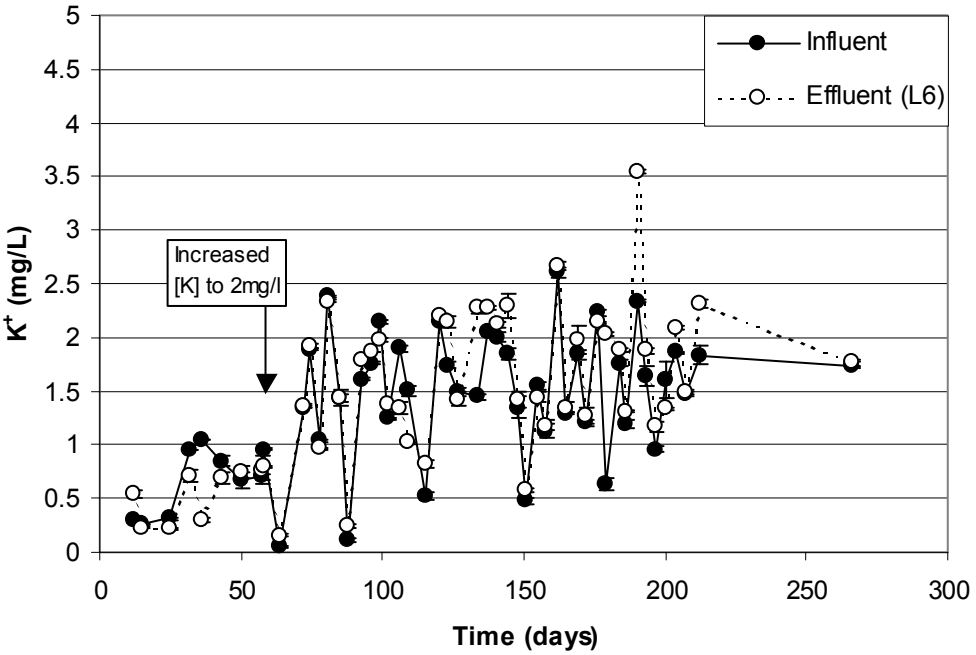

Figure 5.4. Control column influent and effluent K^+ concentrations over time during phase I experimentation. Error bars indicate standard deviation of triplicate analysis; some error bars are within the symbol size. Arrow denotes an increase in the influent K^+ concentration from 0.5 to 2.0 mg/L on day 58.

The pH data from the control column during phase I showed variation that may have been due to unknown inconsistencies that occurred when preparing the SC media

bottles. The influent pH ranged from 8.1 to 6.9, and the effluent ranged from 8.1 to 6.5 (Figure 5.5B). The lowest pH of 6.5 occurred in the effluent on day 127, and could not be explained by changes made to the column. In general, bacteria can function normally between pH 6.5 – 8, but will experience a decrease in function at pH values less than 4 and greater than 10 (Chong *et al.*, 1997). pH data are located in Appendix C-Table C.3.

Planktonic bacterial concentrations in the control column were expected to remain fairly constant. Control column effluent HPC data indicate that planktonic cell concentrations remained similar over the course of the experiment (Figure 5.5C). The highest planktonic bacteria concentrations were seen on day 115, along with high variability between plate counts. A significant decrease in planktonic bacteria was not seen after the BOFS concentration was reduced to 0.5 mg/L as COD on day 171. An independent sample t-test confirmed the observation; the t-distribution variable ($t_{obs}(10df) = 1.2897$) was not greater than the critical value ($\alpha_{0.025}(10df) = 2.228$) with removal of the outlier from day 115. HPC data are compiled in Appendix C-Table C.5.

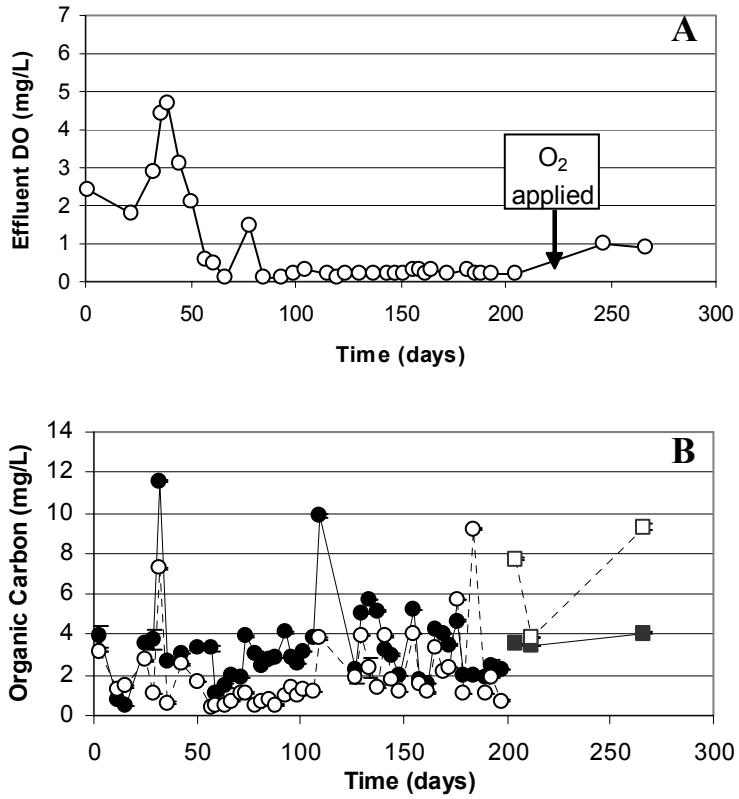

Figure 5.3. Phase I control column (A) effluent DO, arrow shows pure O_2 pressure application on day 225; (B) organic carbon concentration: influent (●) and L6 effluent (○) TOC, and influent (■) and L6 effluent (□) DOC; error bars indicate the standard deviation of triplicate samples; some error bars are within the symbol size.

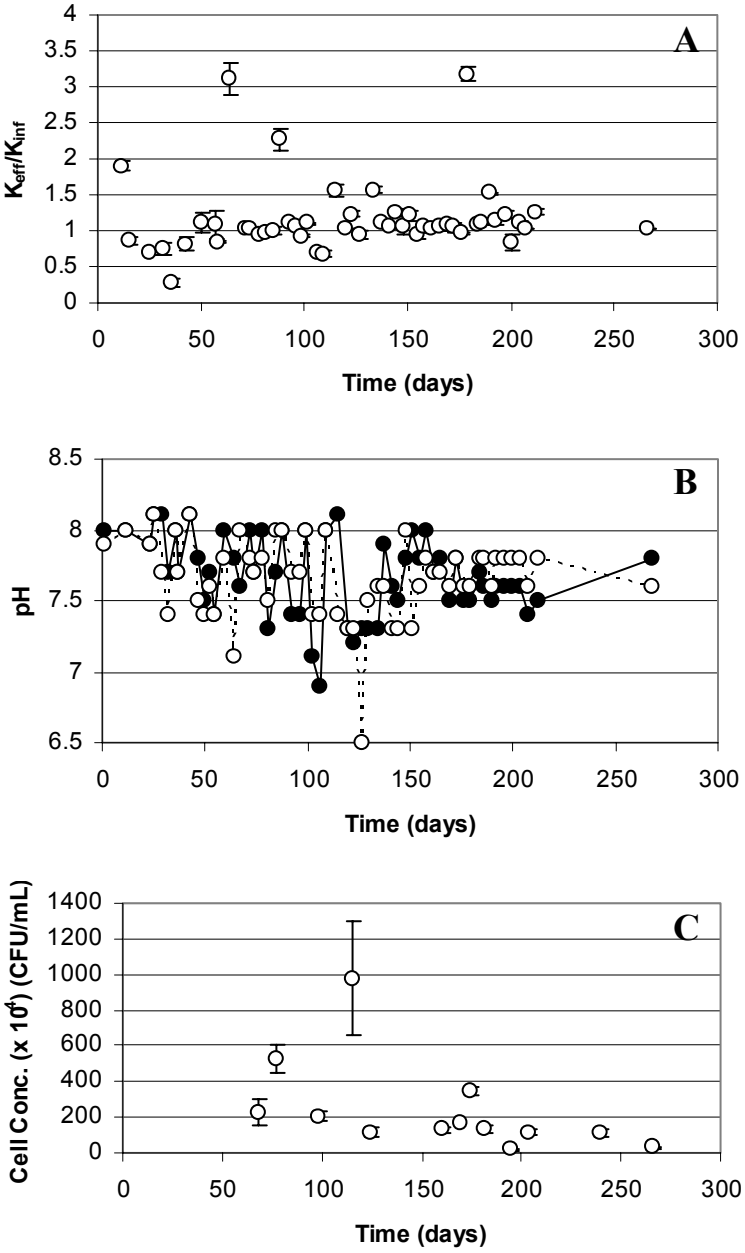

Figure 5.5. Phase I control column (A) effluent K^+ normalized by influent K^+; error bars indicate the normalized K^+ uncertainty from triplicate analysis; (B) pH from influent (●) and L7 effluent (○); and (C) effluent (L7) HPC; error bars indicate the standard deviation of counts from triplicate plates. Some error bars are within the symbol size.

5.2.2 Benzene Column

The soil bacterial culture enriched from the Frederick soil was added to the total sand column inoculum. Therefore, it is likely that multiple benzene degrading organisms were included in the initial column inoculum from the enriched soil and mixed liquor cultures. The benzene column seemed to have more biomass growth as the contaminant concentration was increased. A thick biofilm was frequently cleaned from the stainless steel wire mesh supporting the sand whenever backpressure in the influent feed lines increased.

Benzene concentration generally decreased between the influent and effluent of the column, and was likely due to biodegradation. Although the influent benzene concentration was erratic over the course of the experiment, effluent benzene concentrations were typically less than the influent concentrations (Figure 5.6B). Benzene concentrations were intended to increase and decrease step-wise during phase I. Periodically, benzene was not detected at all in the influent, presumably due to volatilization loss in the SC media feed bottle. Volatilization of benzene from the SC media bottle occurred when air or oxygen positive pressure was released, allowing the pressure to equalize with the atmosphere. Loss of positive pressure may have been instigated by backpressure due to growth on the SS wire mesh; 8 of the 19 days showing close to no benzene in the influent also had backpressure in the influent lines. Backpressure was noted when the drip tube feeding the BOFS began to show rising fluid levels. Although increasing and decreasing benzene concentration trends were seen during phase I experimentation, Figure 5.6B also shows variation in the influent benzene concentration when volatilization did not occur. This variation is thought to be due to the method used to prepare the SC media bottles, which included adding less than 1 mL of

pure benzene to individual media bottles the evening prior to a bottle exchange. Each benzene SC media bottle was changed every two days. Benzene concentration data can be found in Appendix D-Table D.1

Column profile samples showed that most of the decrease in benzene occurred between ports L1 and L2, where DO was likely exhausted in the benzene degradation process after day 67. Column profile measurements of benzene concentration that showed examples of incomplete benzene degradation occurred on days 122, 151, 163 where the influent benzene concentrations (port L1) were 14.7, 26.0, and 5.94 mg/L, and were found to be 10.9 $\pm$ 0.2, 21.5 $\pm$ 0.1, and 3.8 $\pm$ 0.2 mg/L benzene between ports L2 and L7. These benzene concentrations coincide with benzene biodegradation losses of 3.8, 4.5, and 2.1 mg/L benzene, requiring 11.7, 13.8, and 6.4 mg/L DO. The average benzene biodegradation was 2.9 mg/L benzene, requiring 8.9 mg/L O_2 (Appendix D-Table D.2). These DO requirements for benzene removal across the column indicate that anaerobic benzene biodegradation may have been occurring, but DO analysis was not performed across the column to validate this.

The DO data from the benzene column during phase I experimentation indicate that oxygen uptake stabilized by day 67 and showed very little dissolved oxygen remained in the effluent after stabilization (Figure 5.6C, Appendix D-Table D.4). The initial variation of the dissolved oxygen can be a result of an unsteady and young biofilm, and low influent benzene concentration. The final two sample points show that the effluent DO concentrations were slightly elevated to 0.4 and 0.2 mg/L. This slight elevation indicated that the DO was penetrating deeper into the sand column after the

pure oxygen positive pressure was applied on day 225, indicating an aerobic or micro-aerobic system throughout the column.

TOC and DOC data show the BOFS feed was degraded within the benzene column during the experiment. Organic carbon samples during phase I show that effluent TOC and DOC were less than influent concentrations, with the exception of three samples; days 3, 22, and 148 (Figure 5.6D, Appendix D-Table D.6). On day 22, the drip tube for the BOFS feed was unclogged with the use of a syringe, and may have attributed to the observed increase in effluent TOC. Days 3 and 148 did not correlate with any known factor related to operation or maintenance.

Potassium results from the benzene column during phase I experimentation show several effluent K^+ concentrations that were greater than influent K^+ concentrations (Figure 5.7). Correlations between high effluent K^+ and benzene concentrations are not possible because K^+ and benzene samples were not taken on the same day. Similar to the control column, increases in effluent K^+ concentrations over influent concentrations are likely due to the sampling procedure as samples were unfiltered and acidified (Figure 5.8B). Without filtration, planktonic bacterial cells were lysed as the sample was acidified, resulting in an increase in K^+ concentration. K^+ concentration fluctuation throughout phase I experimentation is likely due to the dilution effect of adding 0.9 mL of K^+ stock to 9 L of SC media. Influent, effluent, and normalized K^+ data can be found in Appendix D-Table D.3.

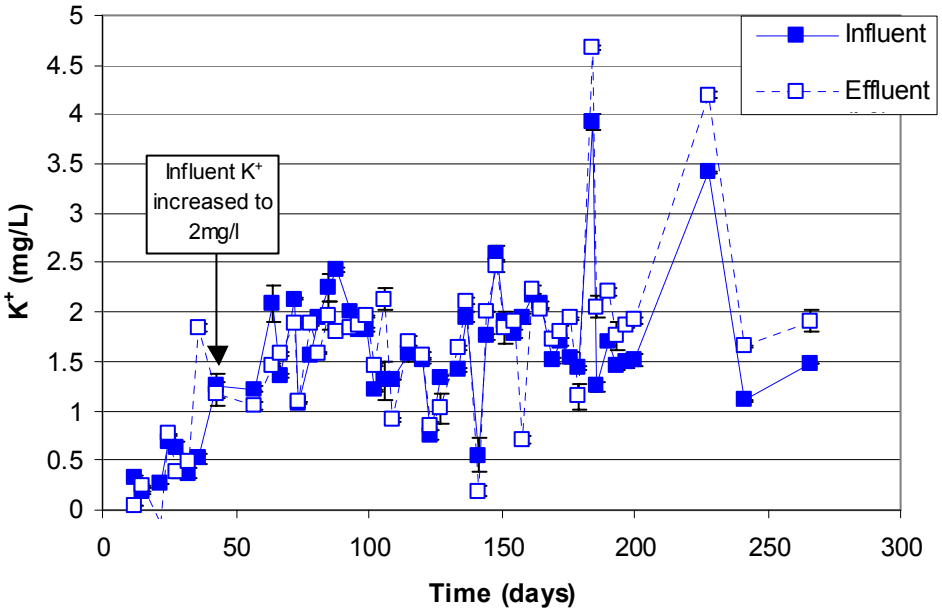

Figure 5.7. Influent and effluent benzene K^+ measurements during phase I experimentation. Error bars indicate the standard deviation of triplicate analysis; some error bars are within the symbol size. The arrow denotes an increase in the influent K^+ concentration from 0.5 to 2.0 mg/L on day 58.

The phase I benzene column influent and effluent pH fluctuated, and like the control column, is believed to be caused by unknown variations during media preparation.. The influent pH ranged from 8.1 to 6.9 while the effluent ranged from 8.1 to 6.5 (Figure 5.8C, Appendix D-Table D.5). The sharp decrease in the effluent pH to 6.5 on day 137 could not be attributed to known problems with column maintenance.

HPC data indicate that planktonic cell concentrations increased over the course of the phase I benzene experiment. The highest planktonic bacterial concentrations were seen after the highest benzene concentrations were fed to the benzene column (Figure 5.8D, Appendix D-Table D.7). In comparison to the benzene concentration, the planktonic bacterial increase was seen just as benzene concentrations decreased. This suggests that bacteria were migrating into the pore water from a robust biofilm.

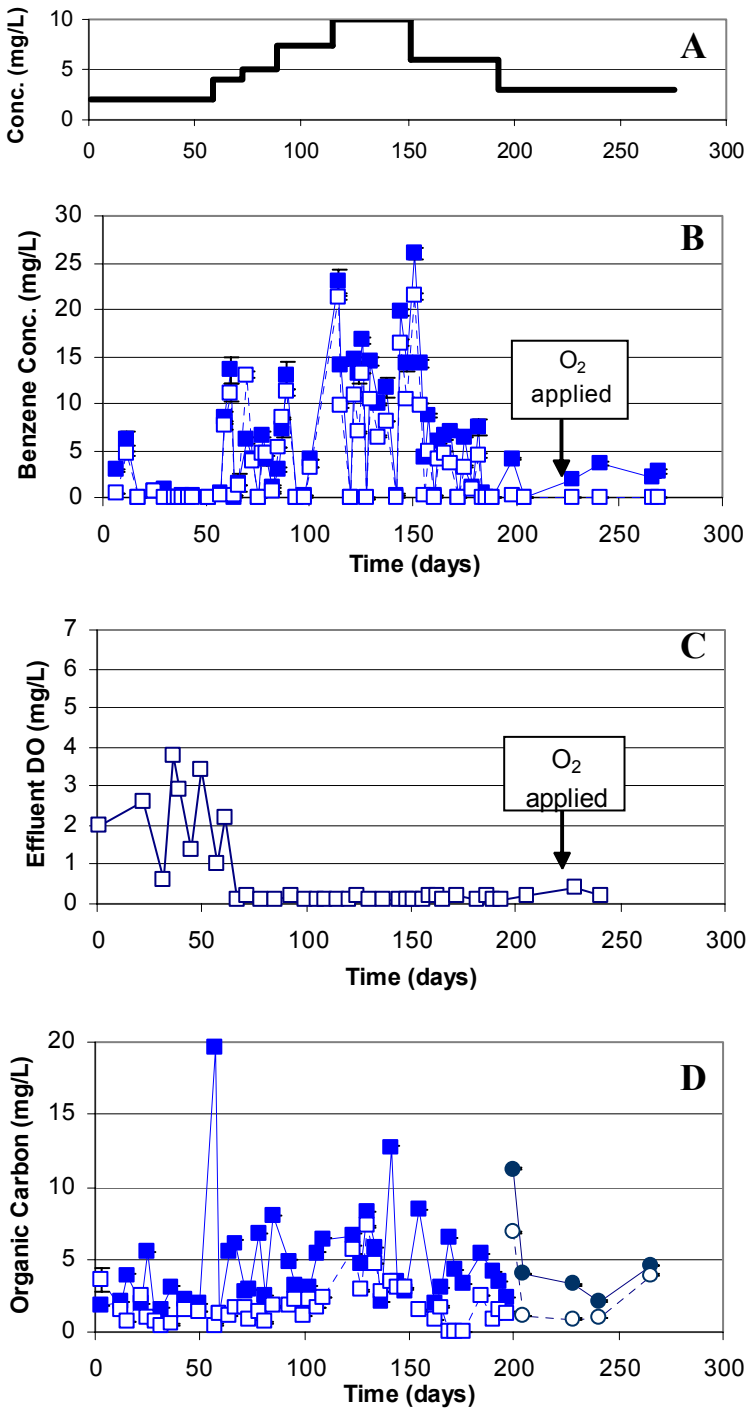

Figure 5.6. Phase I benzene column (A) target benzene concentration; (B) benzene concentration at influent (■) and L7 effluent (□); error bars indicate the standard deviation of triplicate samples; (C) effluent DO; arrow denotes change from air to O_2 positive pressure; and (D) organic carbon: TOC concentration influent (■)and L6 effluent (□); DOC and influent (●)and L6 effluent (○); error bars are the range of duplicate analysis. Some error bars are within the symbol size.

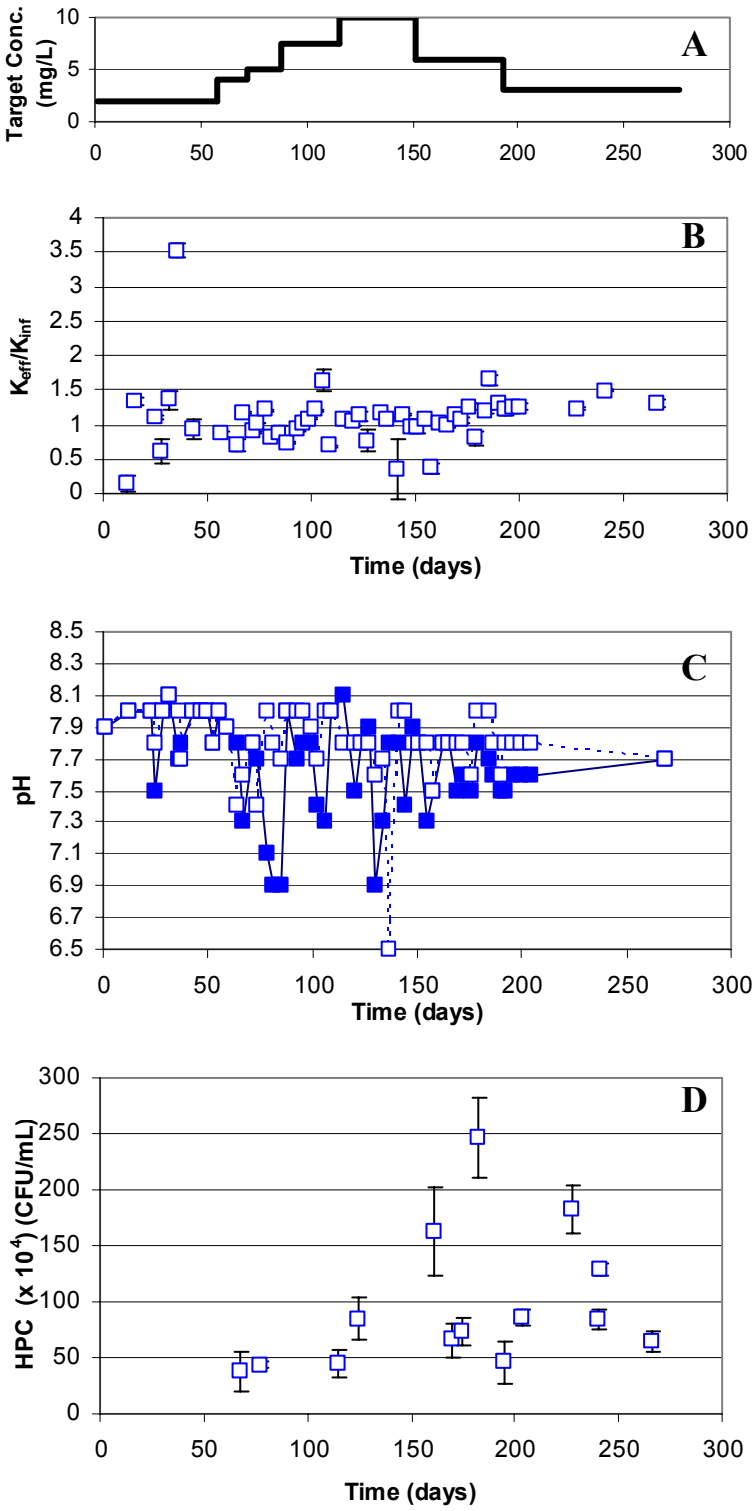

Figure 5.8. Phase I benzene column (A) target benzene concentration (B) normalized K^+; error bars indicate the standard deviation of triplicate analysis; (C) influent (■) and effluent (□) pH; and (D) effluent (L7) HPC; error bars indicate the standard deviation of counts from triplicate plates. Some error bars are within the symbol size.

5.2.3 PCP Column

PCP degradability by soil bacteria cultured from an uncontaminated Frederick soil was tested prior to column inoculation and was not found to degrade PCP. Although the soil culture was not found to degrade PCP, it was used as a component of the microbial consortium for column inoculation due to the ability of the culture to degrade benzene.

The column influent PCP concentrations followed the intended concentrations for increasing, steady, and decreasing ranges, with the exception of days 114, 151, 142, and 175 when the concentration was lower than surrounding days (Figure 5.9B). No effluent PCP concentrations were greater than the influent concentration. PCP loss averaged 8.4 $\pm$ 5.1 %. The greatest PCP removal during targeted concentration was found during the 3 mg/L PCP application on days 193 through 266 with 10.4 $\pm$ 7.5% PCP removed, but a t-test determined this removal was not statistically different from the average (t_{obs}(64 df) = 0.924 < $\alpha_{0.025}$(60 df) = 2.000). As expected due to the outcome of the batch biodegradation study, little to no PCP biodegradation could be inferred. Instead, sorption to biomass was the likely source of PCP removal (Welp *et al.*, 1998; Bellin *et al.*, 1990; Jacobsen *et al.*, 1996). Therefore, PCP was a conservative electrophilic contaminant during this study, despite addition of a known PCP degrader to the inoculum at the beginning of the experiment. PCP data are located in Appendix E-Table E.1.

Effluent DO data from the PCP column showed fluctuations during days 1 through 78 then remained between 0.1 and 0.6 mg/L DO between days 85 and 165 (Figure 5.9C, Appendix E-Table E.3). After day 165, the effluent DO fluctuated again, increasing to 3.1 mg/L DO on day 172 after decreasing the influent BOFS feed to 0.5 mg/L on day 171. The fluctuations in effluent DO prior to day 85 indicate that PCP

column biomass possibly had not reached a steady state. It is also possible that as PCP concentrations were increased to the maximum targeted concentrations between days 85 and 165 that oxidative uncoupling became an oxygen consuming process (Escher *et al.*, 1996; Escher *et al.*, 1999). The DO again increased on day 193 to 0.9 mg/L DO after decreasing the PCP concentration to 3 mg/L on the same day. The influent DO increased from 0.3 mg/L on day 205 to 2.0 mg/L on day 218 without a correlated change. The effluent DO increased on day 233 to 0.4 mg/L and continued to increase to 1.0 mg/L DO on day 267 after the air tank was replaced with pure oxygen as the gas source for positive pressure.

Organic carbon sampled during phase I show that effluent TOC and DOC samples were less than influent concentrations, with the exception of five sample sets; days 3, 43, 50, 204 and 212 (Figure 5.9D, Appendix E-Table E.5). These days do not correlate with concentration change days, nor do they correlate with changes made to the columns. The decreases in TOC and DOC indicate that biodegradation of BOFS occurred within the column.

Phase I K^+ data from the PCP column showed slight variation in the influent K^+ concentration, with a maximum and minimum of 2.68 and 1.30 mg/L K^+ after the target influent K^+ concentration was increased to 2.0 mg/L (Figure 5.10). Normalized K^+ data showed an increase in the K^+ concentration from influent to effluent several times throughout phase I experimentation (Figure 5.11B); however deviations from 1.0 occurred less frequently than was observed with benzene (visually determined). Large K^+ increases, where the effluent K^+ was 1.5 times the influent K^+ concentration, occurred on days 43 and 134 (Figure 5.11B.). These increases in effluent K^+ on these days do not

correlate with any changes made to the PCP column. Similar to the control column, increases in effluent K^+ concentrations over influent concentrations are likely due to the sampling procedure as samples were unfiltered and acidified. Without filtration, planktonic bacterial cells were lysed as the sample was acidified, resulting in an increase in K^+ concentration. K^+ concentration fluctuation throughout phase I experimentation is likely due to the batch preparation method of all media bottles. PCP column influent, effluent, and normalized K^+ data are located in Appendix E-Table E.2.

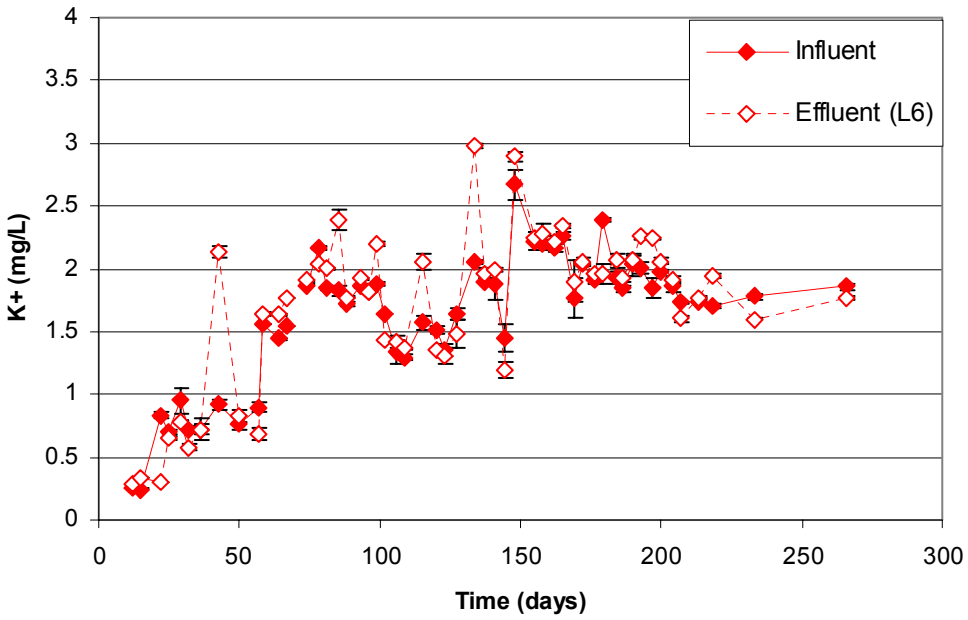

Figure 5.10. PCP column influent and effluent K^+ during phase I experimentation. Error bars indicate the standard deviation of triplicate analysis; some error bars are within the symbol size. Arrow denotes an increase in the influent K^+ concentration from 0.5 to 2.0 mg/L on day 58.

The PCP column pH data during phase I showed variation over time, which is believed to be due to the method of PCP SC media bottle preparation (Figure 5.11C, Appendix E-Table E.4). The specific method of PCP bottle preparation involved increasing the pH to 11, adding PCP, then decreasing the pH back to the original buffered

pH of 7.8. The maximum and minimum influent pH for the PCP column were 8.1 and 6.7, and were 8.0 and 7.0 for the effluent, respectively. Although the pH was variable during phase I, PCP speciation was not likely to vary considerably due to the low pKa (4.35) of PCP, with the predominant form being the deprotonated PCP^- form at the pH maintained in the column.

The phase I PCP column HPC data, shown in Figure 5.11D, give evidence to support the hypothesis statement for non-biodegradable electrophiles. Although PCP was used in this study as a biodegradable electrophile, the PCP concentration data do not suggest the loss of PCP was due to biodegradation. It is hypothesized that biofilm detachment will not occur when the GGKE system is initiated by electrophilic compounds that are biodegradable, and biofilm detachment will occur as a result of GGKE activation by non-biodegradable electrophiles. The PCP column HPC data suggest support for the non-biodegrading electrophile hypothesis, which showed bacterial concentrations increased by 347% between days 77 and 98, after PCP concentrations increased from 5.6 to 8.1 mg/L, respectively (Figure 5.11D). Planktonic bacterial concentrations peaked near day 124, when the PCP concentration was 10.5 mg/L (Figure 5.11D). Fewer planktonic bacteria were seen as the PCP concentration was decreased. The increasing then decreasing HPC trend is similar to the HPC trend seen in the benzene column although PCP degradation was likely not occurring, suggesting the increase in the PCP column HPC was caused by a different mechanism than the benzene column HPC increase. HPC data are located in Appendix E-Table E.6.

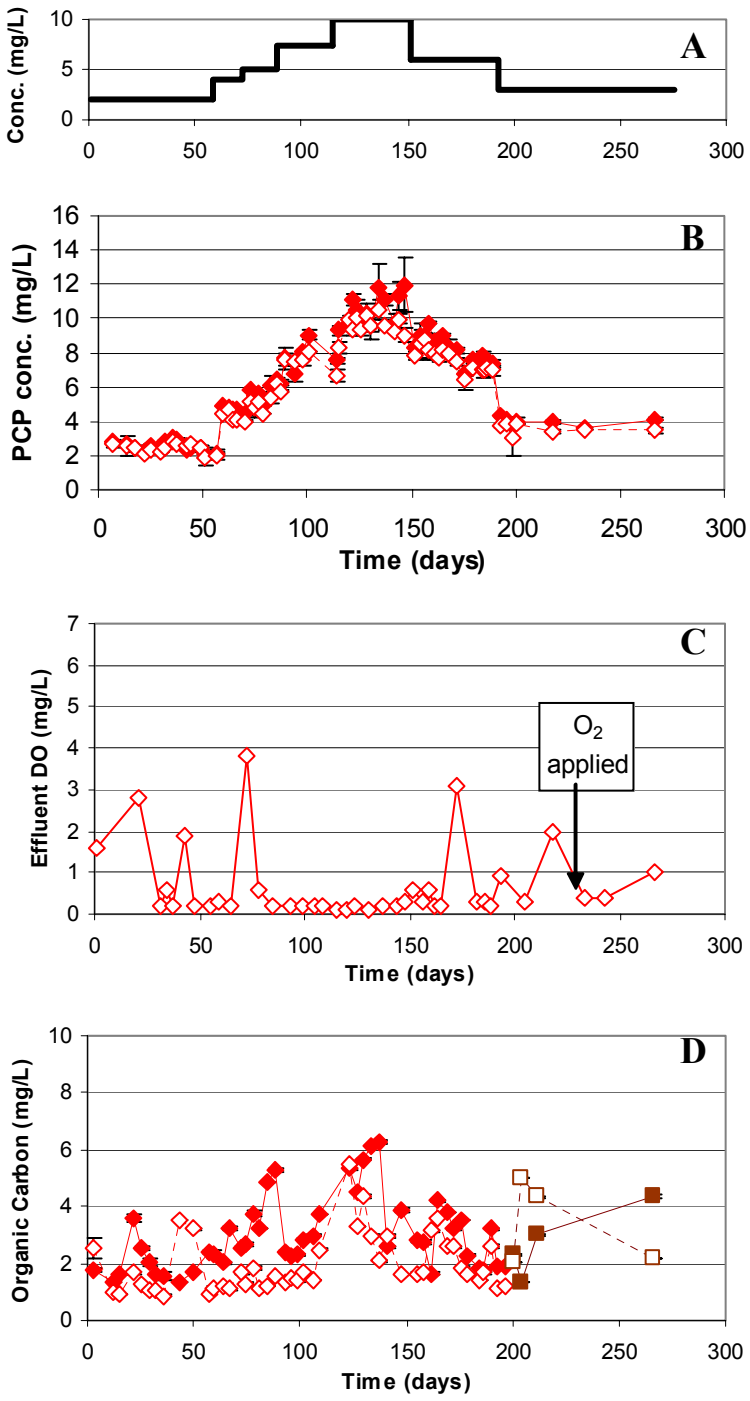

Figure 5.9. Phase I PCP column (A) target PCP concentration; (B) PCP concentration in the influent (♦) and L7 effluent (◊); error bars indicate the standard deviation of triplicate samples; (C) effluent DO; (D) organic carbon: TOC influent (♦) and L6 effluent (◊); DOC influent (■) and L6 effluent (□); error bars indicate the range of duplicate samples. Some error bars are within the symbol size.

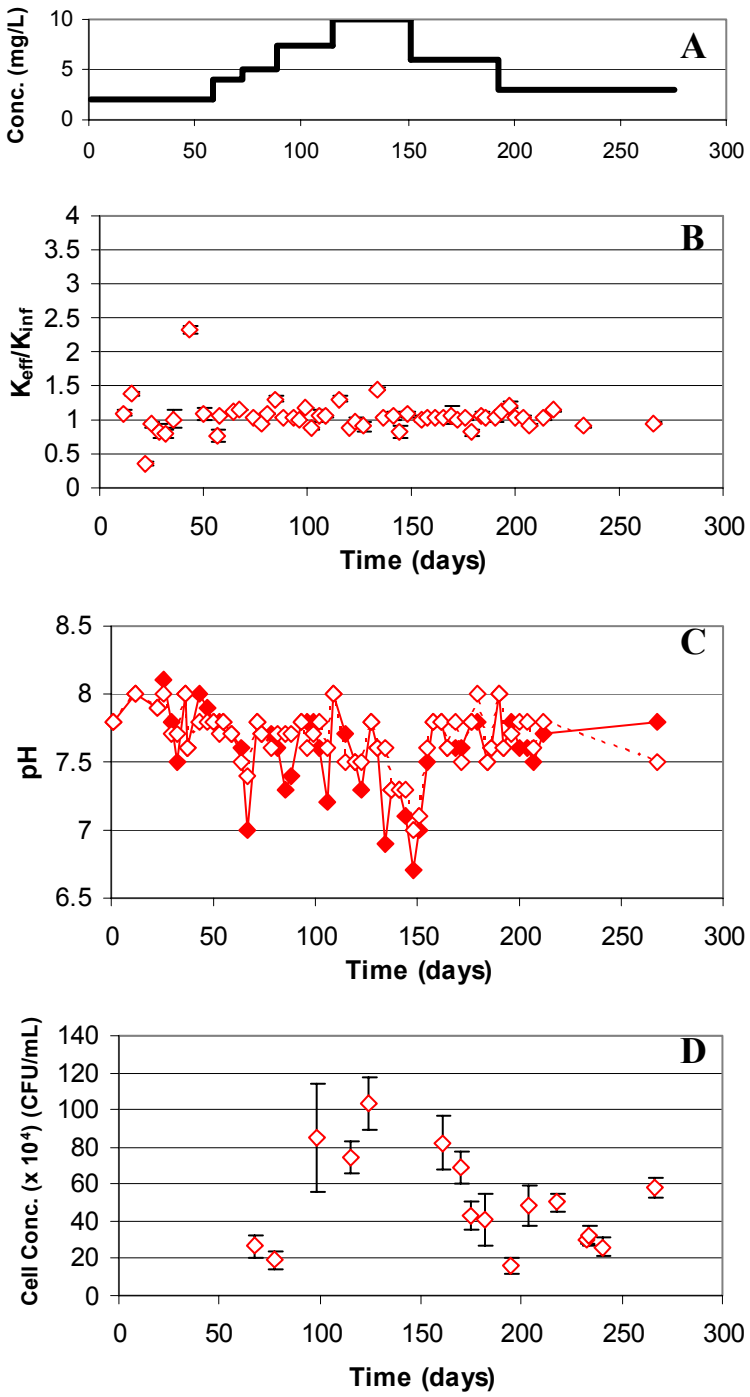

Figure 5.11. Phase I PCP column (A) target PCP concentration; (B) normalized K^+; error bars are the standard deviation of triplicate analysis; (C) influent (♦) and L7 effluent (◊) pH; (D) L7 effluent HPC; error bars are the standard deviation of counts from triplicate plates. Some error bars are within the symbol size.

5.2.4 Cadmium Column

Cadmium column concentrations followed the expected concentration plan during the course of phase I experimentation (Figures 5.12A and 5.12B). Fifty five percent of the effluent Cd concentration measurements were found to be greater than influent measurements, and of those 73% were from samples taken after the Cd concentrations were decreased after day 151, suggesting that Cd desorption occurred (Figure 5.13). A t-test supports the observed findings that the percent difference in influent and effluent Cd concentrations after day 151 are statistically different ($\pm t_{obs}(45\ df) = 2.889 > \alpha_{0.025}(40\ df) = 2.021$) from those sampled as Cd concentrations were increased. However, sorption tests were not performed to validate this observation. Cd concentration and Cd percent removed data are located in Appendix F-Table F.1.

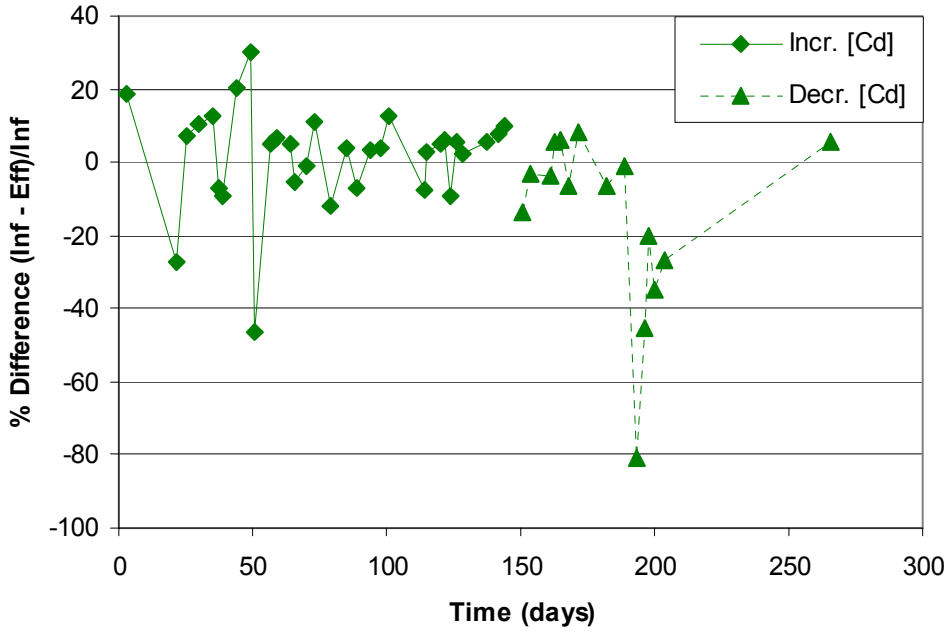

Figure 5.13 Cadmium column percent difference in influent and effluent data during phase I experimentation.

Effluent DO data show that Cd column biomass may have been tolerant of Cd concentrations of 5.0 mg/L and below, but experienced toxicity above 5.9 (7.5) mg/L Cd (targeted Cd concentrations are shown in parenthesis). Effluent dissolved oxygen from the cadmium column show increasing oxygen uptake occurred within the column between days 37 and 99, correlating with step increases in Cd concentrations from 1.6 (2) mg/L to 5.9 (7.5) mg/L (Figure 5.12C, Appendix F-Table F.3). A decrease in oxygen uptake occurred, showing an average effluent DO of 5.3 $\pm$ 0.9 mg/L between days 105 and 159, correlating with an increase from 5.9 (7.5) mg/L to 8.3 (10) mg/L Cd concentration. The cadmium concentration was decreased on day 151, followed by increasing uptake of DO by recovering biomass. On day 225, the positive pressure was changed to pure oxygen, and on day 266 the SC media was changed to SC-Tris-HCl buffered media, resulting in a steadily increasing effluent DO concentration. This indicates that the change in buffer caused an additional stress on the cadmium column biomass.

Organic carbon analysis of cadmium samples showed that most effluent TOC and all DOC samples were less than influent TOC and DOC samples (Figure 5.12D). The reduction in TOC and DOC within the column during phase I experimentation suggests that BOFS biodegradation was likely occurring even in the presence of Cd concentrations which appeared to be inhibitory, as determined by the DO data. Effluent TOC samples were greater than influent samples on days 15, 130, and 179, but could not be correlated to any known factor related to operation or maintenance. Cd column TOC/DOC data are located in Appendix F-Table F.5.

Cadmium column K^+ concentrations ranged between 2.70 and 0.84 mg/L in the influent, and 2.74 and 1.73 mg/L in the effluent (Figure 5.14). Effluent K^+ concentrations were greater than influent concentrations on days 22, 50, 57, 64, 67, 88, 109, 148, 151, 155, 176, 212, and 266 (Figure 5.15B). Five days, 88, 109, 151, 155, and 266, where found to correlate with changes made to the cadmium column. On day 88, the Cd concentration increased from a target of 5.0 to 7.5 mg/L; on day 109 the influent tubing and end cap were cleaned and replaced; on day 151 the Cd concentration was decreased from 10 mg/L to 6 mg/L; on day 155 the fritted end cap was replaced with a fritless end cap; and on day 266 the SC media was changed to SC-Tris buffered media. Similar to the control column, increases in effluent K^+ concentrations over influent concentrations are likely due to the sampling procedure as samples were unfiltered and acidified. Without filtration, planktonic bacterial cells were lysed as the sample was acidified, resulting in an increase in K^+ concentration. K^+ concentration fluctuation throughout phase I experimentation is likely due to the batch preparation method of all media bottles. Although some correlations were made explaining K^+ concentration increases, the constant variation in K^+ and the improper K^+ sampling procedure did not allow a correlation to be made between K^+ efflux and xenobiotic concentration. Cd column influent, effluent, and normalized K^+ data are located in Appendix F-Table F.2.

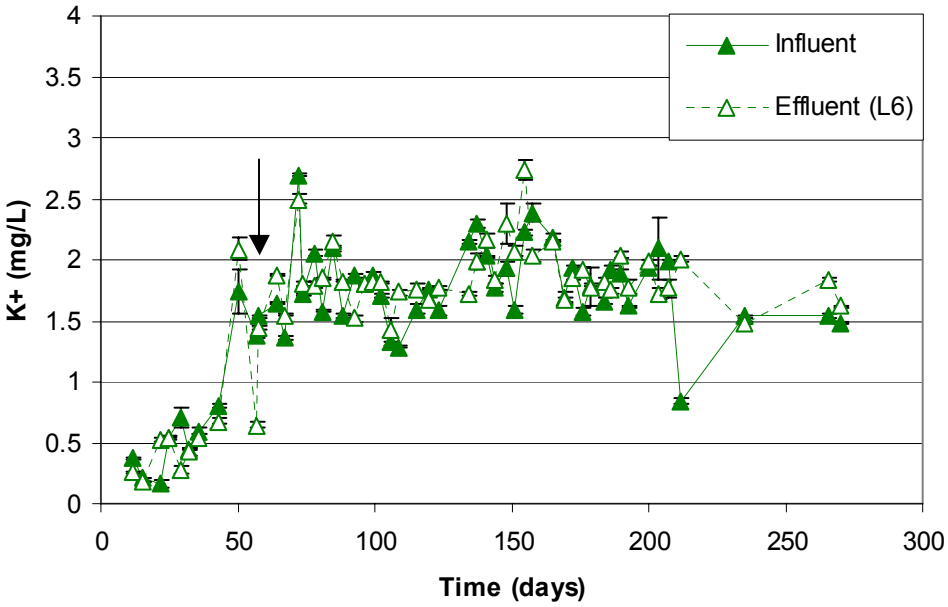

Figure 5.14. Cadmium column influent and effluent potassium concentrations during phase I experimentation. Error bars indicate standard deviation of triplicate analysis, and some error bars are within the symbol size. The increase from 0.5 to 2.0 mg/L K^+ on day 58 is denoted.

The Cd column phase I data showed pH variation as was observed with the other SC media feed bottles. The maximum and minimum pH in the influent were 8.1 and 6.9, and in the effluent were 8.1 and 7.4, respectively (Figure 5.15C). The average pH was found to be 7.7 $\pm$ 0.2 in the influent, and 7.8 $\pm$ 0.2 in the effluent, indicating that pH variability most likely did not have an impact on the Cd column during phase I experimentation. Cd column influent and effluent pH data are located in Appendix F-Table F.4.

HPC data from the Cd column during phase I experimentation indicate that biomass detachment may have occurred as the Cd concentration increased from a target concentration of 5.0 to 7.5 mg/L. The first and second HPC measurement showed a 497% increase between days 68 and 77, when the influent Cd concentrations were 3.0

and 4.3 mg/L, respectively (Figure 5.15D). The highest planktonic bacteria concentration was found on day 98, when the Cd concentration was 6.1 mg/L. Figure 5.15D shows a distinct increase in planktonic bacteria between days 77 and 124, coinciding with an increase in Cd concentration. A t-test confirmed that the planktonic bacterial concentrations were statistically different during the increasing Cd concentration phase than during the decreasing Cd concentration phase (t_{obs} (15 df) = 4.812 > $\alpha_{0.025}$ (15 df) = 2.131). In addition, a decreasing affect on the planktonic bacteria by the decrease in BOFS from 2 mg/L to 0.5 mg/L could not be ruled out by a t-test (t_{obs} (15 df) = 3.6034 > $\alpha_{0.025}$ (15 df) = 2.131). However, it is likely that the effect by the decrease in BOFS on the Cd column was similar to the control column. Since Cd is not a growth substrate, but is thiol reactive (electrophilic), this result appears to be consistent with the hypothesis that biomass detachment occurs in response to electrophilic shock. Cd column HPC data are located in Appendix F-Table F.6.

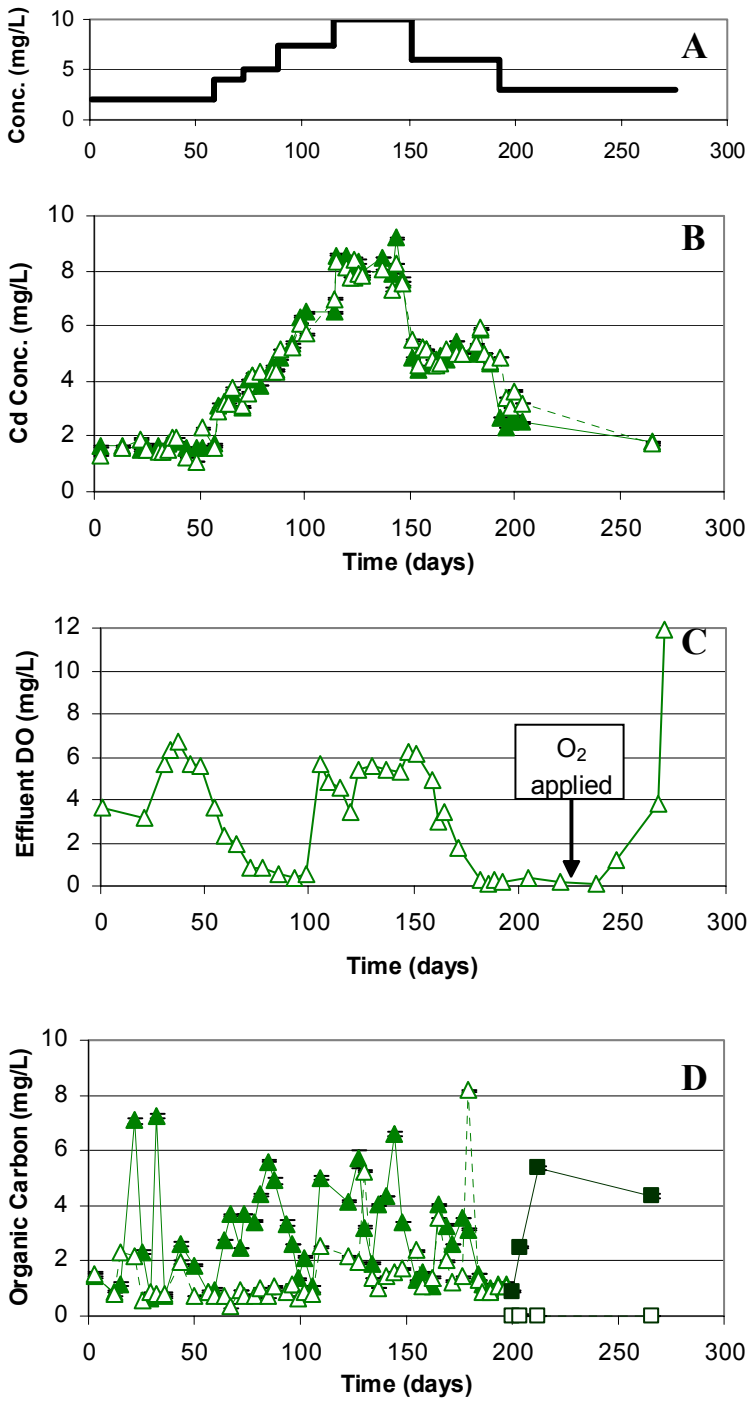

Figure 5.12. Phase I Cd column (A) target Cd concentration; (B) Cd concentration in the influent (▲) and L7 effluent (Δ); error bars indicate the standard deviation of triplicate analysis; (C) effluent DO; and (D) organic carbon: TOC influent (▲) and L6 effluent (Δ); DOC influent (■) and L6 effluent (□); error bars indicate the standard deviation of triplicate analysis. Some error bars are within the symbol size.

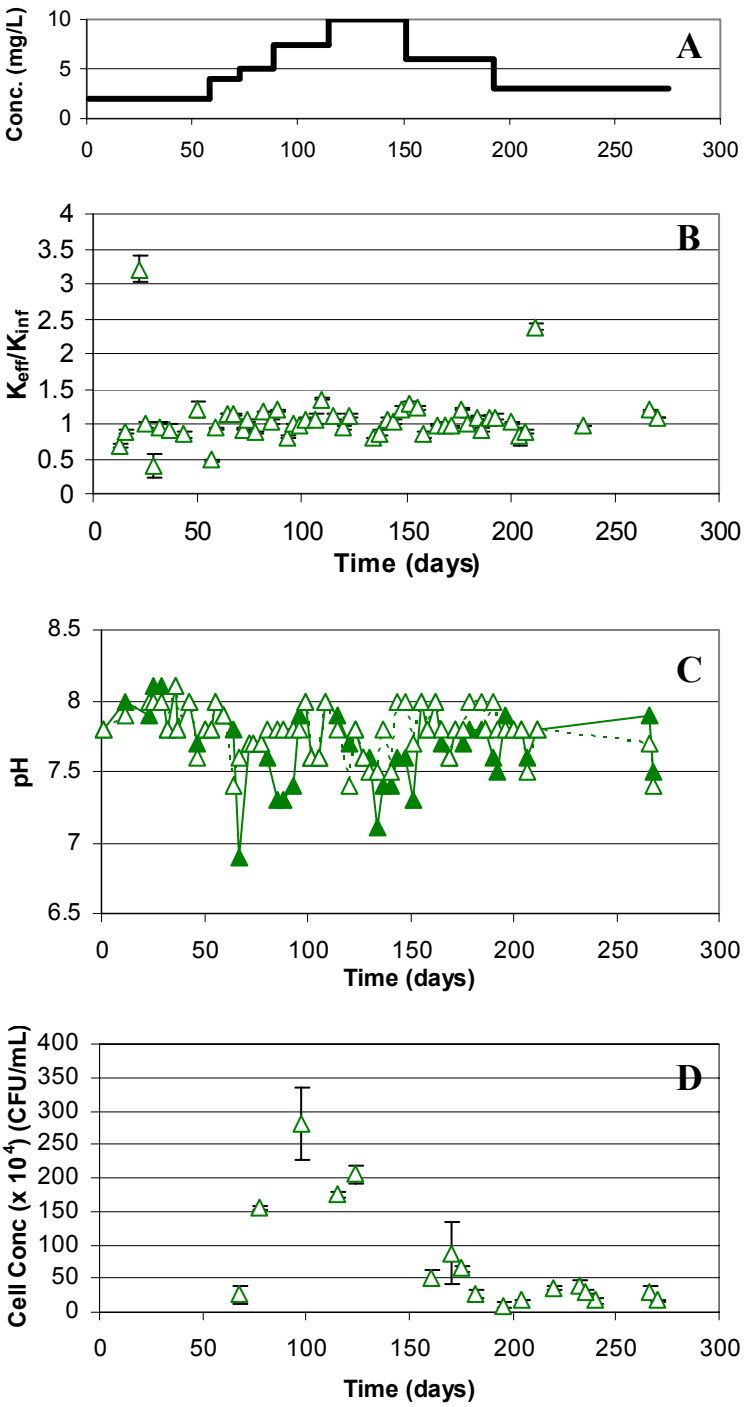

Figure 5.15. Phase I Cd column (A) target Cd concentration; (B) normalized K+; error bars indicate the standard deviation of triplicate analysis; (C) influent (▲) and L7 effluent (Δ) pH; and (D) effluent (L7) HPC; error bars indicate the standard deviation of counts from triplicate plates. Some error bars are within the symbol size.

5.2.5 Phase I Column Comparisons

Variations associated with media bottle preparation and replenishment due to dilution effects of adding small stock volumes and diluting to 9L were found in all columns for K^+, pH, TOC/DOC, and contaminant concentrations. However, comparisons can be made between the columns concerning DO, planktonic bacterial concentrations, and percent contaminant removed during phase I experimentation.

Contaminant removal was found to be greatest for benzene, and is likely due to biodegradation of benzene (Figure 5.16B). The percent of benzene removed between days 58 to 151 is low, but correlated to oxygen limitations after a small percentage of the influent benzene concentration was removed. PCP and Cd show comparable removal, suggesting that removal of each compound was associated with sorption or other loss mechanisms. Percent contaminant removed data are located in Appendix D-Table D.1 (benzene); Appendix E-Table E.1 (PCP); and Appendix F-Table F.1 (Cd).

All columns showed effluent DO fluctuations until day 85, indicating that the biomass had not reached steady state (Figure 5.16C). Following this, the effluent DO were similar until day 115, where the target contaminant concentrations increased to 10 mg/L, resulting in an increase in effluent DO in the control column, and sustained DO removal in the benzene and PCP columns. This suggests that aerobic benzene biodegradation resulted in complete removal of DO. In comparison, the PCP column effluent DO decrease was not likely associated with PCP biodegradation, strongly suggesting oxidative uncoupling was causing excessive DO uptake. The Cd column showed a marked increase in DO when no other column's effluent DO increased, suggesting toxicity to the Cd column bacterial community due to Cd concentration

increases. Effluent DO data are located in Appendix D-Table D.4 (benzene); Appendix E-Table E.3 (PCP); and Appendix F-Table F.3 (Cd).

Planktonic bacterial concentrations showed individual fluctuations, but showed an overall trend that strongly correlated with the contaminant concentration (Figure 5.16D). Initially, the control column showed the greatest planktonic concentrations, followed by the Cd column. This was followed by an increase in the Cd column planktonic bacterial concentrations relative the control column correlate with increases in Cd concentration, indicating a loss of biomass possibly due to biofilm detachment. The Cd column planktonic bacterial concentrations dramatically decreased after Cd concentrations decreased to 6 mg/L. This suggests that the Cd column biomass was not inhibited, or was acclimated to Cd concentrations below 6 mg/L. Interestingly, the benzene column showed lower planktonic bacterial concentrations compared to the control column through day 125, with increases after day 161, possibly due to release of excess biomass as the benzene concentrations decreased. The PCP column planktonic bacterial concentrations remained lower that the control column throughout experimentation, with a small increase as PCP concentrations increased, suggesting that biomass detachment did not occur. HPC data can be found in Appendix D-Table D.7 (benzene); Appendix E-Table E.6 (PCP); and Appendix F-Table F.6 (Cd).

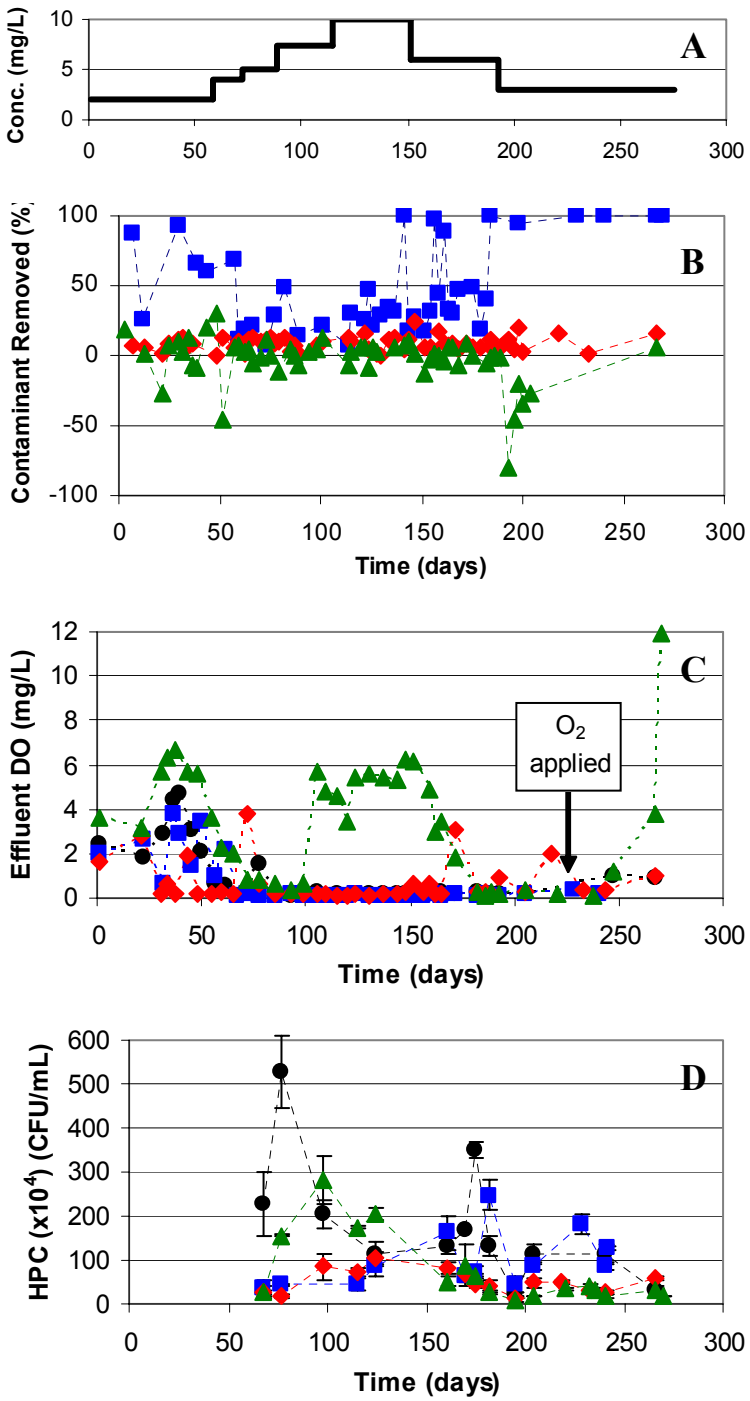

Figure 5.16. Phase I column comparison of (A) target contaminant concentration; (B) percent contaminant removed; (C) L7 effluent DO; arrow denotes the change from positive air to O_2 pressure on day 225; (D) effluent (L7) HPC; error bars indicate the standard deviation of counts of triplicate plates. Some error bars are within the symbol size. For all graphs: control (●); benzene (■), PCP (♦); and Cd (▲).

5.2.6. Relevance of Phase I Data

Aerobic benzene biodegradation was found within the benzene column, which supports the use of benzene as a biodegradable contaminant for this research. PCP removal percentages were similar to those seen for non-biodegradable Cd, indicating that PCP was not biodegraded within the PCP treated sand column. Based on this data, the hypothesis for a biodegradable electrophile could not be proven with the use of PCP during this research. However, the PCP column did show increased oxygen uptake when PCP concentrations were between 7.5 and 10 mg/L PCP (target concentrations), indicating that oxidative phosphorylation uncoupling may have occurred in the aerobic zone of the sand column. Within the Cd column, the combined increase in planktonic bacterial concentrations and bacterial inhibition indicate that the Cd column biomass was stressed when Cd concentrations were between 5 and 10 mg/L (targeted concentration). In general, phase I experimentation did not provide information to support or refute K^+ efflux resulting from exposure to benzene, PCP, or Cd. Subsequent to the end of Phase I, other research occurring in our laboratory and in the laboratory of our collaborators at the University of Cincinnati indicated that GGKE was most likely to be detected when observed over short-term perturbation experiments. For this reason, the Phase II line of experiments were conceived and implemented (discussed in Section 5.5).

5.3 Phase I – Sand Samples

Sand samples were removed from 7 sacrificial flowcell channels on days 53, 113, 135, 149, 170, 191, 275, and from the column on the final day (276). Flowcell sacrifice days and corresponding chemical concentrations are listed in Table 5.1. All sand samples were handled in an aseptic manner during sand sacrifices. It is important to note that flowcells did not receive perturbing concentrations that the columns were subjected to during phase II experimentation. Therefore, differences observed between the flowcell sacrificed on day 275 and the column sacrificed on day 276 are presumably due to the impact of perturbations on the soil microbiota. Inherent differences between how the biomass evolved in the flowcells and the column cannot be ruled out.

Results from the control, benzene, PCP, and Cd columns are presented individually. These sections are followed by sections were VS, carbohydrates, and proteins (5.3.5) and the carbohydrate to protein ratio (5.3.6) are discussed. The last sub-section (5.3.7) provides information on the relevance of phase I sand associated data.

Table 5.1. Range of days when target chemical concentrations were applied and flowcell channel sacrifice days.

Concentration (mg/L)	Day Range of Chemical Concentration (day)	Flowcell Sacrifice (day)
2	1 - 57	53
4	58 - 71	N/A
5	72 - 87	N/A
7.5	88 - 114	113
10	115 - 150	135 , 149
6	151 - 192	170 , 191
3	193 - 276	275

5.3.1 Control Column

The control column showed increasing biomass trends at early ports through day 135 during phase I experimentation. The control column biomass was expected to increase as the young biofilm inoculum matured during phase I experimentation. The volatile solids in the control flowcells showed an average increase through day 135 (Figure 5.17A). Carbohydrate and protein analysis showed an increasing trend for all flowcells (Figures 5.17B and 5.17C). The decrease of 2.0 to 0.5 mg/L BOFS as COD on day 171 did not show a decrease in any of the parameters measured from samples after day 170 at ports F1 and F2, but the change from positive air to pure oxygen may have allowed biomass growth at greater depths as seen at ports F3 and F4 on day 275 (Figures 5.17B and 5.17C). These results suggest that aerobic BOFS degradation allowed biomass concentrations to increase throughout the column. Control column VS, carbohydrate, and protein data are located in Appendix C-Tables C.6, C.7, C.8, respectively.

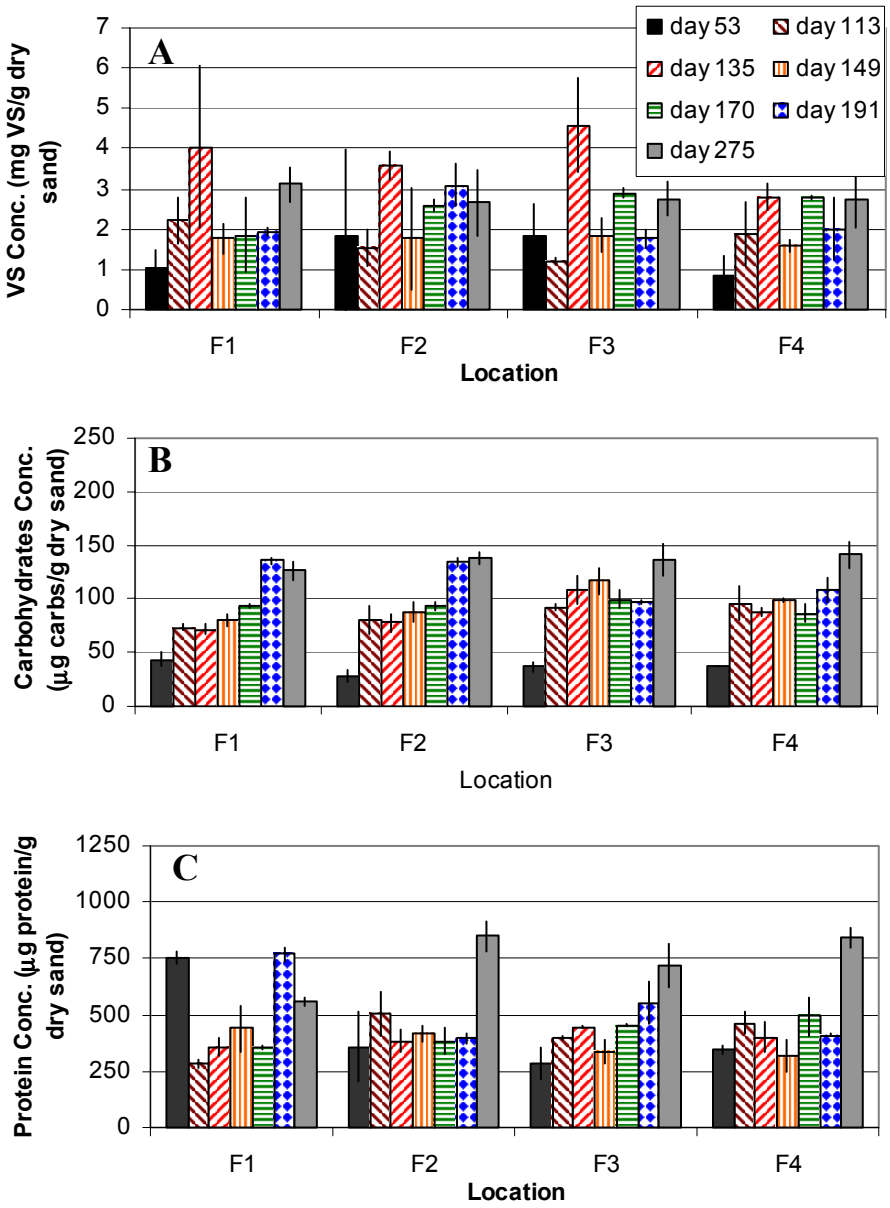

Figure 5.17. Phase I control column (A) VS concentrations; (B) carbohydrate concentrations; and (C) protein concentrations during phase I experimentation. Error bars represent the range of duplicate samples.

5.3.2 Benzene Column

Benzene column data was expected to show an increase and decrease in biomass as the benzene concentration increased and decreased, respectively. Benzene column VS were variable during phase I experimentation (Figure 5.18B). The VS sand sample for day 53 is not reported for flowcells 2 and 3 (F2 and F3) due to an analysis problem. Benzene column carbohydrate and protein data showed a general increasing trend throughout phase I experimentation, although the protein data show some variation (Figures 5.18C and 5.18D). The variation seen in the VS and protein data are likely due to the variable benzene influent concentrations throughout phase I experimentation. Benzene column VS, carbohydrate, and protein data are located in Appendix D-Tables D.8, D.9, D.10, respectively.

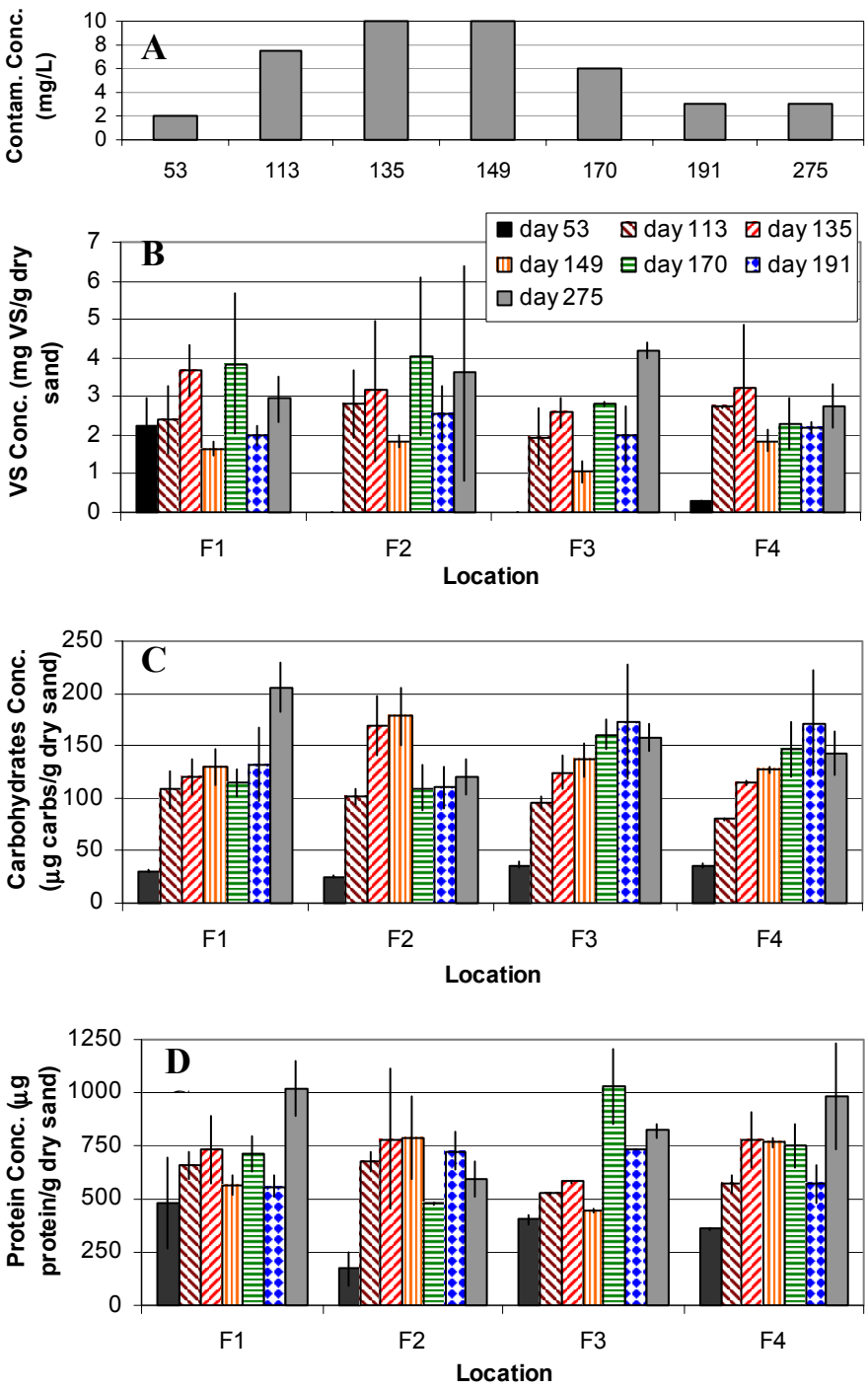

Figure 5.18. Phase I benzene column (A) target benzene concentration; (B) VS concentrations; (C) carbohydrate concentrations; and (D) protein concentrations during phase I experimentation. Error bars represent the range of duplicate samples.

5.3.3 PCP Column

The PCP column carbohydrate and protein data indicate an increase in biomass concentrations, but VS data showed variation in total biomass concentrations during phase I experimentation. Based on results presented in sections 5.1.2 and 5.2.3 disproving PCP biodegradation, biomass concentrations were expected to decrease due to GGKE activation resulting in biomass detachment as PCP concentrations increased. VS data showed a statistically significant ($t_{obs}(6df)=3.464 > \alpha_{0.025}(6df)=2.447$) decrease occurred on day 149, coinciding with the 10 mg/L target PCP concentration, supporting the occurrence of biomass loss (Figure 5.19B). PCP column carbohydrate concentrations were constant at F1, but showed an increase on day 170 after PCP concentrations were decreased to 6 mg/L, although carbohydrates at ports F2, F3 and F4 showed an increasing trend (Figure 5.19C). The carbohydrate concentration increase on day 170 suggest biomass recovery occurred as the PCP concentration was decreased. PCP column protein data showed an increasing trend at F1, F2 and F4, but showed a possible loss of biomass with increasing PCP concentrations at port F3 (Figure 5.19D). In general, the PCP column biomass data show a loss of total biomass at the highest PCP concentrations, but losses are not seen by the carbohydrate and protein data on day 149, indicating that carbohydrate and protein production was only stalled until PCP concentrations were reduced. Following the PCP concentration decrease, carbohydrate and protein concentrations showed increasing trends, suggesting bacterial growth or recovery by PCP resistant bacteria. PCP column VS, carbohydrate, and protein data are located in Appendix E-Tables E.7, E.8, E.9, respectively.

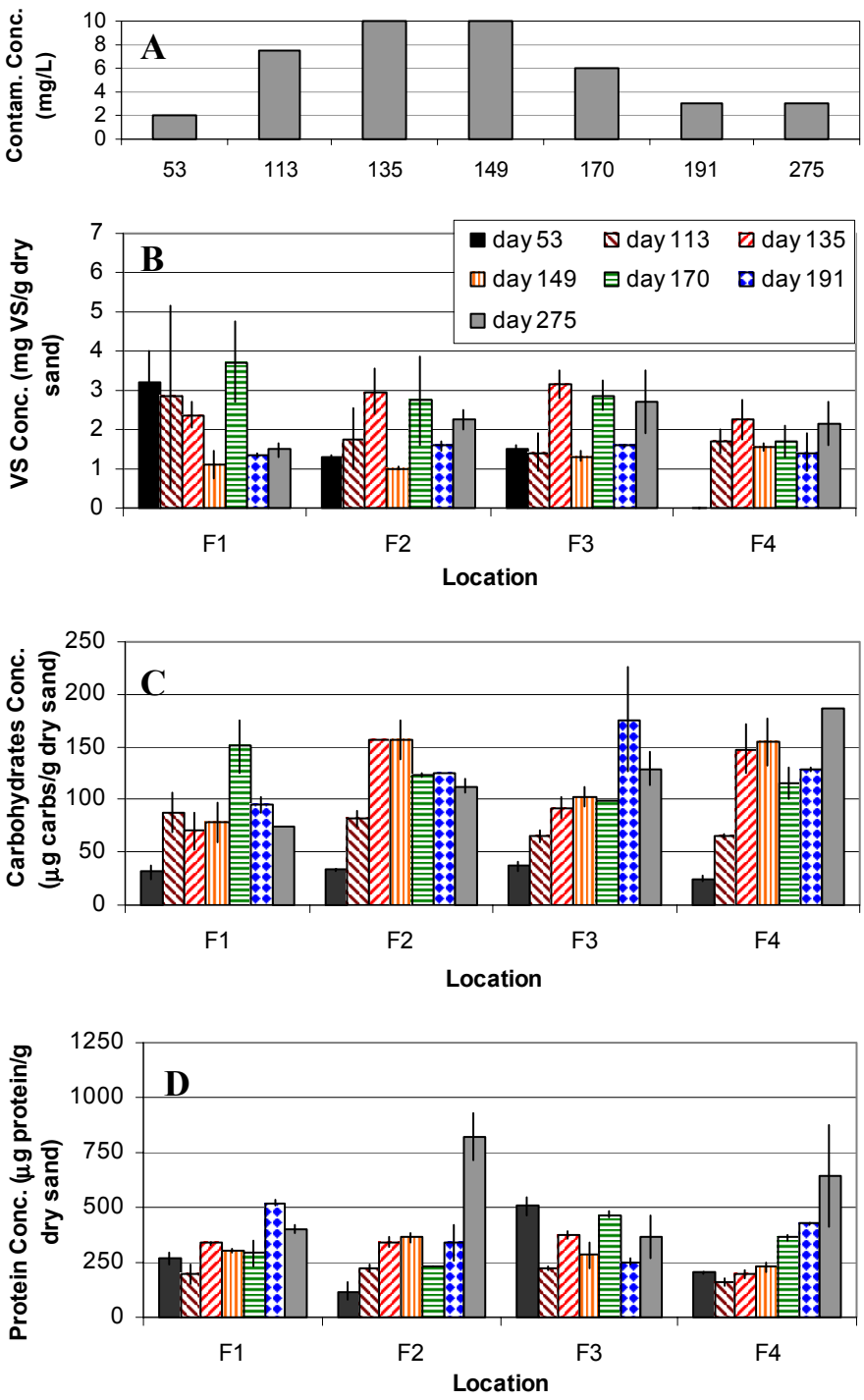

Figure 5.19. Phase I PCP column (A) target PCP concentration; (B) VS concentrations; (C) carbohydrate concentrations; and (D) protein concentrations. Error bars represent the range of duplicate samples.

5.3.4 Cadmium Column

Cadmium column biomass concentrations showed an increasing trend that became more pronounced after Cd concentrations were decreased during phase I experimentation. Cadmium column biomass was expected to decrease as the Cd concentration increased, then recover as Cd concentrations decreased. Cadmium column VS behavior at ports F1 and F4 strongly supported the expectations for biomass concentration changes, with ports F2 and F3 seemingly recovering earlier on day 149 (Figure 5.20B). Cadmium column carbohydrate concentrations at port F1 remained steady, ports F2 and F3 showed predominant increases after Cd concentrations were decreased after day 149, and port F4 showed large variation during days 135 and 149, but did show an increasing trend in carbohydrate concentration after Cd concentrations were decreased (Figure 5.20C). Cadmium column protein concentrations showed prominent increases at port F2 after day 149, but remained steady at ports F1, F3 and F4 (Figure 5.20D). The VS, carbohydrate, and protein data do not indicate a large loss of biomass occurred due to Cd induced biofilm detachment. Rather, the biofilm community likely became acclimated to Cd, which was observed as increases in carbohydrate and protein production for EPS, and/or growth as Cd concentrations decreased. Cadmium column VS, carbohydrate, and protein data are located in Appendix F-Tables F.7, F.8, F.9, respectively.

.

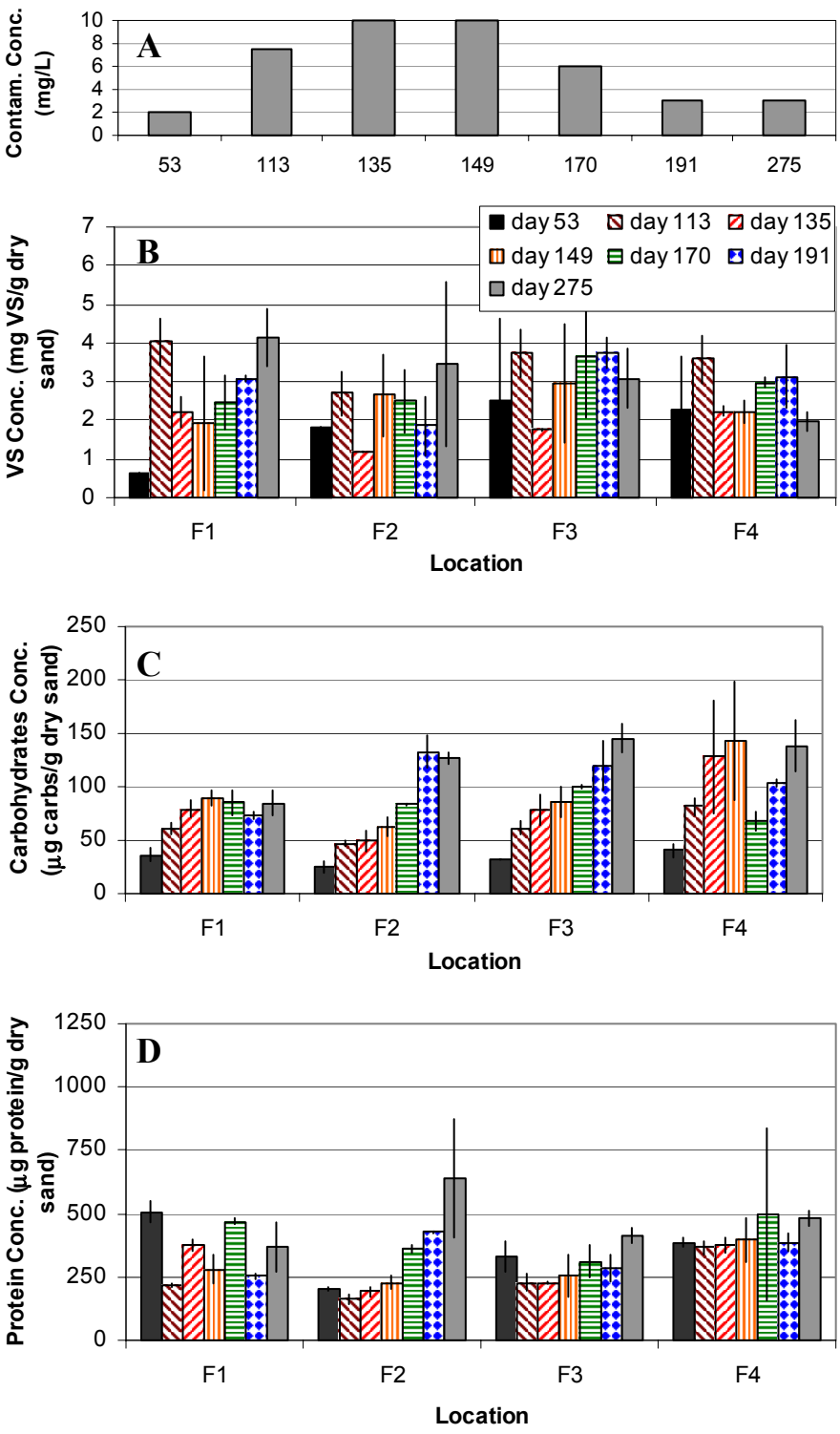

Figure 5.20. Phase I PCP column (A) target Cd concentration; (B) VS concentrations; (C) carbohydrate concentrations; and (D) protein concentrations. Error bars represent the range of duplicate samples.

5.3.5 Sand Sample Column Comparisons

Sand samples were removed multiple times during each concentration phase to measure the total biomass using two indicators: VS, and EPS measured as total carbohydrate and total protein concentrations. Flowcell ports F1 and F2 are considered to be more useful in evaluating the aerobic sand-associated functional response due the decreasing availability of DO with column depth; therefore, flowcell comparisons at ports F3 and F4 are not presented. However, all data are shown for day 276 column sacrifices. Figure 5.21 provides the average measured contaminant concentration applied when each flowcell was sacrificed (Appendix G-Table G.1).

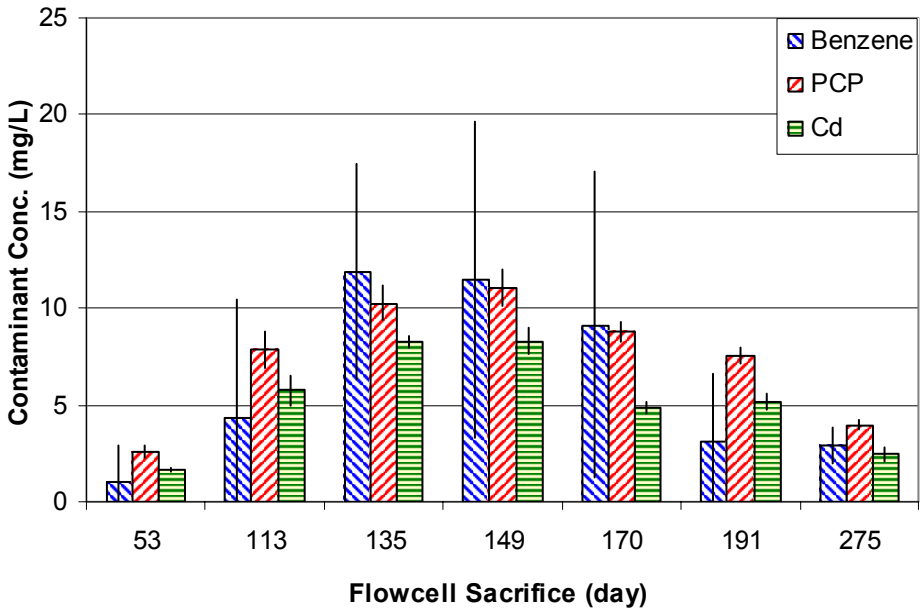

Figure 5.21. Average contaminant concentration prior to each flowcell sacrifice and column sacrifice (day 276). Error bars indicate the range of concentrations applied to the column.

Volatile solids data at port F1 is relevant due to the availability of substrates, such as oxygen and BOFS, and the likelihood that biochemical interactions occurred with

benzene, PCP, and Cd on aerobically grown biomass. The benzene column was expected to have the greatest biomass concentrations throughout phase I due to the availability of an additional readily biodegradable substrate (benzene). The control column was expected to have lower, but steadily increasing biomass concentrations, and the PCP and Cd columns were expected to have the lowest biomass concentrations due to stress responses and toxicity. Volatile solids data from flowcell port 1 (F1) showed fluctuation between columns, but showed an increasing trend for each column through day 113, followed by a decrease through day 149, corresponding with high contaminant concentrations in the Cd and PCP columns (Figure 5.22B). After the contaminant concentration was decreased on day 149, the Cd column showed a sustained increase in total biomass until day 275, whereas benzene and PCP showed a greater degree of variability (Figure 5.22B). In general, the columns behaved as expected in relation to each contaminant, although benzene VS was unexpectedly similar to control VS concentrations. The PCP column also behaved as expected with non-biodegradable contaminant interaction, but the Cd column was found to have far better recovery than the PCP column when compared to the control column. This recovery difference between the PCP and Cd columns is possibly due to the additional uncoupling effect on the PCP column.

Flowcell port 2 (F2) samples showed that all columns were similar throughout phase I experimentation, with the exception of high benzene VS concentrations on days 170 and 275 (Figure 5.22C), which correlate with 6 mg/L target benzene concentration on day 170 and post-perturbation on day 275 where benzene was targeted at 25 mg/L. Cadmium VS was unexpectedly similar to benzene VS concentrations, which were both

greater than the control column, although day 135 does show a decrease possibly related to increasing Cd concentrations (Figure 5.22C). Similar to F1 data, the PCP column VS concentrations on day 149 were expectedly lower that the control and Cd columns as PCP concentrations increased, with recovery comparable to Cd VS concentrations after PCP concentrations decreased on day 170. This indicates that as the column depth increased, PCP and Cd toxicity affected the biomass to a similar degree, which could be related to a lack of substrate (O_2 or BOFS) at increased column depth.

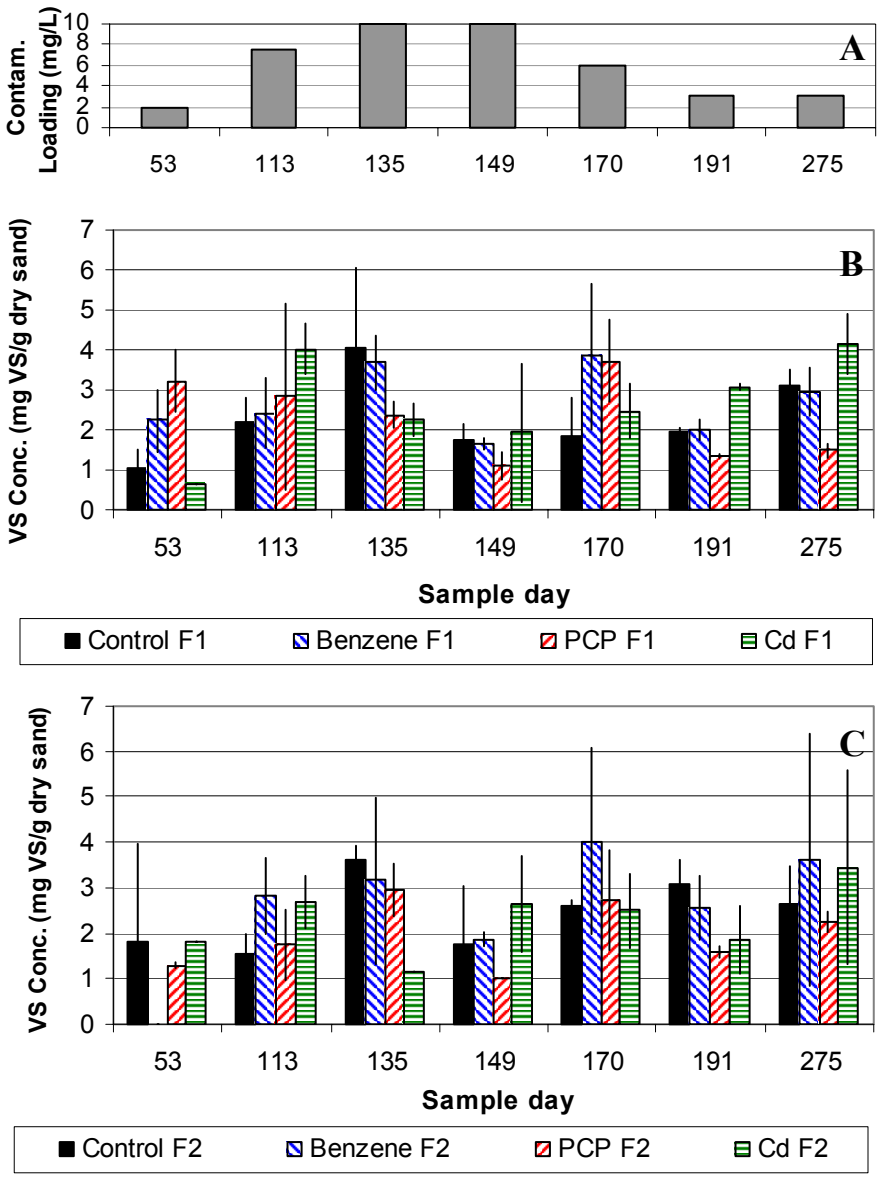

Figure 5.22. Phase I sand column comparison with (A) showing target contaminant concentration; and (B) VS samples from flowcell F1 and (C) flowcell F2. Error bars indicate the range of duplicate samples.

The column sacrifice on day 276 showed that each respective column had much lower total biomass concentrations than was found in the flowcells. The flowcells and column sand samples are not comparable as a result of differences in materials used for flowcells versus glass used for the column, flow regime, sand packing, and application of perturbing contaminant concentrations within the 58 days before column sacrifice. The control column performed as expected, with VS concentrations slightly lower or less than benzene VS concentrations (Figure 5.23). The benzene column showed the highest concentration at the influent, as was expected from visual observation during phase I experimentation (Figure 5.23). Unexpectedly, the benzene column VS increased at port F4 and at the effluent. The PCP column had the lowest VS concentrations of all columns at all ports (Figure 5.23), which likely due to biomass toxicity by combined electrophilic and uncoupling stress. Unexpectedly, the Cd column showed VS concentrations comparable to the control column, indicating that total biomass did not decrease after 3 Cd perturbation experiments. Appendix G-Table G.2 provides data for all VS comparisons and day 276 VS data.

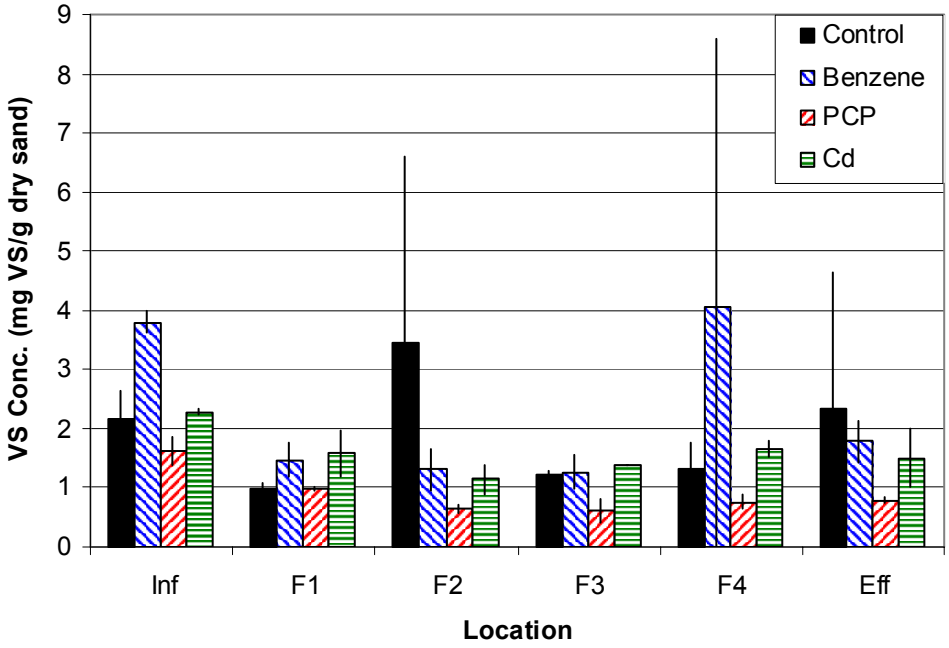

Figure 5.23 Volatile solids data from column sacrifice on day 276 from all ports and all columns. Error bars indicate the range of duplicate samples.

Port F1 carbohydrate concentrations were expected to steadily increase in the control column with time, steadily increase (to a greater degree than the control due to the extra substrate) then decrease as benzene concentrations increased and decreased in the benzene column, steadily decrease as PCP and Cd concentrations increased, then increase some after day 149 for the PCP and Cd columns when the contaminant concentrations were decreased. These carbohydrate results were expected based on BOFS feed, possible oxygen availability at the first flowcell port, and the biodegradability of each contaminant. The control column carbohydrate concentrations showed the expected increasing trend throughout phase I experimentation (Figure 5.24B). Benzene column carbohydrate concentrations increased throughout phase I experimentation, and were greater than the control column, but did not decrease as benzene concentration decreased (Figure 5.24B). The benzene column had the greatest carbohydrate concentrations on

day 275, suggesting that application of pure oxygen pressure after day 225 increased growth. PCP column carbohydrate concentrations remained steady and similar to the control column as PCP concentrations increased until day 149, followed by an increase in carbohydrate concentrations on day 170 as PCP concentrations decreased to the targeted 6 mg/L, but unexpectedly the PCP column carbohydrate concentrations decreased on days 191 and 275 (Figure 5.24B). The decrease in carbohydrate concentrations within the PCP column on day 191 was not expected, but the additional decrease on day 275 is likely due to PCP perturbation inhibitions from day 218 and 233 perturbation experiments.

The Cd column carbohydrate concentrations remained steady throughout phase I experimentation, and were unexpectedly similar to the control column through day 170 (Figure 5.24B), which may be a result of detoxification of cadmium that may have occurred due to metal ion complexation with negatively charged functional groups on the surface of carbohydrate molecules (Zhang *et al.*, 1998). Research on the effect of Cd to biofilms and EPS by White and Gadd (1998) and Fang *et al*. (2002) are in agreement with the Cd column results presented here, showing no decreasing effect on carbohydrate concentration with increasing Cd concentration.

Carbohydrate concentrations in flowcell F2 for the control and benzene columns steadily increased as expected in both columns, with larger increases occurring through day 149 in the benzene column. The increase in the benzene column was followed by a decrease in carbohydrate concentrations after benzene concentrations were decreased (Figure 5.24C). The PCP column showed greater carbohydrate concentrations than the control column, which were similar to the benzene column, suggesting that the increase

in PCP concentration promoted carbohydrate production through day 149 (Figure 5.24C). The cadmium column showed steady carbohydrate concentrations that were slightly less than those found in the control column through day 149, followed by an increase that showed carbohydrate concentrations as high as all other columns (Figure 5.24C). The PCP and Cd column findings were unexpected, and may be due to a detoxifying or protecting effect of carbohydrates within EPS, therefore encouraging carbohydrate or EPS production.

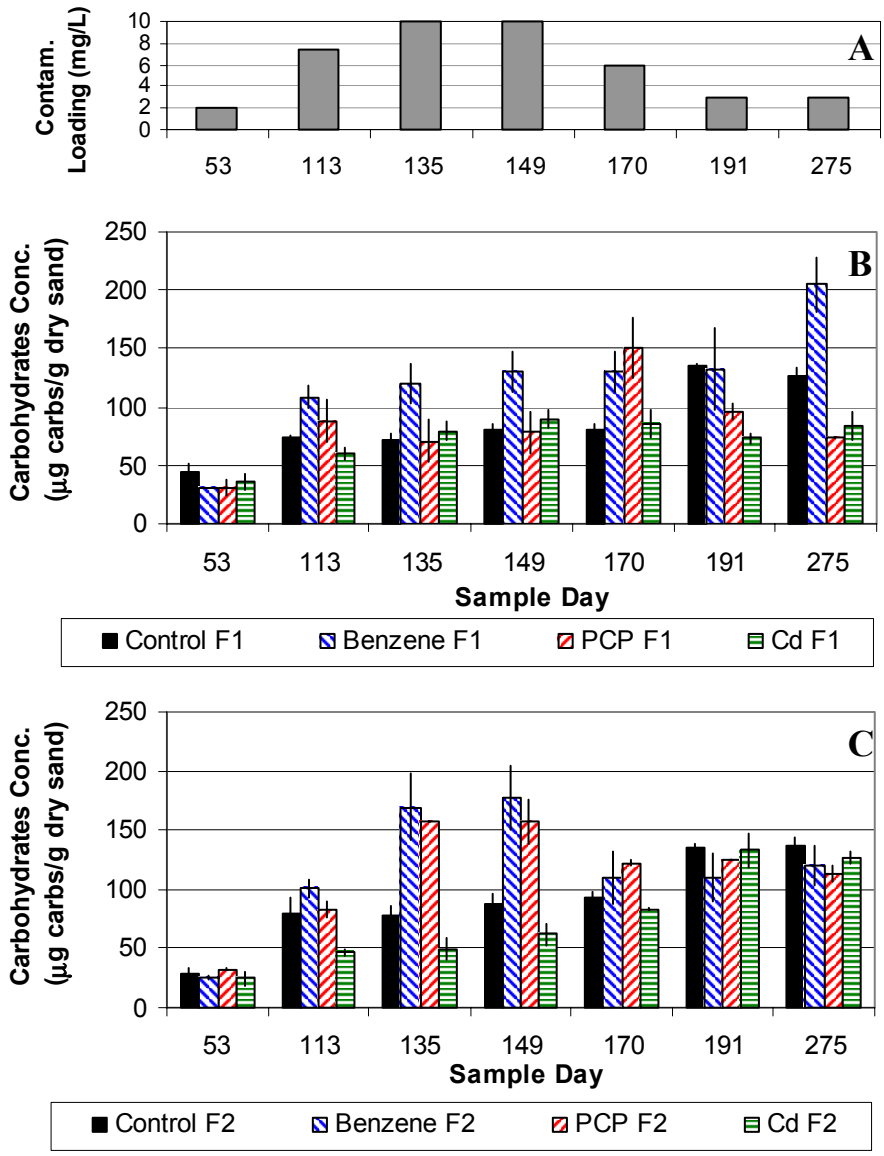

Figure 5.24. Phase I carbohydrate concentration comparisons with (A) target contaminant concentrations; and carbohydrate concentrations between all columns at (B) flowcell port F1 and (C) flowcell port F2. Error bars indicate the range of duplicate samples.

Carbohydrate concentrations within the columns on day 276 were found to be much lower than the flowcells (Figure 5.25). Influent carbohydrate concentrations from the benzene column were 230% greater than the control column, which is consistent with visual observation of thick biomass at the influent of the sand zone (Figure 5.25). The benzene column also showed a decreasing trend throughout the column, but also showed a statistically significant increase over the control column at port F1 (t_{obs} (2df)=23.337 > $\alpha_{0.025}$ (2df) = 4.303), which is likely due to an increase in biomass from benzene biodegradation. Although the Cd and PCP columns showed a decreasing carbohydrate concentration trend, they were not statistically different from the control column, indicating that carbohydrate concentrations between ports F1 through F4 were all impacted in the same manor. Appendix G-Table G.3 provides data for all comparisons of carbohydrate concentration data.

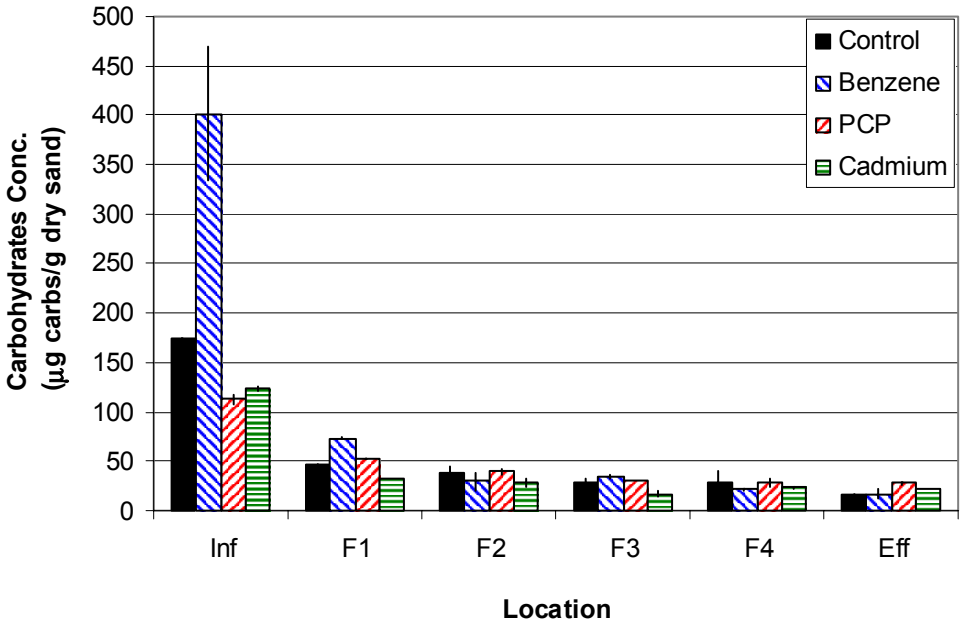

Figure 5.25. Carbohydrate concentration data from column sacrifice on day 276 from all ports and all columns. Error bars indicate the range of duplicate samples.

Protein concentrations were expected to follow the carbohydrate concentration trends. Protein concentrations showed an increasing trend in the control and benzene columns after day 53, with the benzene column showing a large increase after pure oxygen was applied on day 225 at port F1 (Figure 5.26B). PCP column protein concentrations were similar or less than the control, and Cd column protein concentrations were also similar to the control, but fluctuated at port F1 throughout phase I experimentation (Figure 5.26B). Port F1 results suggest that protein production, or growth, was inhibited by Cd and PCP application in comparison to the control. The Cd column showed a decrease in protein on days 113, and 149, correlating with increases in Cd concentrations, but this does not explain the decrease seen on day 191. The PCP column protein concentration does show a small decrease after day 53, correlating with an increase to 7.5 mg/L, and again on day 149 with targeted PCP concentrations of 10 mg/L.

In comparison to the control column, the benzene, Cd and PCP column protein concentrations at F2 were similar to expectations discussed for port F1. The control column protein concentrations at port F2 were steady until day 275, where the application of pure oxygen positive pressure may have supported increased protein production (Figure 5.26C). Benzene column protein concentrations were greater than the control column between days 113 and 191, and did exhibit an increasing and decreasing trend as benzene concentrations increased and decreased (Figure 5.26C). The PCP column protein concentrations were less than the control column through day 170, but were similar to the control on day 191 and 275, indicating that a decrease in PCP likely allowed biomass recovery (Figure 5.26C).

Cd column protein concentrations at port F2 were less than the control between day 53 and 149, but remained steady within the Cd column as Cd concentrations increased (Figure 5.26C). This suggests that the biomass growth remained steady, and increased as Cd concentrations decreased. These results also support the carbohydrate concentration increases seen at ports F2 (Figure 5.26C). Although the Cd column biomass was inhibited compared to the control, the combined data strongly suggest that biomass detachment did not occur at port F2, and indicate that growth remained steady as Cd concentrations increased. White and Gadd (1998) observed an increase in protein with a mixed culture exposed to 200 μM Cd, and Fang *et al.* (2002) measured a 60% increase in proteins with sulfate-reducing bacteria exposed to 20 mg/L Cd(II). These findings suggest that the production of protein and carbohydrates may provide some protection to bacterial cells in the presence of Cd.

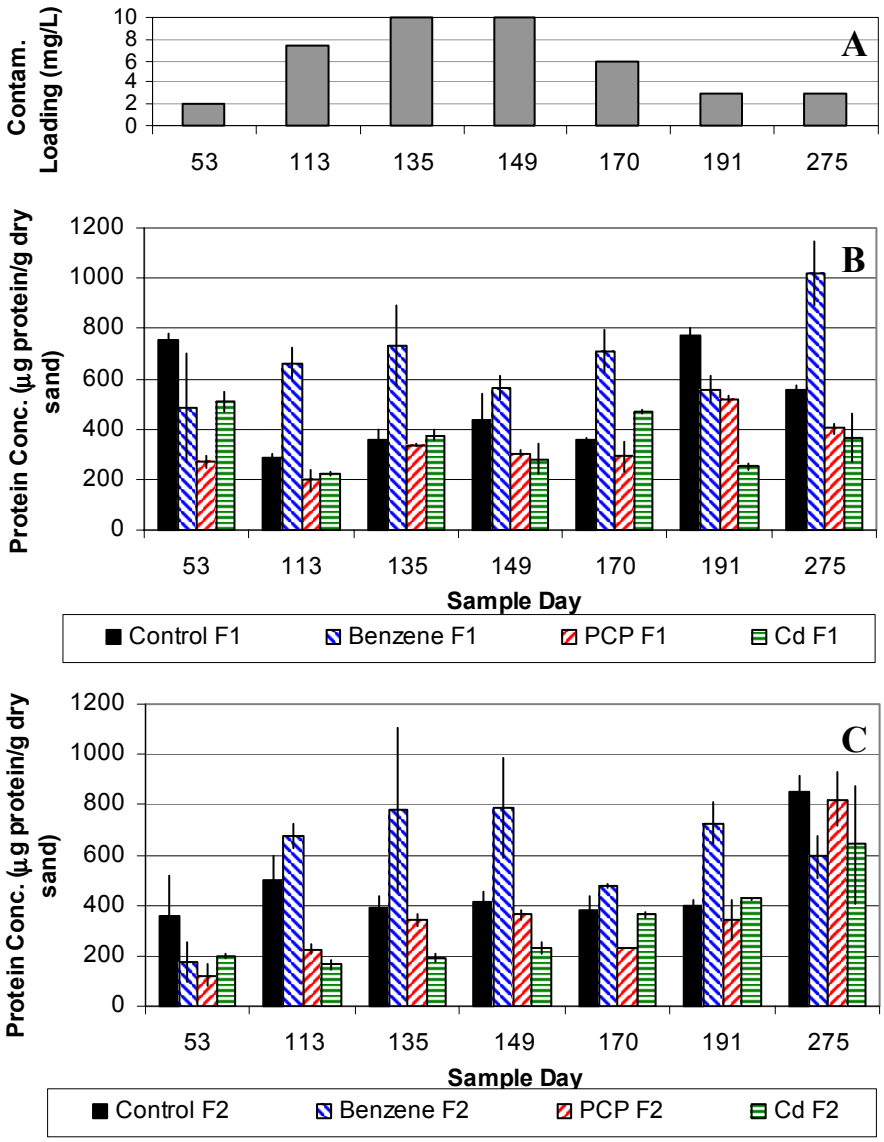

Figure 5.26. Phase I protein concentration comparisons with (A) showing the target contaminant concentration; and the protein concentration from all columns at (B) flowcell port F1 and (C) flowcell port F2. Error bars indicate the range of duplicate samples.

Protein concentrations measured from the column sacrifice on day 276 showed low protein concentrations within the column relative to flowcell protein concentrations (Figure 5.27). The influent from the benzene column contained the greatest protein concentration, 2001 µg protein g^{-1} dry sand, of all protein samples measured (Figure 5.27). This is consistent with the VS and carbohydrate measurements, visual observation of a biofilm matt at the influent to the sand zone, and benzene degradation data showing the largest benzene concentration reductions occurring between liquid ports L1 and L2. The benzene column also showed increases in protein at port F4 and the effluent, indicating additional growth. PCP and Cd influent concentrations were lower than the control, but were similar to the control after port F2 (Figure 5.27). Appendix G-Table G.4 provides all data for protein concentration comparisons between flowcells and on day 276.

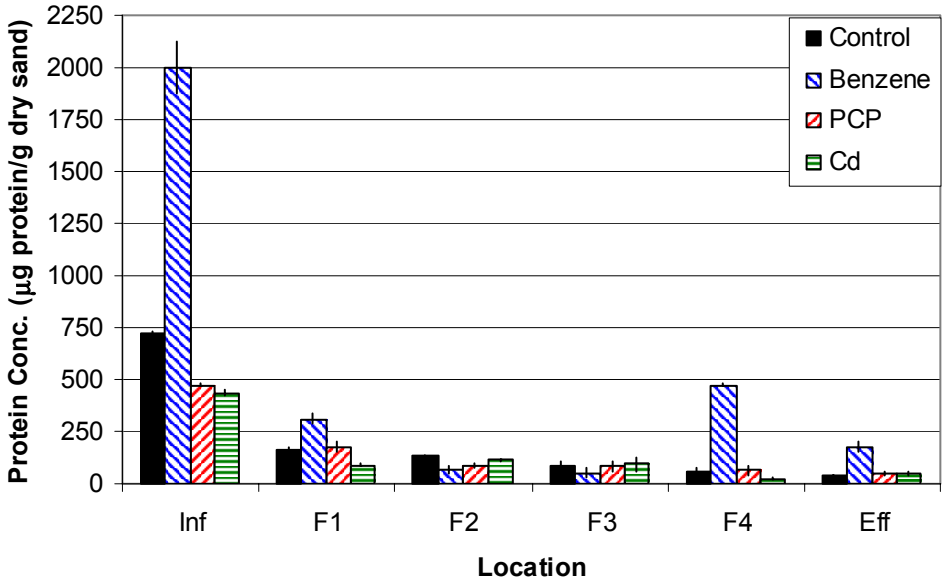

Figure 5.27. Protein concentrations from column sacrifice on day 276 from all ports and all columns. Error bars indicate the range of duplicate samples.

5.3.6 Carbohydrate to Protein Ratios

Carbohydrate to protein ratios were steady overall for the control and benzene column biomass. Carbohydrate concentrations increased relative to protein concentrations between days 53 and 113 for all columns at all flowcell ports (Figure 5.28B; Appendix G-Table G.5a). After day 53 in flowcell F1 the carbohydrate to protein ratios remained steady within the control, benzene, and cadmium columns. Most poignantly, the PCP column biomass showed strong evidence for a change in the functional response relative to PCP presence and PCP concentration increases. Biomass from the PCP column at F2 averaged 0.43 $\pm$ 0.07 μg carbohydrate/ μg protein between chronological PCP concentrations of 7.5 to 3.0 mg/L (days 113 to 191). In comparison, the control column showed a ratio of 0.23 $\pm$ 0.07 μg carbohydrate/ μg protein during the same time period. The Cd column biomass at port F2 also showed a greater increase in the ratio between days 53 and 113 than the control column (Figure 5.28C; Appendix G-Table G.5b). The Cd column showed inconsistent carbohydrate to protein ratio increases over the control column with respect to Cd concentration, showing a slight increase at F2 with increased Cd concentrations.

The carbohydrate to protein ratio has been found to be an important functional response characteristic from bacterial assemblages of activated sludge and biofilm communities. Planktonic bacteria in activated sludge produce carbohydrates and proteins in a ratio of 0.35 to 0.55 (Frølund *et al.*, 1996), whereas biofilm carbohydrate to protein ratios have been found to be much lower at 0.072 $\pm$ 0.02 (Delahaye, 1998) and 0.085 (Nielsen *et al*, 1997). This indicates that the PCP column biomass were producing carbohydrates and proteins in a ratio most similar to planktonic bacteria in activated sludge systems.

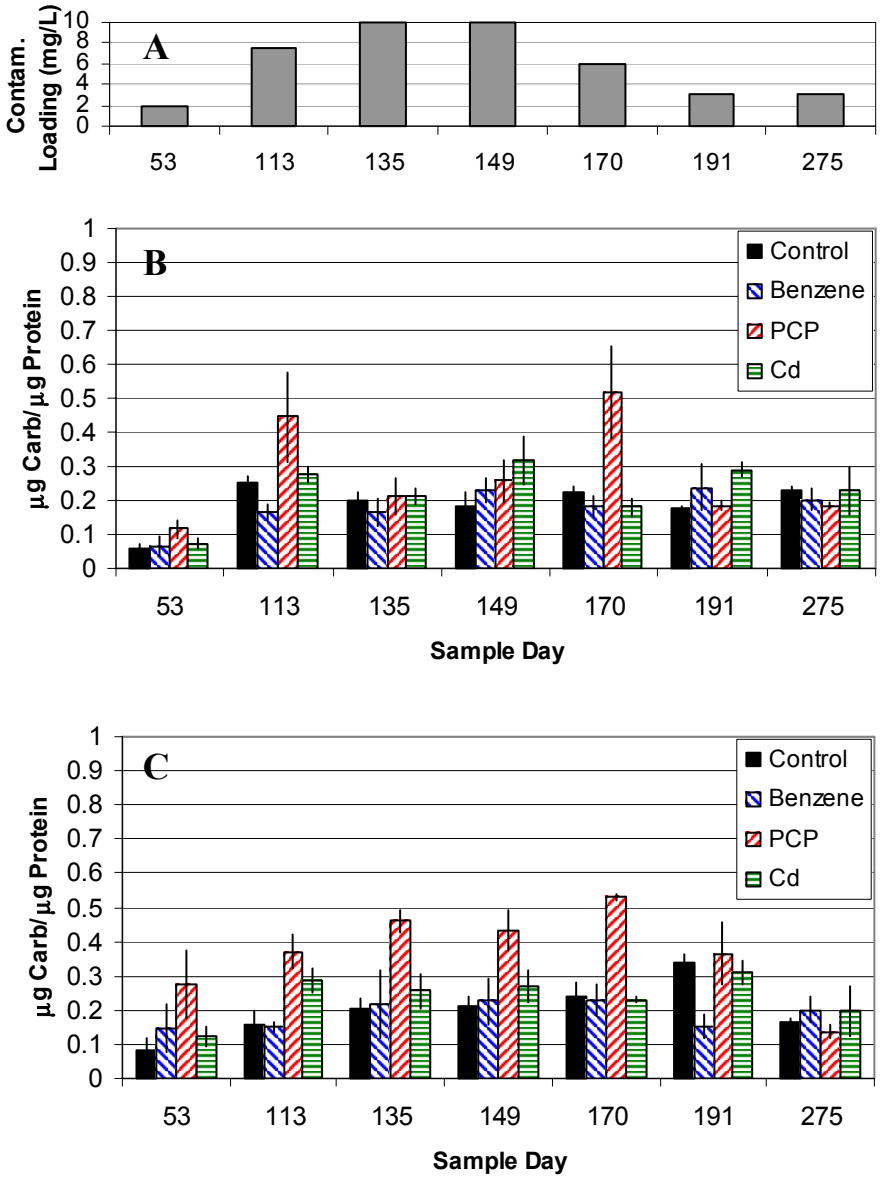

Figure 5.28. Carbohydrate to protein ratio showing the (A) target contaminant concentration; and carbohydrate to protein ratio (B) at flowcell F1 and (C) flowcell F2 during each sample day. Error bars indicate the quotient uncertainty.

5.3.7 Relevance of Sand Associated Characteristics

Several functional responses specific to the contaminant were found to occur in all three contaminant loaded columns. Sand associated biomass characteristics showed that benzene biodegradation stimulated biomass growth. The carbohydrate to protein ratio comparisons showed that a functional shift occurred in the PCP column, indicating that the PCP column bacteria were producing carbohydrates and proteins in a ratio similar to planktonic bacteria from activated sludge systems than typical biofilm bacteria.

Relative to the hypothesis, the benzene column performed as expected. The PCP and Cd columns did not show decreases in carbohydrate or protein concentrations during high contaminant concentrations, but also showed increases in these individual parameters as the contaminant concentrations decreased. This indicates that EPS provided some degree of protection to the PCP and Cd column biomass.

5.4 Tracer Studies

Tracer studies were performed on all columns to determine the experimental mean HRT (HRT_{mean}). Tracer studies were performed on the benzene and PCP columns on days 271 and 272, and on the Cd and control columns on days 273 and 274. Experimental HRT_{mean} values were determined for all columns and compared (Table 5.2). The HRT_{mean} is the time it takes for half of the tracer mass to be measured. All column HRT_{mean} values were within 16% of the control column without flowcells attached, and were within 19% of the control column with flowcells attached. The control column tracer experiment with flowcells attached had the highest HRT_{mean}, which was 4.4% above the average HRT_{mean} of the chemically perturbed columns, and is likely due to the control column having the lowest flow rate rather than flow regime differences between the columns. The similarities between all HRT_{mean} values without flowcells attached indicate that all columns had similar flow regimes and mixing properties. Appendix H provides data from control (Tables H.1, H.2, H.3), benzene (Tables H.4, H.5, H.6), PCP (Tables H.7, H.8, H.9), and Cd (Tables H.10, H.11, H.12) for each of two tracer experiments without flowcells and a final experiment with flowcells attached.

Table 5.2. Experimentally determined mean HRT (HRT_{mean}) values for all columns.

Column	Flowrate (mL/min)	HRT_{mean}[a] (hr)		
		No FC[b] -#1	*No FC* -#2	*With FC*
Control	2.63	2.54	2.52	4.98
Benzene	2.78	2.42	2.92	4.38
PCP	2.72	2.31	2.43	4.41
Cd	2.7	2.46	2.44	4.27

[a]HRT_{mean} was determined through calculations shown in section 4.5.
[b]FC = Flowcell

It is important to note the time when conductance peaked in the effluent, which occurred as the leading edge of the pulse input reached the effluent. The leading edge time is comparable to the perturbation experiments as the time when the step input of the perturbation liquid first exits the column. A comparison of the first appearance of the pulse liquid in the effluent (Leading Edge Time) and calculated HRT values (HRT_{calc}) is shown in Table 5.3. The HRT_{calc} values for tracer studies performed without flowcells are within 38.2 $\pm$ 4.4 % of the experimental HRT_{mean} values. Leading edge times differ from HRT_{calc} values by an average of 18.2 $\pm$ 6.4% with flowcells attached, and by 5.7 $\pm$ 4.0% without flowcells attached. The similarity between the leading edge time and HRT_{calc} indicate that the calculation procedure was correct, and that short-circuiting was not occurring without flowcells attached. However, the leading edge times for tracer studies with flowcell attached show later times than calculated (HRT_{calc}) values predicted. The inconsistencies between the leading edge times and HRT_{calc} for attached flowcells are likely due to discrepancies between actual and expected flow rates leaving the column through the flowcells.

Table 5.3. Comparison of experimentally determined leading edge times and calculated HRT values.

Column	Flowrate (mL/min)	Leading Edge Time (hr)			HRT_{calc}[c] (hr)	
		No FC[b] -#1	*No FC* -#2	*With FC*	*No FC*	*With FC*
Control	2.63	1.67	1.70	3.32	1.59	2.47
Benzene	2.78	1.57	1.75	2.89	1.50	2.49
PCP	2.72	1.55	1.58	2.68	1.53	2.36
Cd	2.7	1.62	1.67	2.87	1.55	2.25

[a]Values reported are the time of greatest conductance detection.
[b]FC = Flowcell
[c]Expected HRT calculations can be found in Appendix H-Table H.13.

5.5 Phase II

Phase II perturbation experiments were designed to determine the immediate bacterial community response to xenobiotic stress. The experiments were performed during the final two months of sand column experimentation. The baseline target chemical concentration was held at 3 mg/L throughout phase II, except during specific column perturbations when the chemical concentrations were increased to a target of 25 mg/L. Samples removed from the columns over time in association with each perturbation and are classified as follows: the pre-perturbation response, set A; the initial perturbation response, set B; the perturbation response after 30 minutes, set C; and the post-perturbation response, sets D and E. Sample sets A, B, C, and D were removed during the first perturbation experiment for each column, whereas all subsequent perturbation experiments included sample set E as well, so that the post-perturbation response could be measured in the event that set D contained perturbing contaminant concentrations. In addition, set A samples during the second perturbation experiments on all columns were taken on time intervals prior to perturbation feed addition. DOC data from all perturbation experiments did not show correlations pertaining to biomass detachment, although the data are provided in Appendix I-Table I.14 (benzene); Appendix J-Table J.13 (PCP); and Appendix K-Table K.20 (Cd). Finally, the results from a tracer study conducted twice on each column after phase II experimentation were used to clarify the information from samples sets A through E.

5.5.1 Benzene Perturbation

Perturbations were conducted on days 227 and 241 for benzene. All benzene perturbation experiments were performed using a positive oxygen pressure over the SC

media bottles in an attempt to increase DO concentration penetration into the column. A DO profile along the column was measured on day 226, showing DO concentrations of at least 0.4 mg/L at all ports (Figure 5.29, Appendix I-Table I.1), indicating adequate oxygen concentrations before perturbing benzene concentrations were added. Benzene concentration samples were removed immediately after HPC, K^+ and DOC samples were removed. Benzene samples were removed from the column at specific time intervals based on the expected HRT of 0.74 hour (44 min.) for the perturbation feed to reach the sand interface, and a theoretical HRT of 1.2 hours (72 min.) within the sand zone, and 1.5 hours to reach the final column effluent (Appendix I-Table I.2), and also included the time required to replace the volume of pore water removed with each sample (Table 5.4).

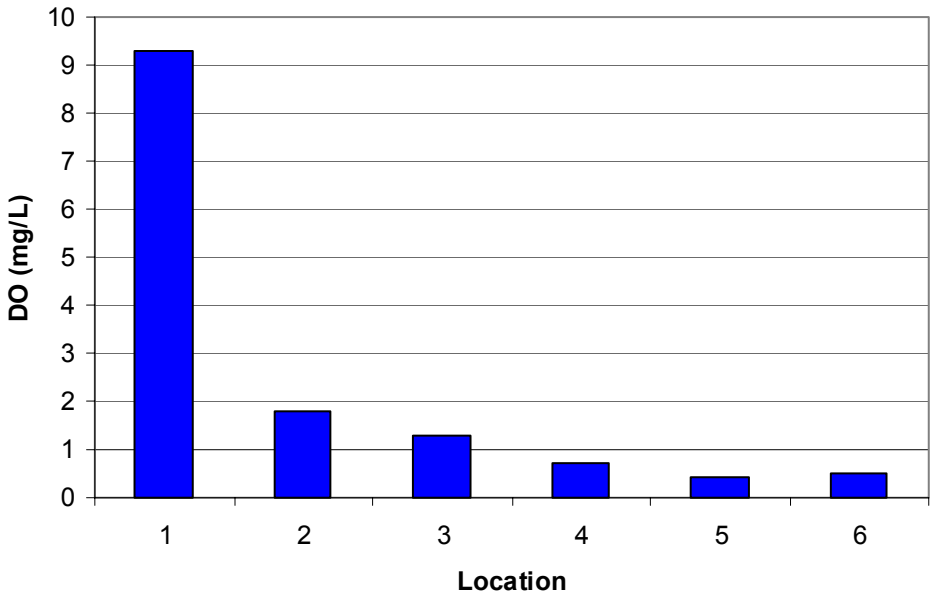

Figure 5.29. DO profile of benzene column on day 226, with positive oxygen pressure over SC-benzene media bottle.

Table 5.4. Sample removal times for benzene perturbation experiment on day 227.

Liquid Port	HRT_{mean}[a] (hr)	Time of Sample Removal (hr)								
		Set A		*Set B*		*Set C*		*Perturb Bottle Removed*	*Set D*	
		HPC, DOC, K	Benzene	HPC, DOC, K	Benzene	HPC, DOC, K	Benzene		HPC, DOC, K	Benzene
1	1.23 - 1.72	Before Start		0.73	0.78	1.31	1.34	2.99	3.75	3.79
2	1.32 - 1.82			0.93	0.96	1.70	1.75		3.93	3.96
3	1.49 - 1.98			1.13	1.17	2.13	2.16		4.09	4.12
4	1.67 - 2.16			1.52	1.58	2.52	2.55		4.26	4.29
5	1.85 - 2.34			1.88	1.99	2.70	2.74		4.43	4.46
6	2.03 - 2.52			2.36	2.40	2.85	2.91		4.59	4.63

[a]HRT_{mean} values apply to set B and were calculated by subtracting the expected HRT between liquid ports from each of duplicate HRT_{mean} values obtained from tracer studies. The expected flow rate of 2.8 mL/min was used, and HRT_{mean} values per port do not account for sample volumes removed from previous ports.

Benzene perturbation experiment data (day 227) show that high benzene concentrations were first measured in set B (Figure 5.30A, Appendix I-Table I.4). Set A shows complete removal of the baseline benzene concentration of 2 mg/L, although the target baseline benzene concentration was 3 mg/L. The final set D, which was expected to show a post-perturbation response, shows the highest measured benzene concentration in the column (Figure 5.30A), suggesting that sample removal created a difference between the actual HRT and the HRT_{mean} of the column Sets B, C, and D show a loss of 6.0, 4.1, and 5.7 mg/L benzene, respectively, between ports L1 and L6, with the majority of benzene biodegradation occurring between ports L1 and L2. Additional losses of benzene after port L2 were not seen. It is believed that the benzene removal is due to aerobic biodegradation of benzene, and that benzene biodegradation ceased after the second port in the column because of DO limitation. The loss of DO was evident in the effluent from the column where DO concentrations were 0 mg/L 1.8 hours after perturbation feed addition (Figure 5.31, Appendix I-Table I.5). DO concentrations of 0.4 mg/L were measured from the effluent at t = 0.2 hrs, just after perturbation feed addition (Figure 5.31). Although the DO measurement occurred after perturbing feed was added,

it corresponds with the pre-perturbation effluent DO because the effluent liquid did not yet contain perturbing benzene concentrations. HRT calculations for the expected time for perturbing benzene concentrations to reach the column effluent correlate with the decrease in effluent DO (HRT_{calc} = 1.94 hrs), confirming that the addition of perturbing benzene concentrations caused benzene column biomass to increase oxygen uptake. Additional O_2 uptake with increasing benzene concentration was also seen in oxygen uptake rate (OUR) experiments performed prior to perturbation experiments (Appendix I-Table I.3).

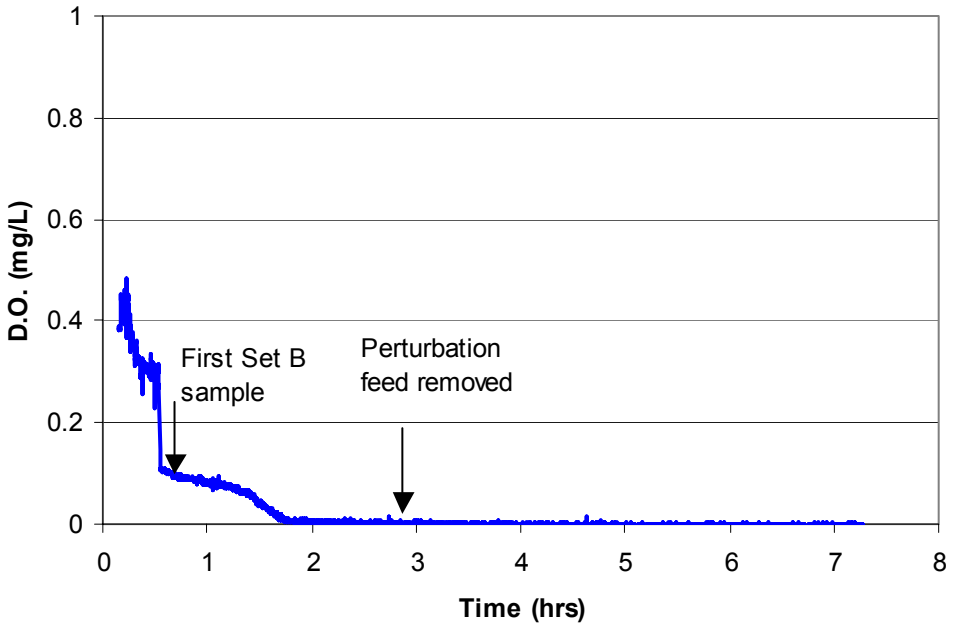

Figure 5.31. Effluent dissolved oxygen concentration during benzene perturbation on day 227. Time zero indicates addition of perturbation feed.

Potassium concentrations normalized by set A at each port showed lower K^+ than in set A, with a large decrease occurring between ports L2 and L4 in set B (Figure 5.30B, Appendix I-Table I.6). Potassium concentrations remained lower than pre-perturbation

concentrations in sets C and D benzene during the benzene perturbation experiment on day 227, which is due to a required bottle exchange possibly containing lower K^+ concentrations than the pre-perturbation media bottle. The decrease in K^+ is likely due to uptake of K^+ for catabolism or cell growth requirements with the additional availability of substrate (benzene).

The responses shown in potassium and HPC data indicate that bacterial growth was likely occurring in the pore water during set B as high benzene concentrations were catabolized. HPC data show bacterial increases in pore liquid during the initial perturbation (set B) between ports L2 and L3 (Figure 5.30C), and is likely due to growth. The lack of growth at other column depths may be due to anaerobic conditions that disallowed growth of biomass. Benzene perturbation HPC data from day 227 is located in Appendix I-Table I.7).

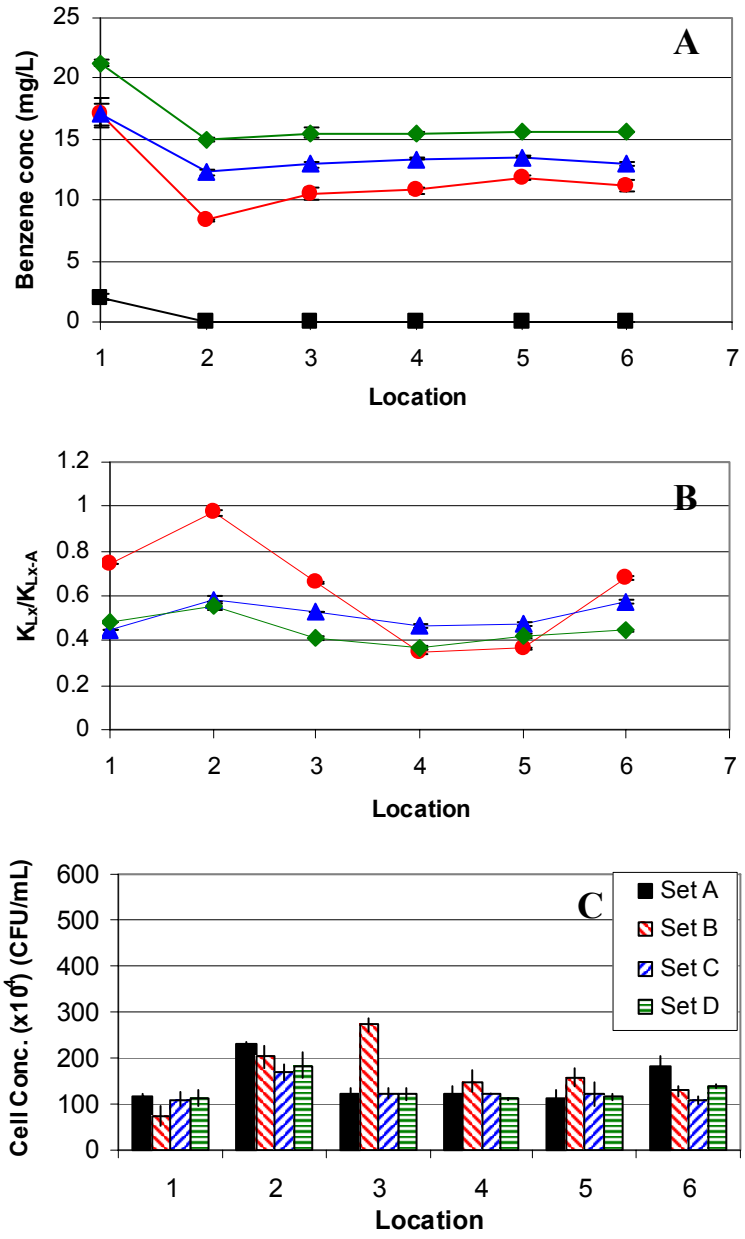

Figure 5.30 Benzene perturbation experiment on day 227 (A) benzene concentration per port; error bars indicate the range of duplicate samples (B) normalized K^+ per port; where each set was normalized by set A per port; error bars indicate the standard deviation of triplicate analysis; and (C) HPC per port. Some error bars are within the symbol size. For graphs A and B: set A (■); set B (●); set C (▲); and set D (♦).

Potassium and HPC comparisons show evidence of concurrent planktonic bacteria increase and potassium concentration decrease at early ports during the initial phase of the benzene perturbation on day 227. Figure 5.32A shows no correlation between the

planktonic bacterial concentration and K^+ concentrations, although planktonic bacterial concentrations decreased between ports L2 and L3 from set A. Figure 5.32B shows an increase in planktonic bacteria in set B between ports L2 - L1, and L3 - L2 (ΔHPC > 0), while K^+ decreased at L3 – L2 by 25%. Figure 5.32C shows a common trend within sets C and D, where the planktonic bacteria concentrations decreased between ports L2 and L3. Post-perturbation planktonic bacteria concentrations (sets C and D) returned to pre-perturbation trends, whereas the initial response to perturbation (set B) showed planktonic increases likely related to catabolism and growth. These results strongly suggest that the initial benzene column biomass response to perturbing benzene concentrations is catabolism and growth when oxygen is available. K^+ and HPC difference data for Figures 5.32A-C are located in Appendix I-Table I-8.

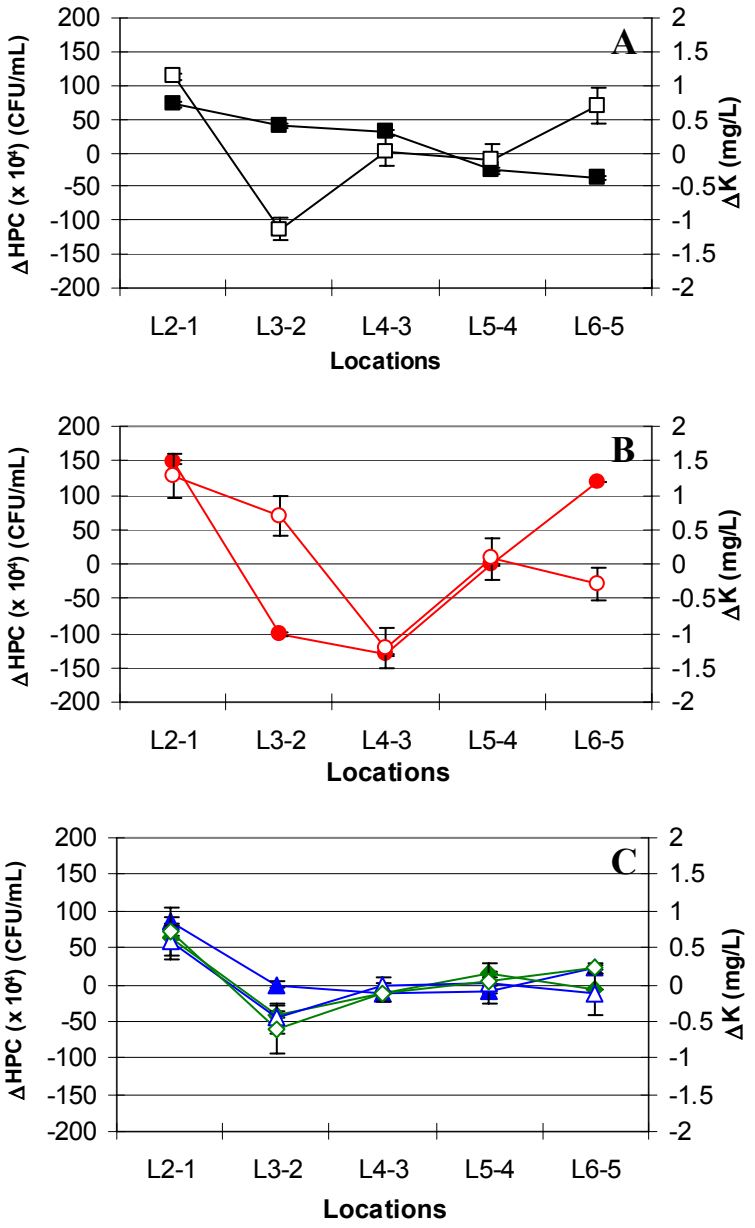

Figure 5.32. Benzene perturbation experiment on day 227 HPC (open symbols) and K+ (closed symbols) difference between ports (L x - L (x-1)) from (A) set A (■); (B) set B (●); (C) sets C (▲) and D (♦). Error bars indicate the standard deviation of the difference; some are within the symbol size.

The second benzene perturbation experiment was performed two weeks after the first perturbation experiment, and was altered to include a fifth sample set (set E) at the end of the experiment to test a post-perturbation response. Sample removal times are shown in Table 5.5.

Table 5.5. Sample removal times for benzene perturbation experiment on day 241.

Liquid Port	HRT_{mean}[a] (hr)	Time of Sample Removal (hr)										
		Set A		*Set B*		*Set C*		*Perturb Bottle Removed*	*Set D*		*Set E*	
		HPC, DOC, K	Benzene	HPC, DOC, K	Benzene	HPC, DOC, K	Benzene		HPC, DOC, K	Benzene	HPC, DOC, K	Benzene
1	1.23 - 1.72	-1.00	-0.92	0.66	0.70	1.16	1.23	2.76	3.27	3.31	5.09	5.14
2	1.32 - 1.82	-0.81	-0.75	0.83	0.91	1.56	1.61		3.44	3.49	5.26	5.30
3	1.49 - 1.98	-0.62	-0.55	1.01	1.07	2.87	1.92		3.59	3.63	5.42	5.46
4	1.67 - 2.16	-0.49	-0.43	1.34	1.40	2.18	2.50		4.81	3.84	5.62	5.66
5	1.85 - 2.34	-0.31	-0.26	1.72	1.75	2.37	2.42		5.99	4.02	5.80	5.83
6	2.03 - 2.52	-0.15	-0.09	2.03	2.10	2.67	2.71		5.12	4.15	5.94	5.96

[a]HRT_{mean} values apply to set B and were calculated by subtracting the expected HRT between liquid ports from each of duplicate HRT_{mean} values obtained from tracer studies. The expected flow rate of 2.8 mL/min was used, and HRT_{mean} values per port do not account for sample volumes removed from previous ports.

The first high benzene concentration is seen in set B, and continues in sets C and D, with set C showing the highest benzene concentration (Figure 5.33A, Appendix I-Table I.9). Sample L2 in set C is missing due to a sampling error, and set A L2 through L6 values are masked by set E (Figure 5.33A). The added set E shows that the influent benzene concentration returned to the target baseline benzene, which was 2.8 mg/L (Figure 5.33A; set E). An increase in benzene relative to L2 is seen in set B at L3 and L4, in set C in L4, and in set D at L6 (Figure 5.33A) on day 241. This response is unlike the first benzene perturbation experiment on day 227, where benzene concentrations remained steady after port L2 in sets B, C and D. The benzene removal was 4.1, 11.7, and -0.69 mg/L between ports L1 and L6 for sets B, C, and D, respectively. This suggests that benzene concentrations were not homogenous within sample sets. Benzene

concentrations of 3.6 and 2.8 mg/L were completely removed between ports L1 and L2 during sets A and E, respectively (Figure 5.33A).

The effluent DO increased during and after the benzene perturbation experiment on day 241. The DO began to increase 2.2 hrs after the perturbation feed was added, peaked at 0.8 mg/L while sampling for set D, and decreased to 0 mg/L at 5.5 hrs until the end of the experiment at 6 hrs (Figure 5.34, Appendix I-Table I.10). The effluent DO increase 2.2 hours into perturbation was slightly longer than the expected HRT (HRT_{calc} = 1.94) for the leading edge time of perturbing benzene to exit the effluent end cap (Figure 5.34). The effluent DO concentration decrease indicates that benzene biodegradation was occurring throughout the experiment, but the effluent DO increase indicates that DO uptake was inhibited by perturbing benzene concentrations. However, this slight inhibition was followed by biomass recovery as effluent DO concentrations decreased to undetectable levels. The inhibition in DO uptake may be a result of substrate inhibition by benzene, degradation byproduct inhibition, or competitive inhibition with benzene and degradation byproducts. Monero *et al.* (2003) found competitive inhibition to have a stronger effect on *Pseudomonas* sp than inhibition by benzene alone.

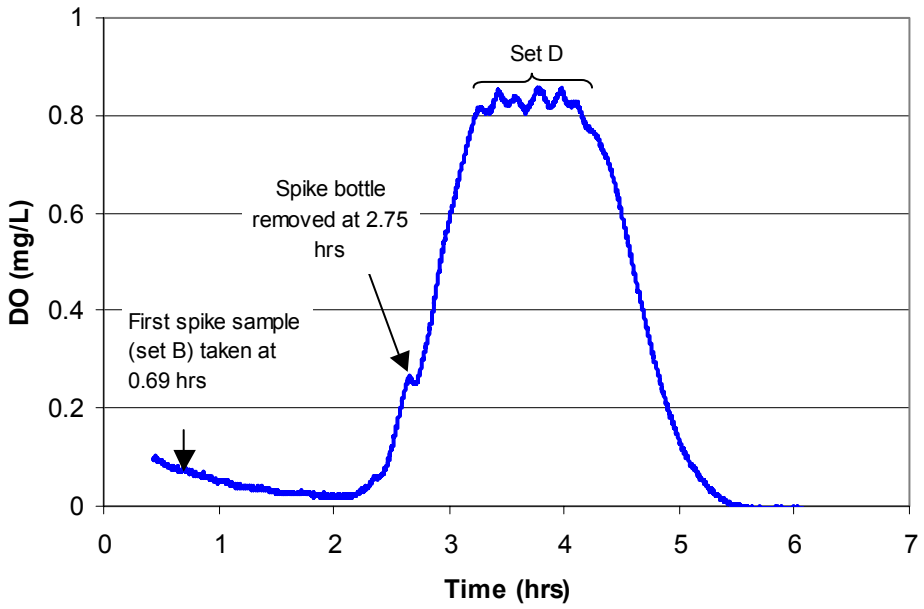

Figure 5.34. Effluent dissolved oxygen during the benzene perturbation experiment on day 241.

Potassium values normalized by set A showed decreasing trends in sets B, C, and E, while set D showed an increase in K^+ between ports L1 through L3 during the benzene perturbation experiment on day 241 (Figure 5.33B, Appendix I-Table I.11). The normalized K^+ values were greater then 1, indicating that K^+ concentrations during and after benzene perturbation were greater overall then the pre-perturbation media solution. Daily records confirmed that the post-perturbation media bottle (set E) was different than the pre-perturbation (set A) feed bottle as part of the normal bottle replenishment schedule. The decreases in K^+ trends within each set on day 241 are similar to day 227, except that set B on day 241 showed an increased uptake over sets C, D, and E, which was likely due to biomass growth requirement limitations during later sample sets. Unlike day 227 (Figure 5.30B), sets C and D showed less uptake of K^+ than set B, which corresponded with the effluent DO increase (Figure 5.33B). This suggests that the K^+

uptake decreased after 30 minutes into benzene perturbation, possibly as a result of growth rate decreases as benzene concentrations decreased, or biomass inhibition.

HPC data show evidence of an increase in planktonic bacteria as perturbing benzene concentrations flowed through the column during the perturbation experiment on day 241 (Figure 5.33C, Appendix I-Table I.12). The highest concentration of planktonic bacteria occurred in set B ports L3 through L6, and in the influent port (L1) of sets C and D, which were all found to be statistically different from set A (t_{obs}(4df)=L3: 4.982 , L4: 6.403, L5: 3.846, L6: 10.641 > $\alpha_{0.025}$(4df)=2.776). Planktonic bacteria concentrations returned to pre-perturbation levels during set C at L2, but continued to decrease below set A concentrations in sets D and E (Figure 5.33C). The increase in planktonic bacterial concentrations in set B indicate catabolism or growth occurred, while the decreasing trends in sets C, D, and E indicate biomass inhibition occurred as perturbation was prolonged.

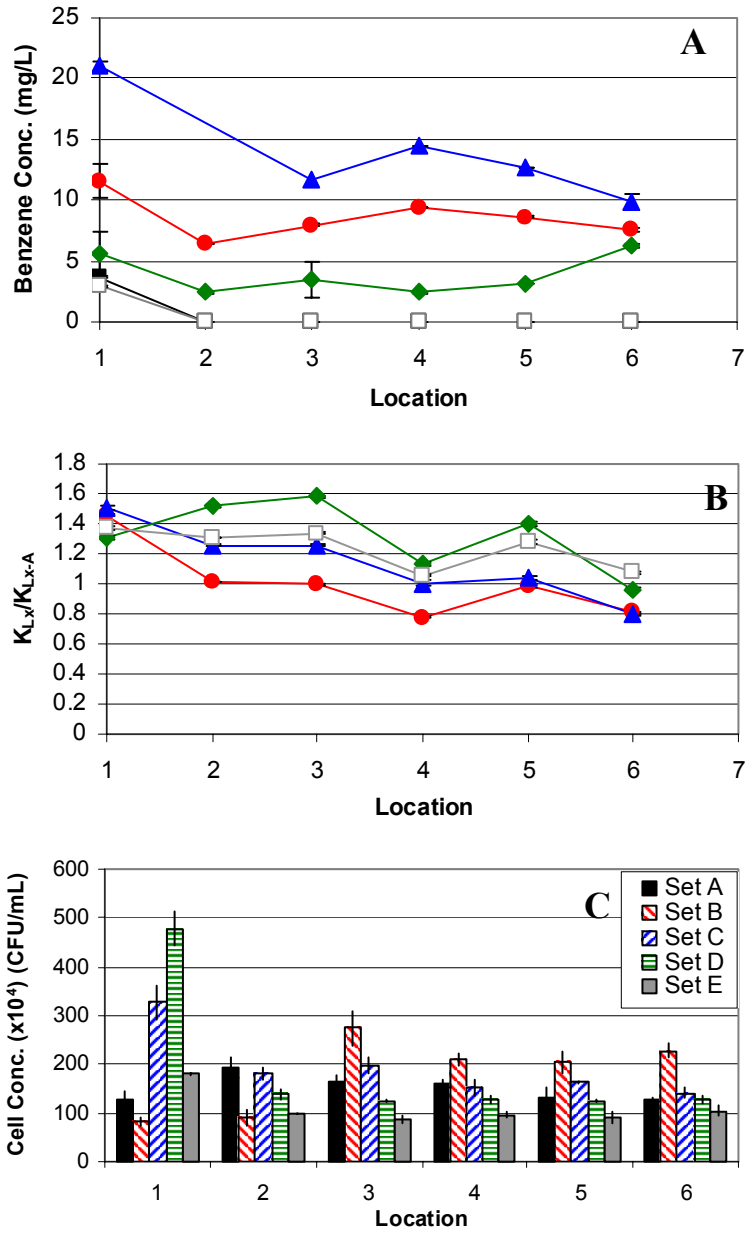

Figure 5.33. Benzene perturbation experiment on day 241 showing (A) benzene concentration per set; error bars indicate the standard deviation of triplicate samples (B) normalized K^+ per port, where each set is normalized by set A per port; error bars indicate the standard deviation of triplicate analysis; and (C) HPC per port; error bars indicate the standard deviation of counts from triplicate plates. For graphs A and B: set A (■); set B (●); set C (▲); set D (♦); and set E (□).

Similar to the benzene perturbation experiment on day 227, K^+ and HPC comparisons show evidence of concurrent planktonic bacteria increase and K^+ concentration decrease at early ports during the initial phase (set B) of the benzene perturbation on day 241. Set B HPC and K^+ comparisons show K^+ concentrations decreased between ports L1 and L2, with K^+ concentrations steady between ports L2 and L3, while planktonic bacteria concentrations were steady between L1 and L2 and increase between L2 and L3 (Figure 5.35B). HPC and K^+ comparisons of sets A, C, and E show no trends for K^+ decrease with planktonic bacteria increase (Figures 5.35A and 5.35C). Set D, however, showed a concurrent increase in K^+ and decrease in planktonic bacteria concentrations between ports L1 and L3 (Figure 5.35C), strongly supporting K^+ efflux due to cell lysis. K^+ and HPC difference data for Figures 5.35A-C are located in Appendix I-Table I.13.

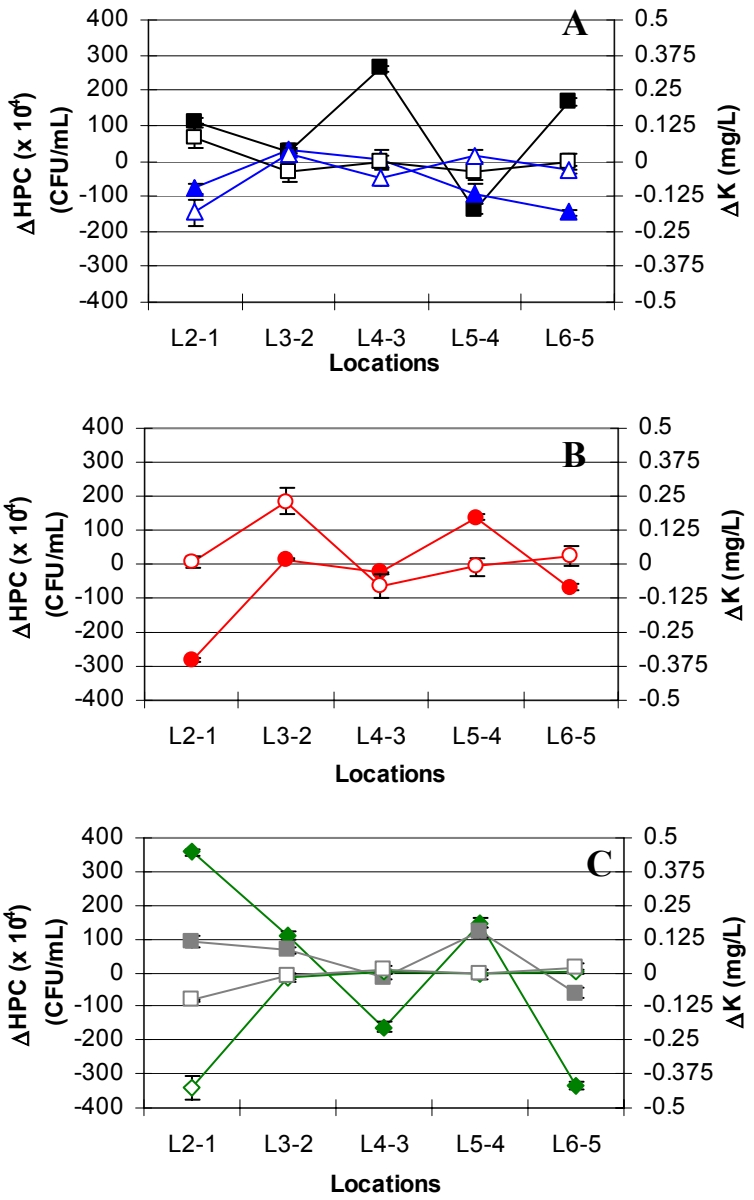

Figure 5.35. Benzene perturbation experiment day 241 HPC (open symbols) and K^+ (closed symbols) difference between ports (L x - L (x-1)) (A) sets A (■) and C (▲); (B) set B (●); and (C) sets D (♦) and E (□). Error bars indicate the standard deviation of the difference; some are within the symbol size.

5.5.2 PCP Perturbation

PCP perturbation experiments were conducted on days 218 and 233. The PCP experiment performed on day 218 used a positive air pressure with the removal of 4

sample sets (Table 5.6), while the second perturbation on day 233 used a positive oxygen pressure over the SC media bottles and included a fifth sample set (set E). PCP concentration samples were removed immediately after HPC, K^+ and DOC samples were removed. The DO profile along the column was measured on day 267 showing DO concentrations of at least 0.8 mg/L at all ports (Figure 5.36, Appendix J-Table J.1). The large decrease in DO between ports L1 and L2 suggest that oxidative uncoupling was an ongoing process throughout experimentation, even at PCP concentrations of 3 mg/L.

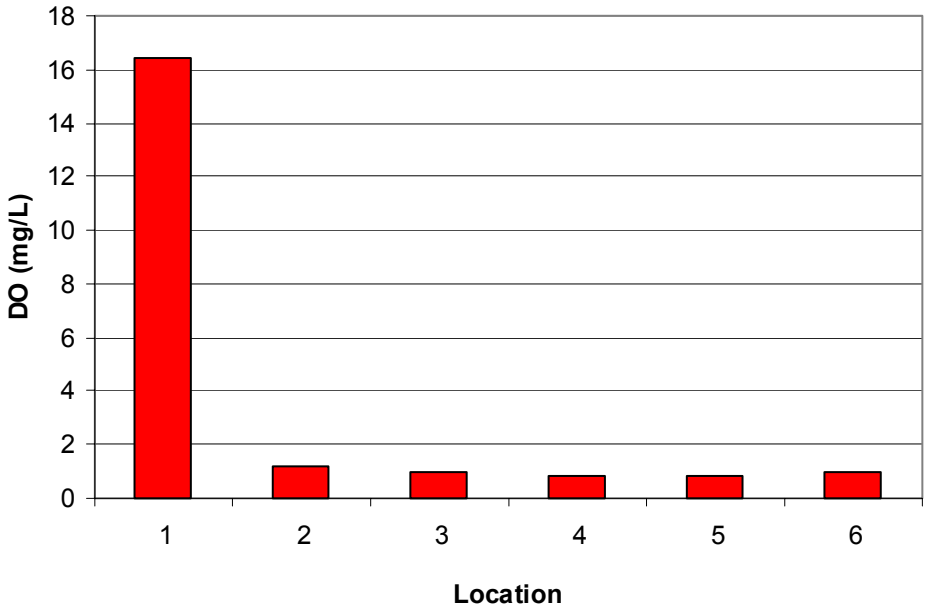

Figure 5.36. DO profile of PCP column on day 267, with positive oxygen pressure over SC-benzene media bottle. The DO at port L1 was greater than 16.4 mg/L, but could not be measured above the maximum measurement of the DO meter.

Table 5.6. Sample removal times for PCP perturbation experiment on day 218.

Liquid Port	HRT_{mean}[a] (hr)	Time of Sample Removal (hr)								
		Set A		*Set B*		*Set C*		*Perturb Bottle Removed*	*Set D*	
		HPC, DOC, K	PCP	HPC, DOC, K	PCP	HPC, DOC, K	PCP		HPC, DOC, K	PCP
1	1.11 - 1.24	Before Start		0.51	0.54	1.01	1.01	2.47	3.14	3.18
2	1.21 - 1.34			0.68	0.71	1.34	1.37		3.34	3.37
3	1.38 - 1.50			0.86	0.89	1.66	1.69		3.55	3.59
4	1.55 - 1.68			1.18	1.22	2.00	2.07		3.72	3.75
5	1.73 - 1.86			1.50	1.55	2.17	2.21		3.85	3.89
6	1.91 - 2.04			1.84	1.87	2.32	2.36		4.04	4.08

[a]HRT_{mean} values apply to set B and were calculated by subtracting the expected HRT between liquid ports from each of duplicate HRT_{mean} values obtained from tracer studies. The expected flow rate of 2.8 mL/min was used, and HRT_{mean} values per port do not account for sample volumes removed from previous ports.

PCP concentration data from the PCP perturbation experiment on day 218 show that the first set that reflected PCP perturbation was set B, followed by the highest PCP concentrations in set C (Figure 5.37A). Set D, taken after the perturbing PCP feed was removed, showed lower PCP concentrations than sets B and C, but does show higher PCP concentrations than baseline (3 mg/L target) PCP concentrations (Figure 5.37A, Appendix J-Table J.3). This indicates that the expected HRT (HRT_{calc}) of the column was different from reality, and was influenced by the liquid volumes removed for samples. Set A showed a removal of 10.2 % PCP between ports L1 and L6 (Figure 5.37A), but this removal could not be attributed to biodegradation due to the results from the preliminary biodegradation experiments (see section 5.1.2). Sorption is the suspected source of PCP removal within the column, given the log k_{ow} = 5.01 (Hickman and Novak, 1984) for PCP, which is highly hydrophobic.

The effluent dissolved oxygen was found to decrease over the course of the experiment (Figure 5.38, Appendix J-Table J.4). The initial DO started at 2 mg/L, and steadily declined to 0 mg/L DO by the end of the PCP experiment on day 218 (Figure 5.38). The previous effluent DO measurement of 0.3 mg/L was made on day 205, which

along with day 218 was when positive air pressure was used over the SC media feed. The steady decrease in effluent DO prior to the HRT_{mean} of 2.37 cannot be explained. Nonetheless, the lack of effluent DO after 2.37 hours could have been caused by the oxidative uncoupling effect of high concentrations of PCP (Bhandari *et al.*, 1997; Hickman and Novak, 1984). Oxidative uncoupling occurs when anionic and neutral forms of a compound, such as PCP, interrupt the proton motive force by shuttling electrons across energy transducing membranes, forcing the bacterial cell to reestablish the proton motive force by increasing respiration (Escher *et al.,* 1999, Escher *et al.*, 1996, and Hickman and Novak, 1984). In support of the occurrence of oxidative uncoupling, increased oxygen uptake was seen during oxygen uptake rate (OUR) experiments when 20 mg/L PCP was applied to cultured planktonic bacteria from the PCP column when compared to the same culture without PCP application (Appendix J-Table J.2).

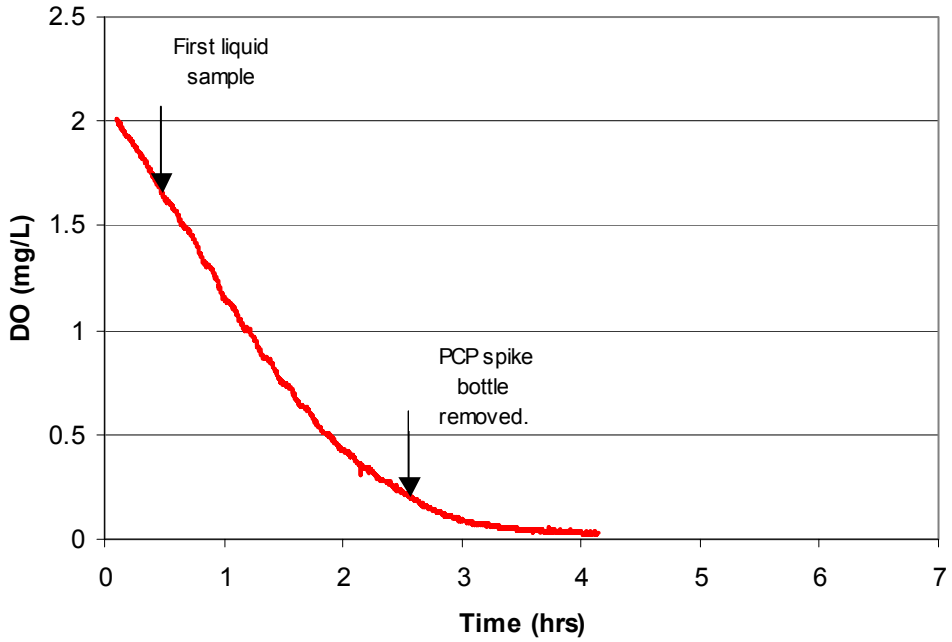

Figure 5.38. Effluent DO concentration during PCP perturbation experiment on day 218.

Figure 5.37B shows an increase in normalized potassium ($K_{Lx}/K_{Lx\text{-}A}$) at ports 1 and 2 between sets C and B and sets C and D, which correlate with PCP concentrations greater than 15 mg/L. Additionally, sets B and D at port L3 were found to be statistically different (Figure 5.37B), possibly indicating an elevation in K^+ as initial perturbing PCP concentrations flowed through the column. Ports L5 through L6 between sets C (greatest PCP concentration) and D (lowest PCP concentration after perturbation) do not show statistically different normalized potassium values, which suggest a lack of GGKE activation at greater column depths. K^+ normalized K^+ data for the PCP perturbation experiment on day 218 are located in Appendix J-Table J-5.

HPC data indicate a mild increase of planktonic bacteria as the perturbation feed flowed through the column during the initial perturbation period, set B. HPC data showed a statistically significant increase of 21% and 74% from set A to set B at ports 2 and 6 ($t_{obs}(4df)$=L2: 3.682; L6: 3.442 > $\alpha_{0.025}(4df)$=2.776) (Figure 5.37C). Planktonic cell concentrations tended to decrease slightly from set B to C, and to an even greater degree from set C to D (Figure 5.37C), indicating a temporal decrease in biofilm detachment or planktonic bacterial growth. The decrease in planktonic bacteria may be due to PCP toxicity or biofilm release exhaustion after set B at port L2. HPC data are located in Appendix J-Table J.6.

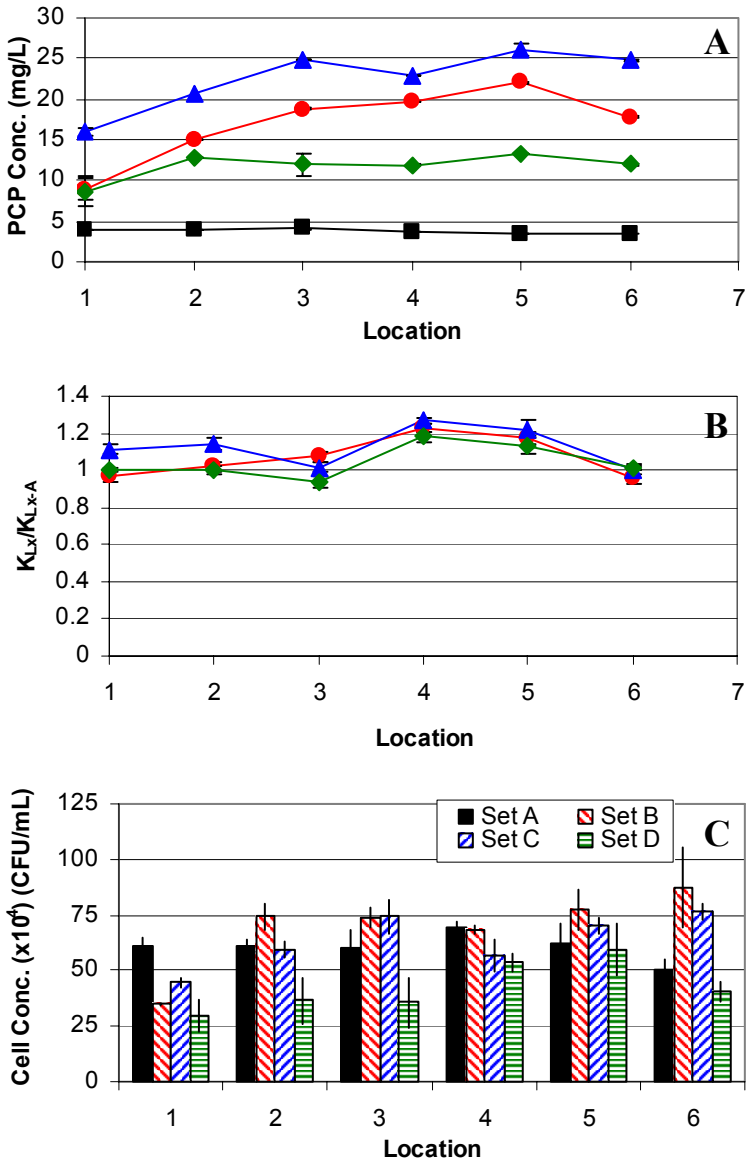

Figure 5.37. PCP perturbation experiment day 218 (A) PCP concentration per port; error bars indicate the standard deviation of duplicate samples; (B) normalized K^+ per port, where each set was normalized by set A per port; error bars indicate the uncertainty in the quotient from triplicate analysis; and (C) HPC per port; error lines indicate the standard deviation of counts from triplicate plates. Some error bars are within the symbol size.

HPC and K^+ comparisons indicate an increase in K^+ and planktonic bacteria concentrations at early port locations after perturbing PCP concentrations were added on day 218. The concurrent increase in K and HPC was seen in sets B, C, and D between ports L1 and L2 (Table 5.7). Within set B, the K^+ concentration increase was 10% and

12% between ports L1 and L2, and between ports L2 and L3, respectively (Table 5.7). The greatest increases in planktonic bacteria concentration were seen in set B between L1 and L2 at 114%, but were only 32% and 25% between the same ports in sets C and D, respectively. No correlations between planktonic bacteria and K^+ concentrations were found in set A, in sets B and C after port L3, or in set D after port L2. This suggests that the perturbing PCP concentrations activated the GGKE response, increasing K^+ and influencing biomass detachment at low column depths, and that a secondary stress response may have been occurring at greater column depths to cause biomass detachment without concurrent K^+ efflux. K^+ and HPC difference data for Table 5.7 are located in Appendix J-Table J.7.

Table 5.7. PCP perturbation experiment day 218 K+ and HPC differences between ports (Lx – (Lx-1) within each set.

Change between ports	Sample Type	Set		
		B	C	D
L2 - L1	ΔK^+ (mg/L)	0.17	0.14	0.08
	ΔHPC (CFU/mL)	3.97E+05	1.43E+05	7.33E+04
L3 - L2	ΔK^+ (mg/L)	0.21	-0.12	-0.01
	ΔHPC (CFU/mL)	-6.67E+03	1.53E+05	-1.00E+04

The second PCP perturbation experiment was performed 15 days after the first. The PCP perturbation experiment on day 233 included positive O_2 bottle pressure, and a fifth sample set E. Sample removal times are shown in Table 5.8.

Table 5.8. Sample removal times for PCP perturbation experiment on day 233.

Liquid Port	HRT_{mean} [a] (hr)	Time of Sample Removal (hr)										
		Set A		*Set B*		*Set C*		*Perturb Bottle Removed*	*Set D*		*Set E*	
		HPC, DOC, K	PCP	HPC, DOC, K	PCP	HPC, DOC, K	PCP		HPC, DOC, K	PCP	HPC, DOC, K	PCP
1	1.11 - 1.24	-1.00	-0.93	0.54	0.57	1.01	1.06	2.50	2.99	3.03	5.01	5.04
2	1.21 - 1.34	-0.81	-0.78	0.67	0.71	1.35	1.40		3.18	3.23	5.18	5.21
3	1.38 - 1.50	-0.66	-0.61	0.84	0.89	1.70	1.74		3.35	3.39	5.34	5.38
4	1.55 - 1.68	-0.49	-0.43	1.20	1.23	2.00	2.03		3.51	3.55	5.50	5.54
5	1.73 - 1.86	-0.33	-0.25	1.53	1.57	2.19	2.22		3.67	3.71	5.66	5.70
6	1.91 - 2.04	-0.15	-0.11	1.84	1.88	2.35	2.38		3.85	3.88	5.86	5.93

[a]HRT_{mean} values apply to set B and were calculated by subtracting the expected HRT between liquid ports from each of duplicate HRT_{mean} values obtained from tracer studies. The expected flow rate of 2.8 mL/min was used, and HRT_{mean} values per port do not account for sample volumes removed from previous ports.

The first set showing high PCP concentration was set B (Figure 5.39A). The decrease in PCP concentration in set B at ports L2 through L4 is possibly due to the staggered method of sample collection started after set B port L3 sampling. Set C port L1 samples, the first 30 minute PCP exposure sample, was retrieved after sample L3-set B, allowing the leading edge of the perturbing PCP concentrations to flow past port L3 to port L4. The post-perturbation samples on day 233 showed that perturbing PCP concentrations greater than 10 mg/L remained in the column during set D, which was similar to the PCP perturbation on day 218, and were between 7.2 and 4.6 mg/L in set E (Figure 5.39A, Appendix J-Table J.8).

The decrease in DO seen in the effluent DO data during the PCP perturbation experiment on day 233 give additional support of an uncoupling response occurring as a result of the perturbing PCP concentrations. Similar to day 218, the effluent DO from the PCP perturbation experiment on day 233 showed a gradual decrease from 0.3 mg/L to 0 mg/L between 0 and 2 hrs, during which no perturbing PCP concentration had yet reached the effluent (Figure 5.40). However, the effluent DO remained undetectable as perturbing PCP concentrations reached the effluent, which provides additional support of

the hypothesis that oxidative uncoupling occurred. PCP perturbation DO data from day 233 is located in Appendix J-Table J.9.

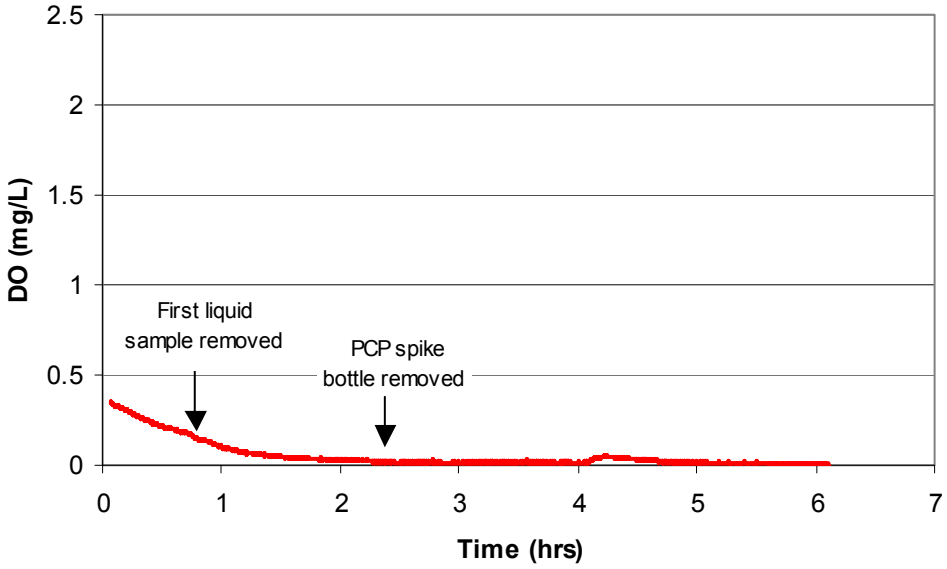

Figure 5.40. Effluent DO concentration during PCP perturbation experiment on day 233.

Figure 5.39B shows that an increase in K^+ occurred in sets B at L2, L3, L5, and L6. The K^+ values normalized by set A at each port showed set B to have the highest elevated K^+ of all sets, followed by set C at ports L2, L4, L5, and L6. This indicates that potassium was elevated during sets B and C at ports L2 and L3 within the sand zone, suggesting K^+ efflux may have occurred for almost 30 minutes. PCP perturbation experiment K^+ and normalized K^+ data from day 233 are located in Appendix J-Table J.10.

HPC data showed evidence of increased planktonic bacteria as perturbing PCP concentrations reached greater depths of the sand column. The increase in planktonic bacteria of 81% was seen at port L6 during set B, with additional increases of 61% and 77% seen in set C at ports L3 and L4 (Figure 5.39C, Appendix J-Table J.11). The

increase in HPC at L3 and L4 in set C correspond with PCP concentrations that were higher than in set B. Planktonic bacteria concentrations decreased below pre-perturbation concentrations as PCP concentrations decreased over time within the column (Figure 5.39C; sets D and E). This decrease in planktonic cell concentrations is possibly due to toxicity by PCP. In addition, HPC data suggest that day 218 PCP perturbation experiment continued to inhibit the biomass based on much lower planktonic bacterial concentration seen prior to perturbation in set A on day 233. A comparison of HPC data from days 218 and 233 at set A show 47.8% fewer planktonic bacteria in the sand zone on day 233.

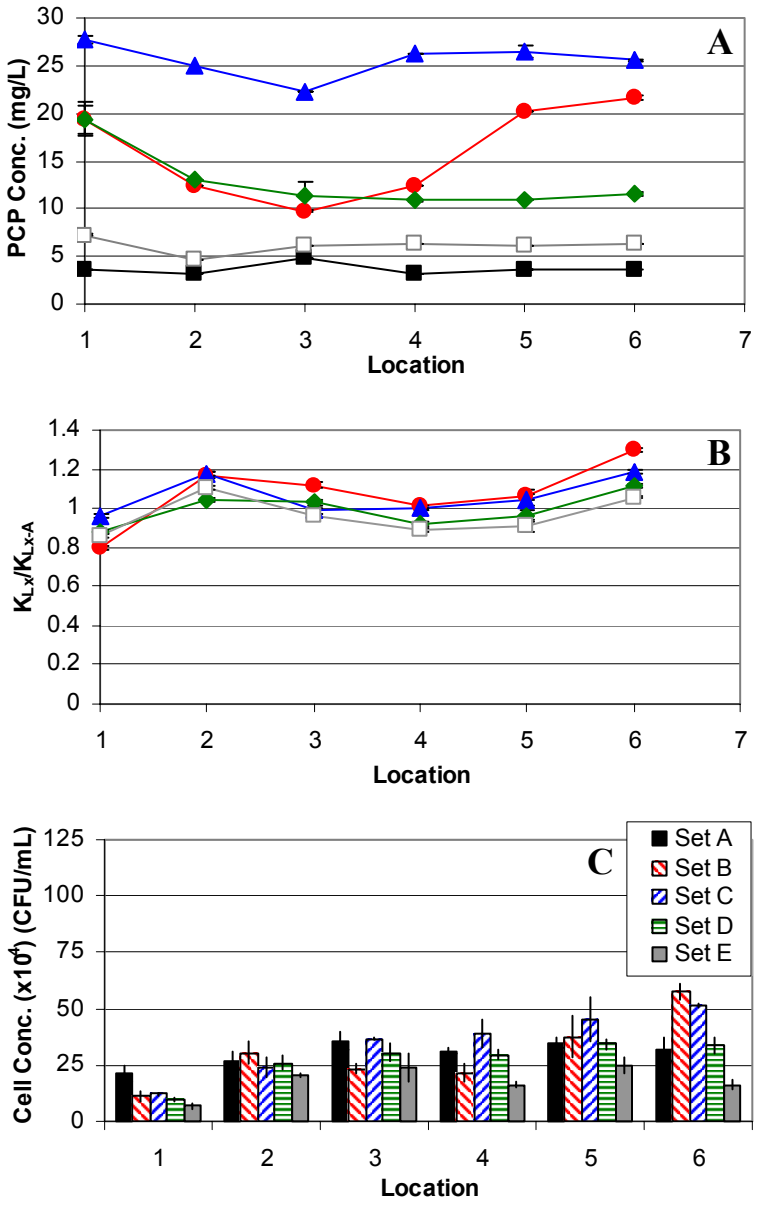

Figure 5.39. PCP perturbation experiment day 233 (A) PCP concentration per port for all sets; error bars show range of duplicate samples; (B) K^+ data per port (Lx) were normalized using each respective set A (Lx-A) potassium concentration; error bars show the range of uncertainty in the normalized data from triplicate analysis; and (C) HPC data for all ports in each sample set; error bars indicate the standard deviation of counts from triplicate plates. Some error bars are within the symbol size. For graphs A and B: set A (■); set B (●); set C (▲); set D (♦); and set E (□).

HPC and K^+ comparisons show evidence to further support a concurrent increase in K^+ and planktonic bacteria concentrations at early ports during the PCP perturbation

experiment on day 233. Sets B, C, D, and E show a synchronous increase in K^+ and planktonic bacteria concentrations between ports L1 and L2 (Table 5.7b). The increase in K^+ concentration may be due to a release of K^+ from attached and planktonic biomass. An increase of 0.2 mg/L is seen during set B between ports L1 and L2, which contained the highest protein concentration in the PCP column, and between ports L5 and L6, which showed the greatest planktonic bacteria concentration during set B (Table 5.7b). This suggests that the larger increases of K^+ were seen at ports with the greatest biomass concentration. K^+ and HPC difference data from the PCP column perturbation on day 233 for Table 5.7b are located in Appendix J-Table J.12.

Table 5.9. PCP perturbation experiment day 233 K+ and HPC differences between specific ports (Lx – (Lx-1) within each set.

Change between ports	Sample Type	Set			
		B	C	D	E
L2 - L1	ΔK^+ (mg/L)	0.46	0.18	0.11	0.25
	ΔHPC (CFU/mL)	1.90E+05	1.14E+05	1.65E+05	1.35E+05
L6 - L5	ΔK^+ (mg/L)	0.14	0.00	0.04	0.04
	ΔHPC (CFU/mL)	2.07E+05	6.33E+04	-6.67E+03	-8.77E+04

5.5.3 Cadmium Perturbation

Three Cd perturbation experiments were performed on days 220, 238, and 270. All SC media perturbation feed was prepared with a target concentration of 25 mg/L Cd. Table 5.10 shows a listing of all changes of positive pressure over media bottles, the type of media buffer, and whether pH was measured during each Cd perturbation experiment. Twelve milliliters of sample were remove for all samples, and was distributed to different vials for HPC, K^+, DOC, and cadmium samples during each Cd perturbation experiment. In addition, a DO profile of the Cd column was made on day 267 to determine the DO decrease over the column when an oxygen positive pressure was applied to the Cd SC media feed bottle (Figure 5.41, Appendix K-Table K.1). Prior to perturbation experiments, OUR experiments showed that 25 mg/L Cd would inhibit Cd biomass by 37%, although the column was only inhibited by 11% based on 5.5 mg/L obtained within the column during perturbations on days 220 and 238, and 19% on day 270 when 11.5 mg/L Cd was reached within the column (Appendix K-Table K.2).

Table 5.10. Altered parameters for all Cd perturbation experiments.

Condition	**Cd Experiment Day**		
	220	*238*	*270*
Positive Pressure	air	O_2	O_2
Media Buffer	N/A	N/A	Tris - HCl
pH Measurement?	no	yes	yes

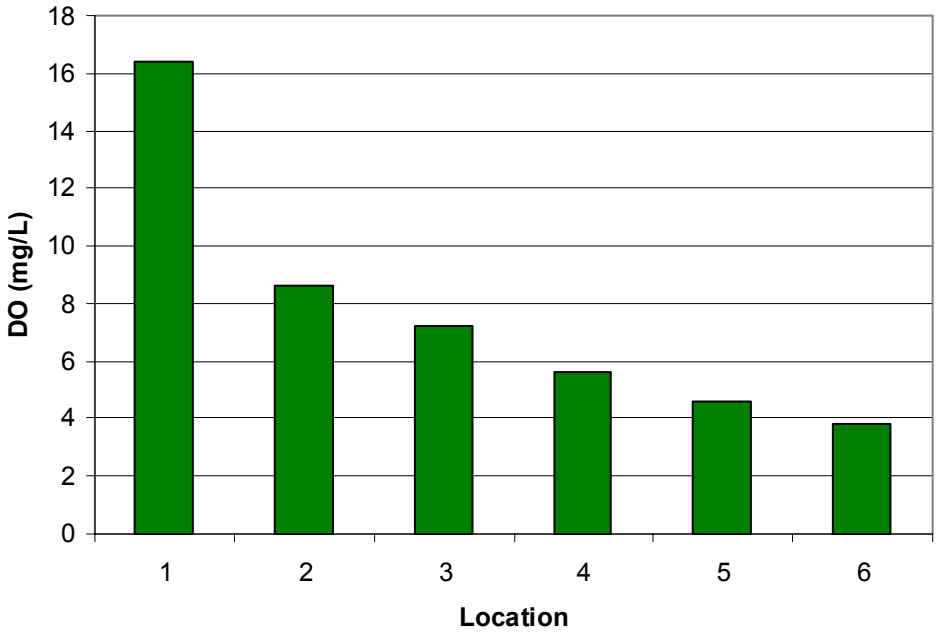

Figure 5.41. DO profile of Cd column with SC media feed under positive O_2 pressure on day 267. The DO at port L1 was greater than 16.4 mg/L, but could not be measured above the maximum measurement of the DO meter.

The first Cd perturbation was performed on day 220, and had air as a positive pressure over the SC media bottles, and four sample sets were taken. The SC buffer was removed from the perturbation media feed due to media precipitation problems with the high phosphate concentration of the pH 7.8 buffer, and high Cd concentration. Table 5.11 provides the sample removal and bottle change times for the first cadmium perturbation experiment.

Table 5.11. Sample removal times for Cd perturbation experiment on day 220.

Liquid Port	HRT_{mean}[a] (hr)	Time of Sample Removal (hr)				
		Set A	*Set B*	*Set C*	*Perturb Bottle Removed*	*Set D*
		HPC, DOC, K, Cd	HPC, DOC, K, Cd	HPC, DOC, K, Cd		HPC, DOC, K, Cd
1	1.24 - 1.27	Before Start	0.66	1.18	2.65	3.34
2	1.34 - 1.36		0.85	1.50		3.51
3	1.50 - 1.53		1.01	1.84		3.67
4	1.68 - 1.71		1.35	2.17		3.83
5	1.86 - 1.89		1.67	2.33		4.00
6	2.04 - 2.06		2.00	2.49		4.17

[a]HRT_{mean} values apply to set B and were calculated by subtracting the expected HRT between liquid ports from each of duplicate HRT_{mean} values obtained from tracer studies. The expected flow rate of 2.8 mL/min was used, and HRT_{mean} values per port do not account for sample volumes removed from previous ports.

The first set showing high Cd concentrations throughout the Cd sand column was set D, but the higher concentrations were found at port L1 in sets B and C (Figure 5.42A, Appendix K-Table K.3). Set D showed the greatest Cd concentration of 5.7 mg/L at port L3, although the target perturbation concentration was 25 mg/L Cd. The port L1-sets B and C Cd concentrations indicate that perturbing Cd concentrations reached the column, but did not infiltrate up to port L2, and were more than 1.0 mg/L below concentrations measured in set A (Figure 5.42A). The inability to detect Cd in the sand zone and the decrease in soluble Cd concentration after set A may have occurred for two reasons: (1) Cd precipitated with 0.01 M phosphate in the buffered SC media before perturbation as the two feeds mixed in the influent end cap and sand zone before port L2; or (2) Cd complexed with negatively charged sites on carbohydrate and protein compounds in EPS (Pümpel and Paknikar, 2001; Vig *et al.*, 2003).

The effluent DO data show strong evidence of biomass inhibition based on the sharp effluent DO increase. The effluent DO began to rise at 2.4 hrs into the Cd perturbation experiment, and peaked at 2.6 mg/L at 4.75 hrs, then immediately decreased

below 0.5 mg/L within 45 minutes of peaking (Figure 5.43, Appendix K-Table K.4). The increase in effluent DO was initiated at 2.4 hrs, which is approximately the HRT required for the initial perturbing Cd concentrations during set B to reach the effluent (Appendix I-Table I.2). It is likely the high initial Cd concentrations during set B caused an inhibition effect on the biomass.

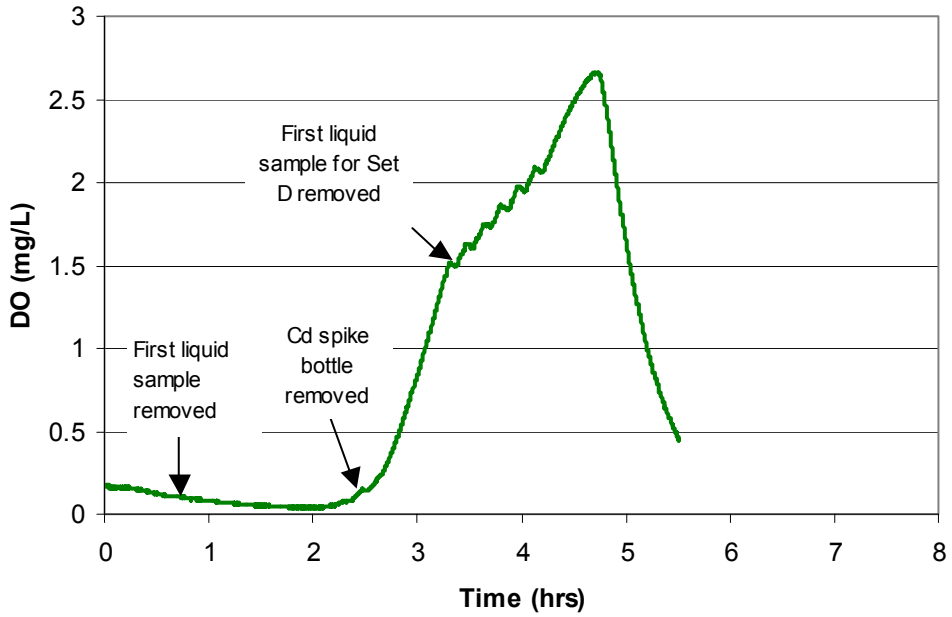

Figure 5.43. Effluent DO concentration during Cd perturbation experiment on day 220.

The K^+ data show strong evidence of K^+ efflux at early column locations during the day 220 Cd perturbation experiment. The K^+ data shown in Figure 5.42B show a K^+ release of 28% between L1 and L2 during set D; the first set showing high Cd concentrations throughout the column profile. Extracellular K^+ was also found to increase by 17% from port L1 to port L5 in set C (Figure 5.42B). Set B showed a K^+ decrease or uptake of 69% between ports L1 and L5, with an increase of 0.6 mg/L K^+

(36%) between L5 and L6 (Figure 5.42B). Set A is not presented due to positive K^+ contamination, therefore K^+ could not be normalized by set A to determine increased K^+ set trends. This strongly suggests that K^+ efflux occurred as high Cd concentrations reached the biomass zone in the Cd column. Cd perturbation K^+ and normalized K^+ data from day 220 are located in Appendix K-Table K.5.

HPC data indicate an increase in planktonic cells occurred during the initial Cd perturbation experiment on day 220, but was not seen when perturbing Cd concentrations were found throughout the column. An increase of 60% and 45% was seen between sets A and B at L1 and L2, respectively (Figure 5.42C, Appendix K-Table K.6). Interestingly, the highest planktonic bacteria concentration was found during set A at L4. This indicates that the Cd column biomass reacted to high concentrations of Cd between port L1 and L2, most likely related to Cd precipitation reactions before soluble Cd concentrations were seen throughout the column (set D). Cd precipitation was found to occur when 25 mg/L Cd was added to 0.01 M phosphate buffered SC media, suggesting that a Cd precipitate formed as the leading edge of the un-buffered Cd SC media interacted with phosphate buffered pre-perturbation feed in the influent end cap and sand zone before port L2. In addition, planktonic bacterial concentrations were statistically lower between set B and C at ports L1 through L5 (t_{obs}(4df)= L1: 18.366; L2: 5.398; L3: 16.800; L4: 14.945; L5 9.430 > $\alpha_{0.025}$(4df)= 2.776), further indicating that planktonic bacterial release was impeded possibly due to precipitation or Cd-EPS complexing within the column.

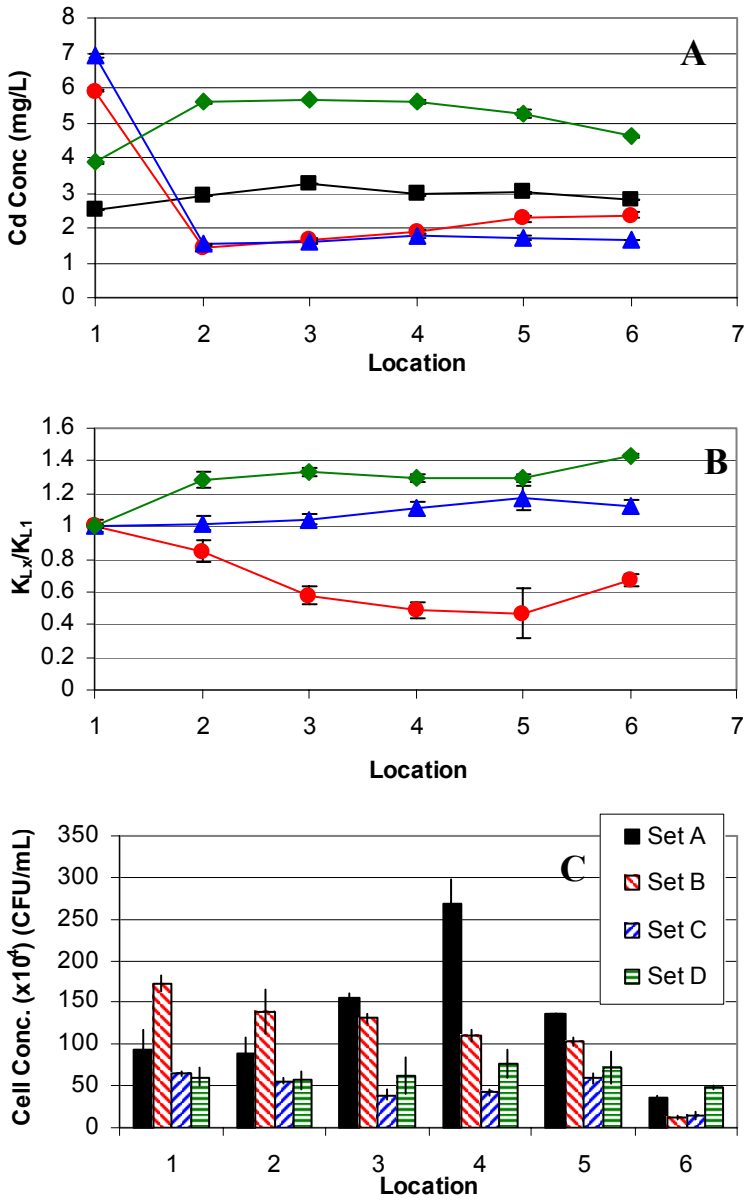

Figure 5.42. Cd perturbation experiment on day 220 (A) Cd concentration per port for all sample sets; error bars indicate the standard deviation of triplicate analysis; (B) K^+ data per port (Lx) were normalized using the influent (L1) K^+ concentration; error bars show the range of uncertainty in the normalized data from triplicate analysis; (C) HPC data for all ports; error bars indicate the standard deviation of triplicate plating. Some error bars are within the symbol size. For graphs A and B: set A (■); set B (●); set C (▲); and set D (♦).

HPC and K^+ comparisons show K^+ concentrations increased at early ports in set D without large changes in planktonic bacteria concentrations as perturbing Cd

concentrations were measured in the sand zone of the column on day 220 (Table 5.12). Sets B and C showed no concurrent increase in K^+ and HPC, although set C did show a steady increase in K^+ between ports L1 and L5 (Table 5.12). This suggests that the Cd column was impacted by high Cd concentrations while Cd was only detected at port L1, and is possibly related to chemical reactions that initially decreased the Cd concentration within the column. K^+ and HPC difference data from the Cd perturbation experiment on day 220 for Table 5.12 are located in Appendix K-Table K.7.

Table 5.12. Cd perturbation experiment day 220 K^+ and HPC differences between specific ports (Lx – (Lx-1) within each set.

Change between ports	Sample Type	Set		
		B	C	D
L2 - L1	ΔK^+ (mg/L)	-0.25	0.04	0.48
	ΔHPC (CFU/mL)	-3.40E+05	-8.67E+04	-3.67E+04
L3 - L2	ΔK^+ (mg/L)	-0.44	0.04	0.08
	ΔHPC (CFU/mL)	-8.67E+04	-1.63E+05	6.00E+04
L4 - L3	ΔK^+ (mg/L)	-0.15	0.11	-0.07
	ΔHPC (CFU/mL)	-2.00E+05	2.67E+04	1.43E+05
L5 - L4	ΔK^+ (mg/L)	-0.03	0.12	0.01
	ΔHPC (CFU/mL)	-7.67E+04	1.73E+05	-4.67E+04
L6 - L5	ΔK^+ (mg/L)	0.34	-0.09	0.22
	ΔHPC (CFU/mL)	-9.07E+05	-4.43E+05	-2.43E+05

The second Cd perturbation experiment was performed on day 238. A positive O_2 pressure was applied to the SC media feed bottles. An additional sample set (E) was added to the end of the perturbation experiment, following the perturbation bottle removal and after set D. The SC buffer was again removed to circumvent Cd precipitation problems, and pH measurements were taken with each sample during all

sets to determine pH fluctuations. Table 5.13 provides the sample removal times during the Cd perturbation on day 238.

Table 5.13. Sample removal times for Cd perturbation experiment on day 238.

Liquid Port	HRT_{mean}[a] (hr)	Time of Sample Removal (hr)					
		Set A	*Set B*	*Set C*	*Perturb Bottle Removed*	*Set D*	*Set E*
		HPC, DOC, K, Cd	HPC, DOC, K, Cd	HPC, DOC, K, Cd		HPC, DOC, K, Cd	HPC, DOC, K, Cd
1	1.24 - 1.27	-1.00	0.69	1.18	2.64	3.39	5.18
2	1.34 - 1.36	-0.81	0.85	1.50		3.53	5.36
3	1.50 - 1.53	-0.67	1.01	1.86		3.69	5.50
4	1.68 - 1.71	-0.50	1.34	2.18		3.85	5.68
5	1.86 - 1.89	-0.33	1.67	2.33		4.00	5.88
6	2.04 - 2.06	-0.17	2.03	2.51		4.17	6.04

[a]HRT_{mean} values apply to set B and were calculated by subtracting the expected HRT between liquid ports from each of duplicate HRT_{mean} values obtained from tracer studies. The expected flow rate of 2.8 mL/min was used, and HRT_{mean} values per port do not account for sample volumes removed from previous ports.

Comparable to the first Cd perturbation experiment on day 220, the second Cd experiment on day 238 showed a lack of sustained high Cd concentrations in set B; the first set taken during cadmium perturbation. The first high cadmium concentration was found in set B at L1, and then again in set C at L1 and L2, but these high concentrations did not continue through the column and were well below the 25 mg/L target. Set D showed the highest cadmium concentrations in the column profile during the day 238 experiment, which reached Cd concentrations similar to those attained during the day 220 Cd perturbation experiment (Figure 5.44A, Appendix K-Table K.8).

The effluent DO data showed strong evidence to support that toxicity by Cd occurred as the initial perturbing concentrations interacted with the column biofilm. The effluent DO was initially 0 mg/L until 2 hours into the experiment, at which time the DO increased to $\geq$16.4 mg/L at t= 4.18 hours (Figure 5.45). This increase in effluent DO occurred slightly later than the expected HRT (HRT_{calc} = 1.94) predicted, but was within a 10% range. The DO reached the maximum detectable concentration at 16.4 mg/L DO.

Therefore, it is likely that the effluent DO was greater then 16.4 mg/L until t = 4.9 hours, when the effluent DO decreased until it reached 0.2 mg/L DO at the end of the experiment (t = 7.2 hours) (Figure 5.45, Appendix K-Table K.9).

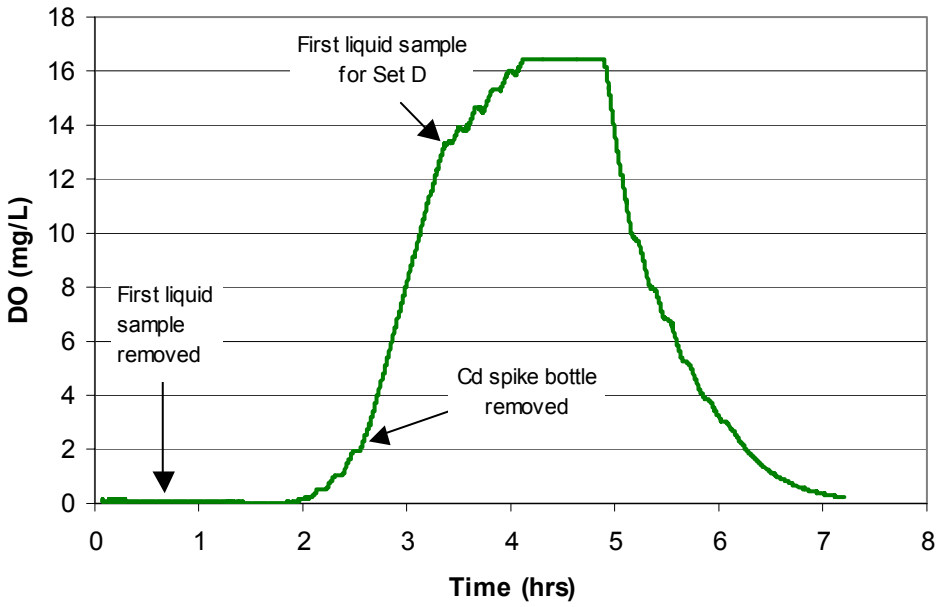

Figure 5.45. Effluent DO concentration during Cd perturbation experiment on day 238.

The lack of a pH buffer in the Cd perturbation media caused pH to become a second experimental variable during the Cd perturbation experiments on day 238. It is also assumed that pH was variable in the experiment on day 220 based on the day 238 pH data. The pH profiles show set A to be constant, which is due to the normal buffered SC media solution (Figure 5.46). Subsequently, sets B, and C showed a pH range of 0.4 and 1.3 units, respectively (Figure 5.46, Appendix K-Table K.10). Bacteria require a narrow range for intracellular pH, 7.8 to 7.6 for *E. coli* (Ferguson *et al.*, 1995), so changes to external pH may have important implications for bacteria, requiring regulation of

intracellular pH that is affected by extracellular pH fluctuations. Regulation of intracellular pH may be performed by various mechanisms: (1) decreased membrane permeability; (2) internal buffering; and (3) proton efflux/influx (Dilworth and Glenn, 1999).

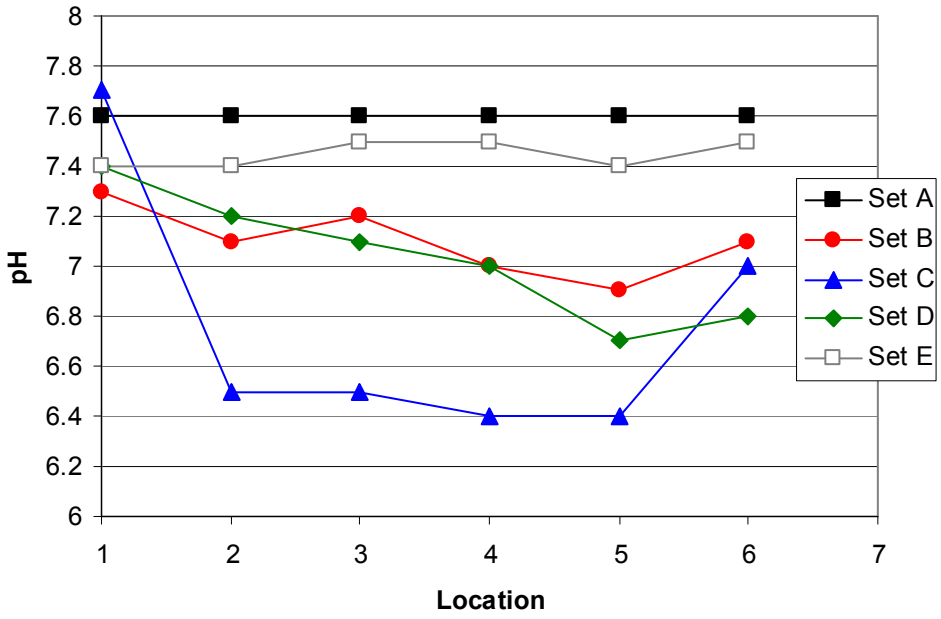

Figure 5.46. pH per port for all sets during the cadmium perturbation on day 238.

K^+ normalization with set A ($K_{Lx}/K_{Lx\text{-}A}$) showed an increase in K^+ corresponding to increases in Cd concentration at port L2 in set compared to set E, and in set D at ports L2 and L3, compared to set E (Figure 5.44B). This suggests that K^+ efflux occurred in response to increases in Cd concentration in the sand zone at early ports. Interestingly, both Cd experiments (days 220 and 238) showed an unexplained K^+ uptake occurred in set B. Cd perturbation experiment day 238 K^+ and normalized K^+ data are located in Appendix K-Table K.11.

HPC data indicate that planktonic bacteria concentrations increased when perturbing Cd concentrations were measured in the sand zone of the column; set D. Fewer planktonic bacteria are seen between sets B and C, and are followed by an average increase of 141 % in planktonic bacteria concentrations at early ports (L1 – L4) between sets C and D (Figure 5.44C, Appendix K-Table K.12). The average planktonic cell concentrations in sample set A from the Cd perturbation experiment on day 238 decreased by 69% after the Cd perturbation experiment on day 220. This indicates that the first Cd perturbation experiment caused some toxicity to the biomass in the column.

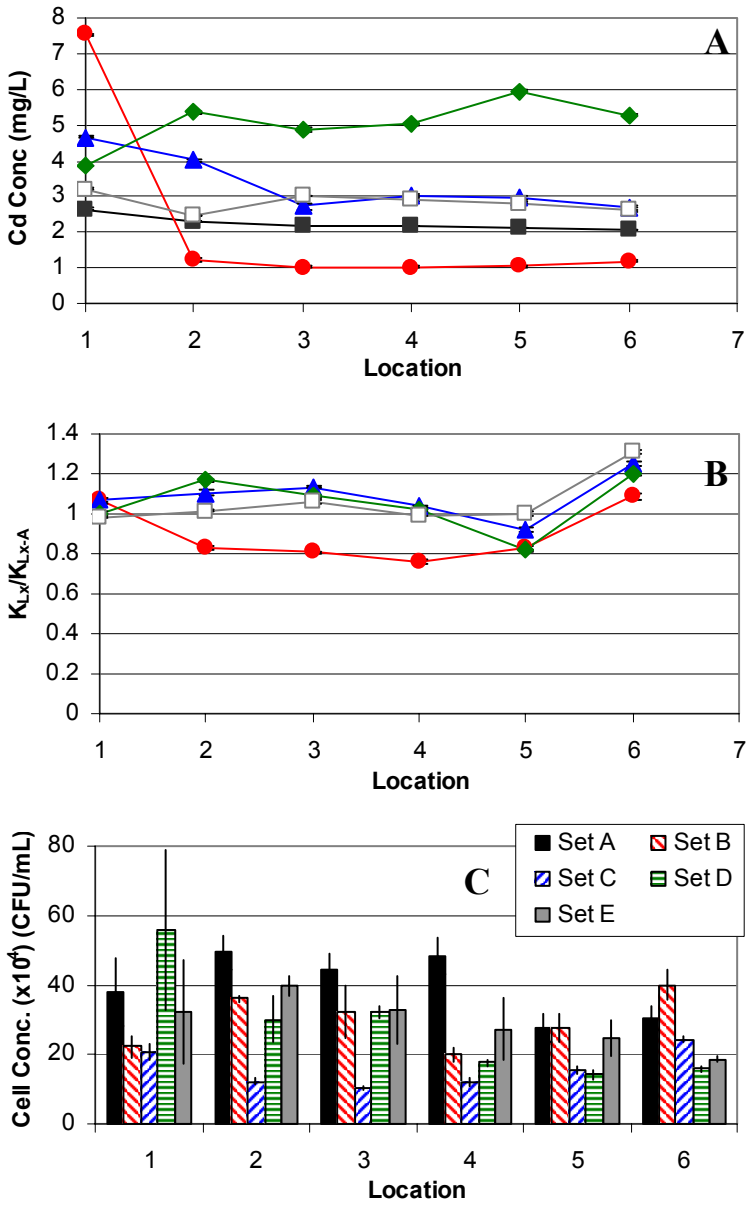

Figure 5.44. Cd perturbation experiment on day 238 (A) Cd concentration per port; error bars represent the standard deviation of triplicate analysis; (B) K+ data per port (Lx) were normalized using each respective set A potassium concentration (Lx-A); error bars show the range of uncertainty in the normalized data from triplicate analysis; and (C) HPC data for all ports; error bars indicate the standard deviation of triplicate plating. Some error bars are within the symbol size. For graphs A and B: set A (■); set B (●); set C (▲); set D (♦); set E (□).

HPC and K^+ comparisons from the Cd perturbation experiment on day 238 indicate an initial increase in K^+ without an increase in planktonic bacteria as perturbing

Cd concentrations moved through the sand zone (set D) (Table 14). Sets A and B do not show correlating increases in K^+ and HPC after and including port L2 while no perturbing Cd concentrations were measured within the sand zone of the column (Table 14), indicating that the Cd column biomass were somehow affected by possible precipitation or EPS-Cd complexing occurring during set B. Set D data show planktonic bacteria concentrations decreased when K^+ concentrations increased at early ports, and vise versa at later ports. Although the reductions in planktonic bacteria within set D were sizable, it is important to note that planktonic bacteria concentrations increased from set C to D (Table 14), which coincided with sustained high Cd concentrations within the sand. Interestingly, set C HPC and K^+ comparisons show an increase in K^+ concentrations at early ports, and a small increase in planktonic bacteria concentrations at later ports (Table 14), which coincides with the lowest pH measurements during the Cd perturbation experiment on day 238. K^+ and HPC differences from the Cd perturbation experiment on day 238 for table 14 are located in Appendix K-Table K.13.

Table 5.14. Cd perturbation experiment day 238 K^+ and HPC differences between specific ports (Lx – (Lx-1) within each set.

Change between ports	Sample Type	Set			
		B	C	D	E
L2 - L1	ΔK^+ (mg/L)	-0.29	0.15	0.34	0.13
	ΔHPC (CFU/mL)	1.4E+05	-8.3E+04	-2.6E+05	7.7E+04
L3 - L2	ΔK^+ (mg/L)	0.01	0.12	-0.06	0.141666667
	ΔHPC (CFU/mL)	-3.67E+04	-2.00E+04	2.00E+04	-6.67E+04
L4 - L3	ΔK^+ (mg/L)	0.05	0.01	0.05	0.043333333
	ΔHPC (CFU/mL)	-1.23E+05	1.87E+04	-1.43E+05	-5.67E+04
L5 - L4	ΔK^+ (mg/L)	0.07	-0.27	-0.42	-0.05
	ΔHPC (CFU/mL)	7.63E+04	3.27E+04	-3.37E+04	-2.67E+04
L6 - L5	ΔK^+ (mg/L)	0.14	0.22	0.33	0.17
	ΔHPC (CFU/mL)	1.23E+05	8.73E+04	1.57E+04	-6.03E+04

A Tris-HCl buffer was used in lieu of the phosphate buffer for the final cadmium perturbation experiment so that pH did not affect the experiment. The SC media was changed to Tris-HCl four days before this final Cd perturbation experiment. The Tris-HCl buffer was designed to maintain a pH of 7.8 $\pm$ 0.2 using the Henderson-Hasselbach equation. The positive O_2 pressure remained on the system, and all five sample sets were taken. Table 5.15 shows a listing of the times for each sample removed from the Cd column during the experiment on day 270.

Table 5.15. Sample removal times for Cd perturbation experiment on day 270.

Liquid Port	HRT_{mean}[a] (hr)	Time of Sample Removal (hr)					
		Set A	*Set B*	*Set C*	*Perturb Bottle Removed*	*Set D*	*Set E*
		HPC, DOC, K, Cd	HPC, DOC, K, Cd	HPC, DOC, K, Cd		HPC, DOC, K, Cd	HPC, DOC, K, Cd
1	1.24 - 1.27	-1.00	0.69	1.17	2.60	3.25	5.12
2	1.34 - 1.36	-0.83	0.84	1.53		3.46	5.27
3	1.50 - 1.53	-0.67	1.00	1.83		3.66	5.43
4	1.68 - 1.71	-0.51	1.35	2.17		3.76	5.59
5	1.86 - 1.89	-0.34	1.67	2.34		3.93	5.75
6	2.04 - 2.06	-0.18	1.99	2.53		4.10	5.91

[a]HRT_{mean} values apply to set B and were calculated by subtracting the expected HRT between liquid ports from each of duplicate HRT_{mean} values obtained from tracer studies. The expected flow rate of 2.8 mL/min was used, and HRT_{mean} values per port do not account for sample volumes removed from previous ports.

Similar to the previous Cd perturbation experiments, the maximum Cd concentration was greater than in past Cd perturbation studies, but still did not measure the 25 mg/L target Cd concentration. The Cd concentration data showed perturbing Cd concentrations in the influent ports of sets B and C, and during sample set D (Figure 5.47A, Appendix K-Table K.14). All media bottles contained the Tris-HCl buffered media, and the samples were expected to show high Cd concentrations within the column during set B due to the media change. The fact that this did not suggests that precipitation reactions with Cd column biomass were occurring (Pümpel and Paknikar, 2001; Vig *et al.*, 2003).

The effluent DO data showed that inhibition was probably occurring prior to perturbation with Cd on day 270 (Figure 5.48), and perturbing Cd concentrations continued to inhibit the column biomass. Unlike previous Cd perturbation experiments, the effluent DO concentration did not immediately recover after perturbing Cd concentrations were removed. The effluent DO was 3.8 mg/L on day 267; 1 day after the buffer was changed to Tris-HCl, and 3 days before the Cd experiment on day 270.

Although, the effluent DO was initially high, the DO additionally increased at 2.6 hrs into perturbation. The expected HRT (HRT_{calc}) for the time when perturbing Cd concentrations were to reach the effluent was 1.94 hrs, which indicates that the expected HRT was underestimated, or Cd precipitation or complexing reactions delayed Cd perturbing inhibition reactions with the biomass. The effluent DO increased to the DO probe upper detection limit following the removal of the cadmium spike bottle (Figure 5.48, Appendix K-Table K.15). This high effluent DO concentration indicated that the bacterial community was inhibited.

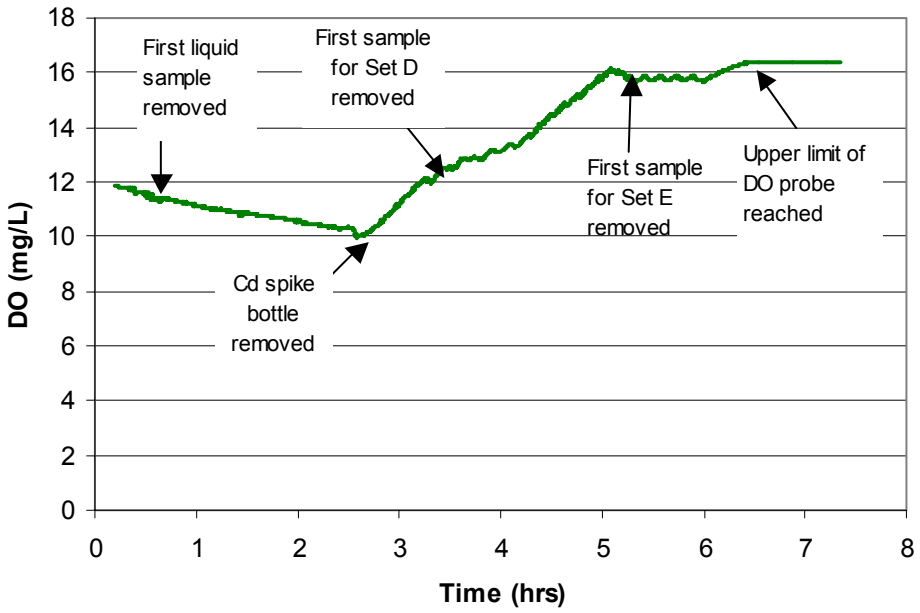

Figure 5.48. Effluent DO concentration during Cd perturbation experiment on day 270.

The Tris-HCl media change removed pH as an experimental variable during the day 270 Cd perturbation experiment. The pH to remained within a 0.2 pH unit range for all samples (Figure 5.49, Appendix K-Table K.16). Although the pH of the Tris-HCl

buffer was adjusted to 7.8, the influent pH was between 7.5 and 7.3, which may be due to the acidic BOFS feed mixing with the Tris-HCl buffered media prior to port L1.

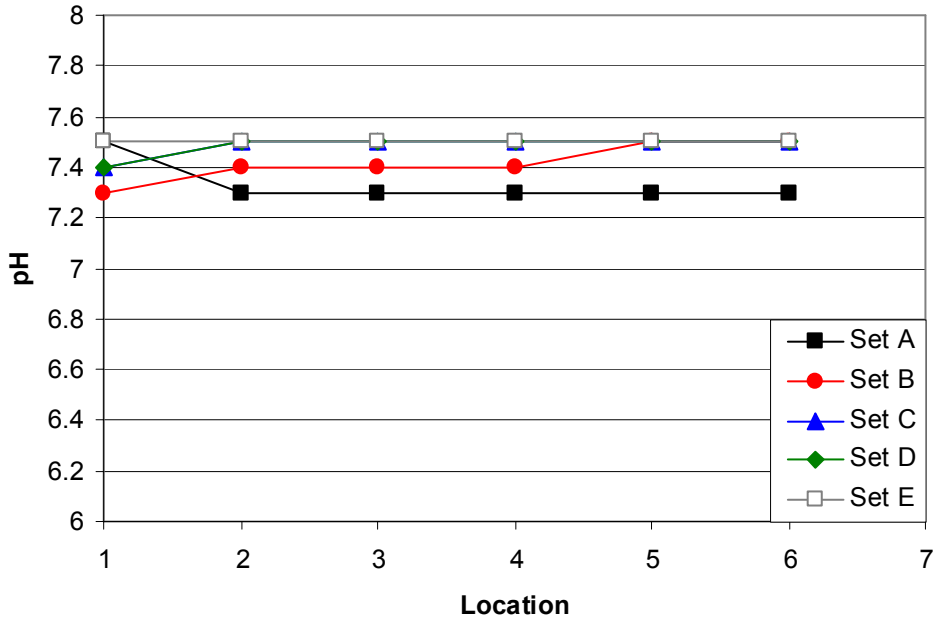

Figure 5.49. pH per port for all sets during the cadmium perturbation on day 270. Sets C and D are hidden by sets D and E.

K^+ normalized at each port by set A showed statistically higher K^+ values at port L2 in set D, and at ports L4 and L5 in sets C and D (Figure 5.47B) than sets B and E. These increases in K^+ concentration, which correlate to increased Cd concentrations within the column, suggest that the GGKE response was activated. Cd perturbation experiment day 270 K^+ and normalized K^+ data are located in Appendix K-Table K.17.

Concurrent with an increase in Cd concentrations, an increase in planktonic bacteria was seen during the Cd perturbation experiment on day 270. Similar to day 238 results, HPC data showed an average increase of 170% in planktonic bacteria concentration between set C and set D, with the exception of L4, where set E showed the increase (Figure 5.47C, Appendix K-Table K.18). Although planktonic bacteria

concentrations in port L1 are comparable to ports L2 through L6 on days 220 and 238, these concentrations were not seen on day 270. Port L1 has typically been found to contain bacteria although the port it is not sand-associated. The increase in planktonic bacteria in set D was seen after planktonic cell concentrations decreased showed continued decreased between sets A and C. This suggests that bacterial release from the biofilm to the pore water was negatively affected by precipitation or complexing reactions with Cd in the sand zone before port L2.

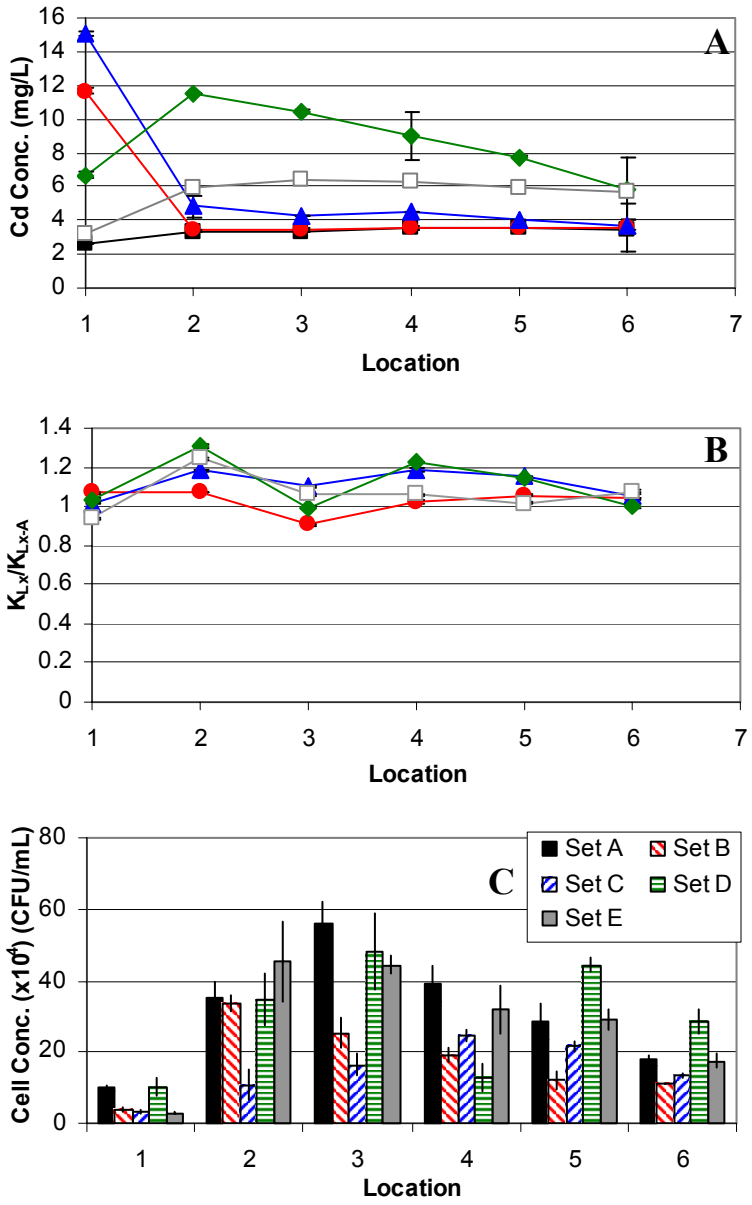

Figure 5.47. Cd perturbation experiment on day 270 (A) Cd concentration per port; error bars indicate the standard deviation of triplicate analysis; (B) K^+ data per port (Lx) for were normalized using the set A (Lx-A) K^+ concentration; error bars show the range of uncertainty in the normalized data from triplicate analysis; and (C) HPC data for all ports; error bars indicate the standard deviation of triplicate plating. Some error bars are within the symbol size. For graphs A and B: set A (■); set B (●); set C (▲); set D (♦); set E (□).

HPC and K^+ comparisons suggest that concurrent increases of K^+ and planktonic bacteria concentrations occurred as the perturbing Cd concentrations peaked. The K^+ and

HPC results from set B at ports L3 through L6 indicate K^+ increase may be caused by a release of K^+ via cell lysis, or K^+ efflux by GGKE activation followed by cell death; either case results in a decrease in planktonic bacterial concentrations (Table 16). This suggests that Cd did affect the biomass, but not as a soluble form based on Cd pore water samples. Similar to day 238, set D data shows planktonic bacteria concentrations decreased when K^+ concentrations increase, and vise versa after port L3 (Table 16). In addition, set E suggests that K^+ efflux occurred with an increase in HPC between port L1 and L2 (Table 16), suggesting that perturbing Cd concentrations were still affecting the Cd column biomass. K^+ and HPC difference data from the Cd perturbation experiment on day 270 for table 16 are located in Appendix K-Table K.19.

Table 5.16. Cd perturbation experiment day 270 K^+ and HPC differences between specific ports (Lx – (Lx-1) within each set.

Change between ports	Sample Type	Set			
		B	C	D	E
L2 - L1	ΔK^+ (mg/L)	-0.12	0.11	0.25	0.31
	ΔHPC (CFU/mL)	3.0E+05	7.5E+04	2.4E+05	4.2E+05
L3 - L2	ΔK^+ (mg/L)	-0.03	0.13	-0.21	-0.03
	ΔHPC (CFU/mL)	-8.3E+04	5.7E+04	1.3E+05	-1.0E+04
L4 - L3	ΔK^+ (mg/L)	0.08	0.02	0.24	-0.11
	ΔHPC (CFU/mL)	-6.1E+04	8.1E+04	-3.5E+05	-1.3E+05
L5 - L4	ΔK^+ (mg/L)	0.08	-0.02	-0.09	-0.04
	ΔHPC (CFU/mL)	-7.2E+04	-2.9E+04	3.1E+05	-2.7E+04
L6 - L5	ΔK^+ (mg/L)	0.09	-0.03	-0.10	0.20
	ΔHPC (CFU/mL)	-1.0E+04	-8.2E+04	-1.6E+05	-1.2E+05

5.5.4 Relevance of Phase II Data

The benzene perturbation results showed evidence of bacterial growth with an increase in pore water, planktonic bacterial concentrations and a decrease in K^+ concentrations. This evidence supports the hypothesis that benzene was not expected to cause K^+ efflux. Cd perturbation experiments suggest that Cd-EPS complexing or Cd precipitation occurred, and Cd biomass was concurrently inhibited showing a sharp increase in effluent DO. Perturbing Cd concentrations (set D) showed an acute K^+ efflux response with acute and minimal biomass loss. PCP perturbation experiments suggest that oxidative phosphorylation uncoupling occurred, as evident by undetectable effluent DO oxygen concentrations. PCP column effluent DO would be expected to be similar to the Cd column due to the toxic and non-biodegradable nature of PCP within the sand

columns. In support of the hypothesis, PCP perturbation results showed acute K^+ efflux with PCP concentrations above 10 mg/L, with concurrent acute and minimal biomass loss.

Literature Cited:

Bellin, C. A., G. A. O'Conner, and Y. Jin. 1990. Sorption and degradation of pentachlorophenol in sludge-amended soils. Journal of Environmental Quality. **19**:603-608.

Chong, N. M., S. L. Pai, and C. H. Chen. 1997. Bioaugmentation of an activated sludge receiving pH shock loadings. Bioresource Technology. **59**:235-240.

Delahaye, A. P. 1998. Distribution and characteristics of biomass in an upflow biological aerated filter. MS thesis. Virginia Tech, Blacksburg, VA.

Dilworth, M. J., and A. R. Glenn. 1999. Problems of adverse pH and bacterial strategies to combat it, p. 4-18. *In* Bacterial Response to pH. Novartis Foundation. **221**. John Wiley & Sons, Chichester, England.

Escher, B. I., M. Snozzi, and R. P. Schwarzenbach. 1996. Uptake, speciation, and uncoupling activity of substituted phenols in energy transducing membranes. Environmental Science and Technology. **30**(10):3071-3079.

Escher, B. I., R. Hunziker, and R. P. Schwarzenbach. 1999. Kinetic model to describe the intrinsic uncoupling activity of substituted phenols in energy transducing membranes. Environmental Science and Technology. **33**(4):560-570.

Fang, H. H. P., X. Li-Chong, and K.-Y. Chan. 2002. Effects of toxic metals and chemicals on biofilm and biocorrosion. Water Research. **36**:4709-4716.

Ferguson, G. P., D. McLaggan, and I. R. Booth. 1995. Potassium channel activation by glutathione-S-conjugates in *Escherichia coli*: protection against methylglyoxal is mediated by cytoplasmic acidification. Molecular Microbiology. **17**(6):1025-1033.

Frølund, B., R. Palmgren, K. Keiding, P.H. Nielson. 1996. Extraction of extracellular polymers from an activated sludge using a cation exchange resin. Water Research. **30**(8):1749-1758.

Hickman, G. T. and J. T. Novak. 1984. Acclimation of activated sludge to pentachlorophenol. Journal of the Water Pollution Control Federation. **56**(4):364-368.

Jacobsen, B. N., E. Arvin, and M. Reinders. 1996. Factors affecting sorption of pentachlorophenol to suspended microbial biomass. Water Research. **30**(1):13-20.

Monero, A., L. Lanza, M. Zilli, L. Sene, and A. Convert. 2003. Batch kinetics of *Pseudomonas* sp. growth on benzene. Modeling of product and substrate inhibitions. Biotechnol. Prog. **19**:676-679.

Neilson, P.H., A. Jahn, and R. Palmgren. 1997. Conceptual model for production and composition of exopolymers in biofilms. Water Science and Technology. **36**(1):11-19.

Pümpel, T. and K. M. Paknikar. 2001. Bioremediation technologies for metal-containing wastewaters using metabolically active microorganisms, p.135 – 169. *In* A. Laskin, G. Gadd, and J. W. Bennett (ed.), Advances in Applied Microbiology, vol. 48. Academic Press, San Diego, CA.

Vig, K., M. Megharaj, N. Sethunathan, and R. Naidu. 2003. Bioavailability and toxicity of cadmium to microorganisms and their activities in soil: a review. Advanced Environmental Research **8**:121-135.

Welp, G., and G. W. Brummer. 1999. Effects of organic pollutants on soil microbial activity: The influence of sorption, solubility, and speciation. Ecotoxicology and Environmental Safety. **43**:83-90.

White, C. and G. M. Gadd. 1998. Accumulation and effects of cadmium on sulfate-reducing bacterial biofilms. Microbiology. **144**:1408-1415.

Zhang, X., P. L. Bishop, M. J. Kupferle. 1998. Measurement of polysaccharides and proteins in biofilm extracellular polymers. Water Science and Technology. **37**(4-5):345-348.

Chapter 6: Discussion

The central hypothesis of the research states that both the concentration and nature of xenobiotic stressors influence microbial adaptation to contaminant plumes in subsurface environments, and will elicit stress responses from the bacterial consortium that will shape the future of the bacterial community. In support of the hypothesis, several objectives were set forth to systematically test for the GGKE response within a saturated subsurface environment: (1) monitor the biodegradative fate of target contaminants in the sand columns; (2) determine the long-term (phase I) biomass response to xenobiotic influx (3) monitor soil biofilm biochemical composition and profiles over time; and (4) monitor the short-term (phase II) biomass response to xenobiotic influx.

Soil column microbial systems were established and operated over 9 months with varying concentrations of benzene, PCP, or Cd to determine the biomass response to increasing, steady, and decreasing concentrations. A control column was also operated to determine the baseline biomass response. In general, it was found that influent parameters of each contaminant, K^+, pH, and TOC varied over the course of experimentation for all columns. In addition, the O_2 concentration in the columns was found to fluctuate during the first 80 days for all columns until the effluent DO decreased to 0.1 mg/L. The aerobic status of the system was critical to determining how the GGKE response affected the bacterial community and biofilm. The GGKE system has primarily been found for aerobically grown gram-negative bacteria, the facultative anaerobe *E. coli* in aerobic systems (Apontoweil and Berends, 1975; Fahey *et al.*, 1978; Ferguson *et al.*, 1997; Meury *et al.*, 1980; Ness *et al.*, 1997), and aerated mixed liquor (Bott and Love,

2002). Fahey *et al.* (1978) showed the majority of gram-positive anaerobes contained less than 0.5 μmol GSH + GSSG/g cell, and gram-negative anaerobes less than 0.02 μmol GSH + GSSG/g cell, indicating that the GGKE mechanism is restricted to aerobic, or oxidative, environments. Meury *et al.* (1980) found that aerobically grown bacteria stop K^+ efflux when O_2 is exhausted. This implies that GGKE activation could have been inhibited at greater depths in the soil columns due to the lack of oxygen.

The potentially biodegradable contaminants, benzene and PCP, were monitored during phase I experimentation by regular sampling of the pore water. Results suggest that benzene was aerobically biodegraded during batch experimentation, phase I, and phase II experimentation. Batch experiments with enriched soil bacteria showed biodegradation of benzene and depletion of DO. Column experimentation showed biodegradation of benzene between 0 and 3.25 cm sand depth. Overall, additional degradation was not seen after 3.25 cm sand depth, as DO was completely consumed during aerobic benzene degradation, although anaerobic benzene degradation could not be ruled out.

Anaerobic benzene degradation requires the presence of terminal electron acceptors, such as Fe (III), sulfate (SO_4^{-2}), carbon dioxide (CO_2), and methanogenic (strictly anaerobic) conditions in non-limiting concentrations, and bacteria capable of performing these metabolisms (Lovley *et al.*, 1995). Lovley *et al.* (1995) additionally considers nitrate (NO_3^-) as a possible terminal electron acceptor, but research by Ma and Love (2001) contradict this, showing that activated sludge did not use nitrate to degrade benzene anaerobically. Hutchins (1991) also showed that benzene biodegradation was not found under denitrifying conditions. The concentrations of alternate terminal electron

acceptors in the SC media were 0.024 mg/L Fe (III) as a trace metal, 4.27 mg/L SO_4^{-2}, and CO_2 from atmospheric sources only. Of the anaerobic electron acceptors presented, only sulfate has a sufficient concentration in the SC media to support possible anaerobic degradation. Under anaerobic conditions, 3.75 mg SO_4^{-2}/mg C_6H_6 is required (Anderson and Lovley, 2000; Phelps *et al.*, 1996) to degrade benzene, allowing biodegradation of 1.14 mg/L benzene with complete exhaustion of the sulfate present in the feed solution. However, electron acceptors other than O_2 were not measured, so anaerobic benzene biodegradation could not be concluded.

Benzene column biomass was hypothesized to show greater concentrations than all other columns due to additional substrate (benzene) availability. All flowcell ports showed greater carbohydrate and protein concentrations overall, but total biomass, measured as VS, fluctuated throughout phase I experimentation. The largest increases of biomass over the control were seen in F1 and F2, where aerobic benzene biodegradation was likely occurring. Flowcell ports F3 and F4 showed lower increases over the control column, indicating that anaerobic metabolism was likely occurring. Energy production is drastically different between aerobic metabolism, which produces 38 ATP via the citric acid cycle, and anaerobic metabolism, which produces 2 ATP via glycolysis (Madigan *et al.*, 2003).

Unlike benzene, batch PCP degradation experiments did not give evidence of PCP degradation with enriched soil bacteria or enriched mixed liquor. The pure culture *S. chlorophenolicum* was added to the pre-established bacterial consortium-sand mixture to introduce a known PCP degrader into the bacterial community added to the sand columns, but PCP concentration profile samples indicated that PCP biodegradation did

not occur. As a result, *S. chlorophenolicum* was assumed to be out-competed within the bacterial community. Definitive evidence of the existence of *S. chlorophenolicum* as a member of the microbial community is under investigation through DGGE analysis of the column bacterial community by Irina Chakraborty. Therefore, for the purposes of this experiment, PCP is considered a non-biodegradable electrophile.

Research that has shown PCP biodegradation is typically accomplished by allowing a mixed culture to acclimate to a chlorophenol substrate, using a chlorophenol-enriched culture, or bioaugmentation with a PCP degrading pure culture. Mäkinen *et al.* (1993) used a recirculating fluidized bed containing activated sludge enriched for 1 year on a mono- and dichlorophenol carbon source, then maintained for 1.5 years on groundwater containing 2,4,6-trichlorophenol, 2,3,4,6-tetrachlorophenol, and PCP prior to experimentation showing PCP biodegradation. Karamanev and Samson (1998) used soil from a site contaminated with PCP for 10 years in an immobilized soil biofilm reactor operated in batch mode for 90 days, and then showed PCP biodegradation in flow-through mode. Jaconsen and Arvin (1996) added *M. chlorophenolicus* to activated sludge sequencing batch reactors (SBRs) and observed total PCP removal. These examples of PCP biodegradation indicate that PCP is a biodegradable contaminant when mixed cultures are bioaugmented with a PCP degrading culture, or when the system is allowed to acclimate for a period of time. The acclimation period has been found to range from 1 hour to several months (Karamanev and Samson, 1998). It is also noteworthy that the reactors used in the examples above for PCP biodegradation research were either batch, SBR, or fluidized bed reactors, which all provided additional oxygen to

the bacterial communities. The availability of oxygen was found to be of great importance during this work.

Biodegradable non-electrophilic chemicals are hypothesized not to elicit the GGKE response. In support of this hypothesis, the benzene column did not show K^+ efflux during perturbations studies. Rather, K^+ was found to decrease with increases in HPC, strongly indicating that bacterial growth was initially occurring as benzene concentrations increased. The uptake of K^+ seen during perturbation experiments is commensurate with increased biomass concentrations measured during the experiment and the large intracellular K^+ concentration requirements in gram-negative bacteria, with concentrations measuring between 0.2 and 0.5 M (Bakker, 1993). Bacterial K^+ requirements are due to a large reliance for the cation for osmotic and pH regulation within the cell. K^+ is used by bacteria for osmotic, or turgor, pressure regulation through the K^+/H^+ TrkA pump, and genetic expression of the *kdp* operon, a reserve K^+ uptake system (Meury *et al.*, 1985, and Epstein, 1986). Intracellular pH also relies on the cytoplasmic K^+ pool, with the pH being raised when the Kdp system brings in additional K^+ (Ferguson *et al.*, 1996; Booth, 1999). Fluxes continually occur between both systems while bacteria regulate intracellular conditions, relying heavily on K^+ and H^+ balances with regard to environmental changes.

The hypothesized response to PCP by sand column biomass was detoxification through PCP biodegradation; therefore the GGKE response would be circumvented. Without GGKE activation, the PCP column biomass was expected to remain attached throughout experimentation. As discussed previously, PCP biodegradation did not occur during experimentation; therefore the hypothesis for a non-biodegradable electrophile

applies. The PCP column biomass was therefore expected to activate the GGKE system to combat electrophilic perturbation, resulting in K^+ efflux and biomass detachment.

In terms of the non-biodegradable electrophile hypothesis, the PCP column showed K^+ efflux only when PCP concentrations were greatest during PCP perturbation. Concurrently with increased K^+ concentrations, elevated planktonic bacterial concentrations were found. These results support the hypothesis for GGKE activation due to a non-biodegradable electrophile. Furthermore, there is strong evidence that oxidative phosphorylation uncoupling occurred, which increased in intensity as PCP concentrations increased. The combined results from phase I, phase II, and the sand column biomass analysis showed that increased oxygen uptake occurred during the PCP experiment, even though PCP biodegradation did not occur concomitantly, further supporting the notion that oxidative phosphorylation uncoupling occurred (Escher *et al.*, 1996).

Uncoupling activities and GGKE activation conflict each other, as both responses utilize the H^+ pool. The proton motive force provides energy for ATP production in aerobic bacteria, which uncoupling dissipates; therefore fewer H^+ are available for cytoplasmic acidification (Ferguson *et al.*, 1995) required during GGKE activation in most aerobic bacteria (Fahey *et al.*, 1978). Therefore, proton motive force dissipation due to oxidative phosphorylation uncoupling (Escher *et al.*, 1996) may shunt GGKE activation after glutathione adducts form.

Meury *et al.* (1980) report that GGKE activation halts without DO. This suggests that the aerobic status of the environment is highly important. DO consumption resulting from oxidative uncoupling, as was shown during high PCP concentrations of phase I

experimentation, and throughout PCP perturbation experiments, could therefore halt the GGKE system. The predominant purpose of cytoplasmic acidification by GGKE activation is protection of macromolecules, detoxification, and repair mechanism activation (Ferguson *et al*., 1997, and Booth, 1999). A secondary cytoplasm acidification method would therefore be required for electrophilic detoxification, possibly by weak acid concentration increases (Ferguson *et al.*, 1995).

PCP column data strongly suggest that GGKE and oxidative uncoupling were in competition, with a PCP concentration threshold determining the dominant stress response. This effect was seen in effluent DO data from phase I experimentation, which showed a continued effluent DO decrease starting on day 72, which coincided with an increase to 4 to 5 mg/L PCP, indicating that uncoupling dominated at this higher PCP concentration. Both PCP perturbation experiments showed GGKE activation at ports L2 and L3 when PCP concentrations approached 20 mg/L. This strongly suggests that uncoupling controls the H^+ pool below 10 mg/L, while the GGKE response controls as the PCP concentration approached 20 mg/L.

An increase of 0.1 K^+/K^+_A due to K^+ efflux was visually determined from Figures 5.37B and 5.39B. On a K^+ concentration basis, PCP perturbation experiments showed increases of 0.175, and 0.172 mg/L on days 218 and 233, respectively. These values were used to calculate the biofilm-associated active biomass that could initiate the GGKE response. To determine the biofilm bacterial concentrations, assumptions (Table 6.1) were used for equations 6.1, 6.2, and 6.3. Biofilm bacterial concentration ranged from $1.6x10^9$ to $6.5x10^9$ CFU/cm^3 for the PCP column using these calculations (Table 6.2). In comparison, Bott (2001) determined that the pre-efflux cell K^+ concentration was

2.11×10^{-14}mmole K^+/cell, and was 0.44×10^{-14}mmole K^+/cell after efflux; an efflux of 1.67×10^{-14}mmole K^+/cell, or 6.53×10^{-13}mg K^+/cell. Using this value and the calculated bacterial concentration range, an expected bulk liquid K^+ concentration increase was calculated (equation 6.4). The expected K^+ efflux seen in the pore water was between 0.003 and 0.008 mg K^+/L based on these calculated bacterial concentrations. These K^+ concentrations are much lower than observed K^+ concentration increases of 0.172 to 0.175 mg K^+/L. Again, using equation 6.3 with the experimental K^+ efflux obtained by Bott (2001) provided that a bacterial concentration greater than 3.4×10^{10} cells/cm^3 biofilm were required to produce the K^+ increases seen in the pore water.

$$D_p = \frac{D_b}{1 - p} \tag{6.1}$$

D_p = particle density (g/cm^3)
D_b = bulk density (g/cm^3)
p = porosity

$$V_f = \frac{VS_{avg} * D_p}{1000 * D_f} \tag{6.2}$$

V_f = Biofilm volume (cm^3)
VS_{avg} = average volatile solids concentration (mg VS/g dry sand)
D_f = biofilm density (g/cm^3)

$$X_f = \frac{\Delta[K]_{\exp t} * V_{liq}}{[K_{cyt}] * V_{cell} * V_f} \tag{6.3}$$

X_f = Bacterial concentration in biomass (CFU/cm^3 biofilm)
$\Delta[K]_{expt}$ = change in K^+ during perturbation (mg/L)
V_{liq} = volume of pore liquid per port (cm^3/port)
$[K_{cyt}]$ = Cytoplasmic K^+ concentration (mg/L)
V_{cell} = Cell volume (cm^3)

$$\Delta[K]_{calc} = \frac{[K]_{efflux} * X_f * V_f * 1000}{V_{liq}} \quad (6.4)$$

$\Delta[K]_{calc}$ = expected increase in pore liquid K^+ after K^+ efflux (mg K^+/L)
$[K^+]_{efflux}$ = K^+ concentration effluxed per cell (mg K^+/cell)

Table 6.1 Assumed variables for biofilm bacterial concentration calculations.

Biofilm Bacterial Concentration Calculation Variables	
Biomass	
Cocci, radius[a] (μm)	0.75
Volume (cm^3)	$1.77x10^{-12}$
K_{cyt}[b] (mg/L)	7820 - 19550
D_f (g/cm^3)[c]	1.002
PCP - VS_{avg} (mg/g dry sand)	2.15
Cd - VS_{avg} (mg/g dry sand)	3.16
Column	
V_{liq} (cm^3/port)	31.0
Sand	
porosity	0.44
D_b (g/cm^3)[d]	1.6
D_p (g/cm^3)	2.857
Average Volatile Solids	
PCP (mg VS/g dry sand)	2.15
Cd (mg VS/g dry sand)	3.16

[a]Madigan *et al.* (2003)
[b]Bakker (1993)
[c]Zhang and Bishop (1994c)
[d]Brady and Weil (2002)

Table 6.2. Biofilm bacterial concentration range for each PCP perturbation experiment.

PCP Perturbation Expt (day)	**ΔK^+ normalized[a]**	**Range of Biofilm Concentration (CFU/cm^3 biofilm)[b]**	**K^+ increase in pore water (mg/L)**
218	0.1	$1.6x10^9$ - $6.5X10^9$	0.003 - 0.008
233	0.1	$1.6x10^9$ - $6.4X10^9$	0.004 - 0.008

[a]Determined by visual inspection from ports L2 or L3 showing $K^+_{Lx}/K^+_{Lx\text{-}A}$ increase.
[b]CFU = colony forming units

A second method of determining the active bacterial concentrations from total protein measurements provided a concentration of 1.4 x 10^9 cells/g sand 5 cm into the sand zone. This value was determined by using the protein concentration from the influent of the PCP column, multiplying by the average fraction of active bacteria in the biofilm (.47) found by Zhang and Bishop (1994a), and dividing by the protein concentration of stationary phase *E. coli* (1.56 x 10^{-7} μg protein/cell) measured by Gudapaty *et al.* (2001) using the BCA method. The column total protein was used due to the inconsistencies noted between the flowcells and column protein concentrations. Consequently, the total protein concentrations may be lower due to duplicate perturbations, making the value most comparable to the second perturbation experiment.

The calculated bacterial concentration ranged from 10^8 to 10^3 cell/cm^3 in the PCP column and is feasible based on other biofilm based bacterial concentrations. Zhang and Bishop (1994a,b) determined that a heterotrophic/autotrophic biofilm contained 10^8 to 10^{10} CFU/cm^3 heterotrophs, and 10^7 to 10^8 CFU/cm^3 facultative bacteria actively respiring in the top layer of the biofilm. The values obtained by Zhang and Bishop (1994a,b) do not reflect a biofilm grown in the presence of xenobiotic compounds, and the concentration of heterotrophs able to activate GGKE are limited to those contained in the aerobic zone of the biofilm, although the concentration ranges were similar. Karthikeyan *et al.* (1999) measured a biofilm with PCP as the sole carbon source to have 2x10^5 CFU/cm^3, which provides an extant bacterial community concentration, and would be expected to be lower than those calculated here.

Losses in ATP production due to ongoing oxidative uncoupling would be expected to exhibit comparatively lower biomass concentrations in the aerobic zone of

the PCP column, although the biofilm based bacterial concentrations calculated do not show a difference between experimentally determined bacterial concentrations. Planktonic bacterial concentrations during phase I did show lower concentrations than all other column during high PCP concentrations. In addition, the column sand samples from the influent are considered to be representative of an aerobic environment, which did show lower protein concentrations in the PCP column than in the control column, however, the PCP column biomass was not statistically different from the Cd column. The flowcell biomass measurements showed that PCP column protein concentrations were lower than the control at F4. Based on the effluent DO measurements throughout phase I experimentation, the majority of the PCP column was likely anaerobic. The biomass data suggests two possibilities: (1) ATP and EPS production were less affected by K^+ efflux-influenced detachment than expected in the aerobic zone; and (2) EPS production was not affected in anaerobic zones due to a lack of uncoupling and GGKE inactivity.

PCP column bacteria showed a specific functional response to PCP by increasing the production of carbohydrates relative to protein production. The PCP column bacteria carbohydrate and protein ratio was 87% greater (0.43 ± 0.07 μg carbohydrate/ μg protein) than the control column (0.23 ± 0.07). This large increase in carbohydrate to protein ratio over the control column suggests that the PCP column bacteria adapted to the presence of PCP and benefited from increasing carbohydrate production relative to protein production. The carbohydrate to protein ratio within the PCP column was similar to detached and loosely attached biofilm fractions (0.39 ± 0.10) measured by Delahaye (1998) from a heterotrophic fixed-film biological aerated filter. The PCP column ratio

was also similar to the ratio (0.35 – 0.55) found by Frølund *et al*. (1996) for activated sludge. In contrast, Delahaye (1998) found a the whole biofilm ratio to be 0.072 $\pm$ 0.02, and Nielsen *et al.* (1997) found a ratio of 0.085 for EPS from a biofilter. This suggests that the biomass in the PCP column has physiological features more similar to floc-immobilized bacteria, such as those in activated sludge, than biofilm bacteria found in attached growth treatment systems with more dense biomass concentrations.

Cd was hypothesized to activate the GGKE system, causing K^+ efflux, and biomass detachment. Phase I experimentation did not support or refute K^+ efflux, although planktonic bacterial concentrations did provide support for biomass detachment. Phase II experimentation provided support for GGKE activation resulting in a temporary increase in planktonic bacterial concentrations. Biomass data did not show decreases in carbohydrate or protein concentrations, although VS concentrations did show decreases during high Cd concentrations.

Phase I experimentation HPC data showed an increase in planktonic bacteria during high Cd concentrations. The Cd column showed the highest planktonic bacterial concentrations of all columns as actual Cd concentrations were between 6.5 and 8.5 mg/L. Increases in planktonic bacteria indicate that viable bacteria were displaced from the biofilm. This suggests that GGKE activation may have occurred, allowing biomass detachment, although K^+ concentration fluctuations would not permit this conclusion from phase I experimentation. Concurrently, effluent DO concentrations increased, indicating that increases in Cd negatively affected oxygen uptake. The increase in effluent DO further indicates that the increase in planktonic bacteria was not due to growth. In an aerobic environment, assumed as DO greater than 0.3 mg/L, bacteria will

preferentially use oxygen as the terminal electron acceptor towards ATP, or energy, production and growth (Madigan *et al.*, 2003). Effluent DO increases were seen during Cd perturbation experiments where Cd concentrations were at least 5.0, 4.8, and 6.0 during Cd perturbations experiments on days 220, 238, and 270, respectively. These results additionally support findings of bacterial inhibition of oxygen uptake with Cd concentrations above 5 mg/L. Bacterial inhibition is typically quantified by the lack of oxygen uptake compared to a control. Uncoupling activity causing increased oxygen uptake is an exception to the inhibition quantification process, as seen with PCP.

Phase II perturbation experiments provided the K^+ information that was lacking from phase I experimentation. Cadmium perturbation experiments performed on days 220, 238, and 270 showed K^+ efflux, although perturbations on days 220 and 238 were performed without pH buffering. The Cd perturbation on day 270 was performed with a Tris-HCl buffer to rule out pH fluctuation seen during the Cd perturbation experiment on day 238. The decrease in pH during the Cd perturbation experiment on day 238 was 1.3 pH units, or a 20-fold decrease in the H^+ concentration of the bulk liquid.

Activated sludge is found to most optimally function between the pH range of 6.5 to 8.0, with detrimental effects occurring at a pH less than 4.0 and greater than 10.0 (Chong *et al.*, 1997). Although, the pH did not decrease below 4.0, pH fluctuations require bacteria to counteract effects that may change the desired intracellular pH of 7.6 to 7.8 (Booth, 1985; Dilworth and Glenn, 1999) by activating the K^+/H^+ antiporter (Foster and Mareno, 1999). Among other intracellular pH maintenance systems is proton release/uptake via the K^+/H^+ antiporter system (Dilworth and Glenn, 1999), with K^+ uptake required to maintain an alkaline cytoplasmic pH (Booth, 1999). In this regard, a

decrease in extracellular pH may encourage the bacteria to counteract H^+ intrusion by increasing the intracellular K^+ concentration. This effect is likely negligible due the acceptable extracellular pH and purposeful cytoplasmic protonation as a result of GGKE activation.

Cd perturbation experiments showed K^+ efflux occurred as Cd concentrations increased within the column. Planktonic bacterial concentration increases were also concurrent with effluent DO increases. This indicates that inhibiting Cd concentrations cause GGKE activation, resulting in biomass detachment. In addition, K^+ and planktonic bacterial increases ceased after Cd concentrations decreased, indicating intracellular Cd detoxification was achieved. Detoxification occurs by glutathione conjugation with the electrophile, forming a non-reactive glutathione adduct that is transported out of the cell (Ness *et al.*, 1997; Ferguson *et al.*, 1997). Cd has been shown to cause an increase in effluent volatile suspended solids (VSS) after addition of 25 mg/L Cd to a sequencing batch reactor (Bott and Love, 2001), with further studies showing that biomass deflocculation was linked to K^+ efflux (Bott and Love, 2002). In addition, flowcell K^+ efflux experiments performed by Gillam (2003) showed a large localized release of 50.67 mg K^+/L 3 minutes after the addition of 10 mg/L Cd feed.

K^+ increases of 0.16, 0.25, and 0.08 mg/L within the first 8.75 cm of sand depth were observed from Cd perturbation experiments on days 220, 238, and 270, respectively. These values were determined using the increase in normalized K^+ over a non-perturbed normalized K^+ set, followed by multiplication by the average K^+ of the baseline set (A). These increases are possibly due to biological K^+ efflux, or physical/chemical cation exchange from the increase in Cd^{+2} ions in the SC media with

K^+ ions within EPS. Both possibilities were observed during Cd perturbations experiments. Physical/chemical K^+ concentration increases were found during Cd-EPS complexation reactions in sets B and C (Tables 5.12, 5.14, and 5.16). Biological K^+ increases would be expected to be localized relative to high biomass concentrations within the column. Based on this assumption, localized K^+ increases during high Cd concentrations from set D are thought to be due to K^+ efflux. However, K^+ efflux resulting from physical/chemical versus biological sources were not specifically tested, and the K^+ concentration increases could not be determined to be significant due to sample volume limitations.

Calculations for the biofilm-based bacterial concentration and possible K^+ efflux concentrations can provide additional clarity for the biological source of K^+ efflux. Equations 6.1, 6.2, 6.3 were used to determine the probable GGKE-activating bacterial concentration located in the biofilm during Cd perturbation experiments (Table 6.3). In addition, equation 6.4 was used to determine the K^+ increase that could be expected from the bacterial concentrations obtained through equation 6.3 calculations (Table 6.3). The assumptions for these calculations were the same as the PCP biofilm bacterial concentrations, except the VS_{avg} was found to be 3.16 mg VS/dry sand. The values obtained for Cd perturbation days 220 and 238 were twice as high as day 270, which may be associated with additional inhibition observed from effluent DO concentrations greater than 10mg/L throughout Cd perturbation experimentation on day 270. The potential K^+ concentration increase in the pore water determined from these calculations does not agree with the observed K^+ increases from Cd column experimentation. Using the K^+ efflux concentration per cell determined by Bott (2001) and the observed K^+ efflux of

0.075 to 0.25 mg K^+/L and equation 6.3, a biofilm bacterial concentration greater than $1.0x10^{10}$ cells/cm^3 biofilm is required. Similar to the PCP column, these bacterial concentrations agree with the heterotrophic and facultative bacterial concentrations found by Zhang and Bishop (1994a,b).

Table 6.3. Biofilm bacterial concentration range from each Cd perturbation experiment

Cd Perturbation Expt (day)	ΔK^+ normalized[a]	Biofilm Concentration (CFU/cm^3 biofilm)	K^+ increase in pore water (mg/L)
220	0.1	$1.0x10^9$ - $4.1X10^9$	0.003 - 0.008
238	0.1 - 0.15	$1.0x10^9$ - $6.3X10^9$	0.003 -0.01
270	0.05	$1.9X10^8$ - $4.7x10^8$	0.001 - 0.003

[a]Determined by visual inspection from ports L2 or L3 showing $K^+_{Lx}/K^+_{Lx\text{-}A}$ increase.

Using the second method previously described for PCP, an active bacterial concentration within the first 5 cm of the Cd column of 1.3 x 10^9 cell/g dry sand was calculated. Biomass inhibition, observed from the effluent DO data, during each perturbation experiment may have decreased the active bacterial-protein concentration within the column. Therefore, this value is most comparable to the final Cd perturbation experiment on day 270.

Sand associated biomass measurements were expected to show decreases in all parameters due to biomass detachment as Cd concentrations increased during phase I experimentation. In addition, increases in sand associated biomass concentrations after Cd concentrations decreased indicate that biofilm bacterial concentrations were possibly in the range of 10^8 to 10^{10} cells/cm^3 biofilm, which would be required to observe an increase in K^+ due to GGKE activation during Cd perturbation experiments after phase I. Carbohydrate and protein concentrations did show that EPS production was inhibited compared to the control column. This response was expected due to GGKE activation,

which halts ATP formation when the H^+ pool is redirected for cytoplasmic acidification. In addition, VS data showed decreases on days 135 and 149 at F1, corresponding with high Cd concentrations (8 mg/L actual), although carbohydrate and protein concentrations did not. Rather, steady and slowly increasing carbohydrate and protein concentrations were observed through day 149, and both were found to steadily increase as Cd concentrations decreased. These results were unexpected due results from Cd perturbations showing GGKE activation with planktonic bacterial concentration increases. However, research using Cd and biofilm systems have also shown similar results, and are discussed next.

EPS has been found to precipitate with (Wang *et al.,* 2001), or bind with large concentrations of heavy metals, providing a decrease in metal toxicity to microorganisms (Fang *et al.*, 2002; White and Gadd, 1998; Teitzel and Parsek, 2003). Research on biofilms to which 200 μM Cd was applied showed that protein concentrations increased over the control. White and Gadd (1998), and Fang *et al.* (2002) found an increase in protein-EPS after a 20 day exposure to 10 mg/L Cd. The mechanism for binding is believed to be charge attraction between positively charged heavy metals and negatively charged functional groups, such as acetyl, succinyl, pyruvyl, and sulfonate on carbohydrates (Fang *et al.*, 2002). This information indicates that increases in carbohydrate or protein concentration provide bacteria with an additional barrier, which decreases toxicity, and reinforces EPS production.

The Cd column biomass and perturbation results indicate that GGKE activation occurs with shock loads, but without considerable biomass detachment. In addition, the observed increases in carbohydrate and protein concentrations after Cd concentrations

decreased indicate either community adaptation followed by growth and EPS production. Increased Cd concentrations may have reduced low EPS producing bacteria, therefore encouraging high EPS producing bacteria.

Future Studies

Several factors will need to be considered during future research on subsurface biofilm communities concerning K^+ efflux: (1) the reactor size; (2) DO availability; (3) interfering reactions. Future work should be focused toward minimizing the reactor size to better differentiate biofilm responses of K^+ efflux, and to better control O_2 availability. Experiments using only the multi-channel flowcells could be done with triplicate channels for active or non-active biomass, allowing sampling for effluent liquid samples of the contaminant, K^+, DO, pH, and sand associated characteristics such as precipitate, carbohydrates, and proteins.

Future studies with sand columns loaded with contaminants that have been shown to be biodegradable or recalcitrant, depending on the environment, should be done with concern directed toward measuring by-product formation. Biofilms contain oxygen gradients, allowing bacteria to use aerobic and anaerobic metabolisms, which give rise to complex community structures. In addition, by-product measurements could help to determine the redox condition under which they were made.

Competitive stress response research may be an important application for subsurface bioremediation of electrophilic uncouplers, especially to determine the initial adaptation by the bacterial community. Future studies should be performed with special

attention to oxygenation. Air-lift percolators, described by Mäkinen *et al.* (1993), could be utilized to better control DO concentrations. In addition, a PCP-acclimated and PCP-unacclimated mixed culture could be used to elucidate the contribution of PCP biodegradation to GGKE and oxidative uncoupling.

Literature Cited:

Alagappan, G., and R. Cowan. Substrate inhibition kinetics for toluene and benzene degrading pure cultures and a method for collection for strongly inhibited cultures. Biotechnology and Bioengineering. **83**(7):798-809.

Anderson, R. T. and D. R. Lovley. 2000. Anaerobic bioremediation of benzene under sulfate-reducing conditions in a petroleum-contaminated aquifer. Environmental Science and Technology. **34**:2261-2266.

Apontoweil, P. and W. Berends. 1975. Isolation and initial characterization of glutathione-deficient mutants of *Escherichia coli* K 12. Biochemica et Biophysica Acta. **399**:10-22.

Bakker, E. P. 1993. Cell K^+ and K^+ transport systems in prokaryotes, p.205-224. *In* Bakker, E. P. (ed.), Alkali cation transport systems in prokaryotes. CRC Press, Boca Raton, FL.

Booth, I. R. 1985. Regulation of cytoplasmic pH in bacteria. Microbiol. Rev. **49**:359-378.

Booth, I. R. 1999. The regulation of intracellular pH in bacteria, p. 19-37. *In* Bacterial responses to pH. Novartis Foundation Symposium 221. John Wiley & Sons, Chichester, England.

Bott, C. B. 2001. Elucidating the role of toxin-induced microbial stress responses in biological wastewater treatment process upset. Ph.D. dissertation. Virginia Tech, Blacksburg, VA.

Bott, C. B., and N. G. Love. 2002. Investigating a mechanistic cause for activated-sludge deflocculation in response to shock loads of toxic electrophilic chemicals. Water Environment Research. **74**(3):306-315.

Brady, N. C, and R. R. Weil. 2002. The nature and properties of soils. Prentice Hall, Upper Saddle River, NJ.

Cunningham, A. B., W. G. Characklis, F. Abedeen, D. Crawford. 1991. Influence of biofilm accumulation on porous media hydrodynamics. Environmental Science and Technology. **25**:1305-1311.

Delahaye, A. P. 1998. Distribution and characteristics of biomass in an upflow biological aerated filter. MS thesis. Virginia Tech, Blacksburg, VA.

Dilworth, M. J., and A. R. Glenn. 1999. Problems of adverse pH and bacterial strategies to combat it, p. 4-18. *In* Bacterial Response to pH. Novartis Foundation. **221**. John Wiley & Sons, Chichester, England.

Epstein, W. 1986. Osmoregulation by potassium transport in *Escherichia coli*. FEMS Microbiology Reviews. **39**:73-78.

Escher, B. I., M. Snozzi, and R. P. Schwarzenbach. 1996. Uptake, speciation, and uncoupling activity of substituted phenols in energy transducing membranes. Environmental Science and Technology. **30**(10):3071-3079.

Fahey, R. C., W. C. Brown, W. B. Adams, and M. B. Worsham. 1978. Occurrence of glutathione in bacteria. Journal of Bacteriology. **133**(3):1126-1129.

Fang, H. H. P, L. C. Xu, K. Y. Chan. 2002. Effects of toxic metals and chemicals on biofilm and biocorrosion. Water Research. **36**:4709-4716.

Ferguson, G. P., D. McLaggan, and I. R. Booth. 1995. Potassium channel activation by glutathione-S-conjugates in *Escherichia coli*: protection against methylglyoxal is mediated by cytoplasmic acidification. Molecular Microbiology. **17**(6):1025-1033.

Ferguson, G.P., A. D. Chacko, C. Lee, I. R. Booth. 1996. The activity of the high affinity potassium uptake system Kdp sensitizes cells of *Escherichia coli* towards methylglyoxal. Journal of Bacteriology. **178**:3957-3961.

Ferguson, G. P., Y. Nikolaev, D. MacLaggan, M. Maclean, and I. R. Booth. 1997. Survival during exposure to the electrophilic reagent *N*-Ethylmaleimide in *Escherichia coli*: Role of KefB and KefC potassium channels. Journal of Bacteriology. **179**(4):1007-1012.

Foster, J. W., and M. Mareno. 1999. Inducible acid tolerance mechanisms in enteric bacteria, p. 55-74. *In* Bacterial Response to pH. Novartis Foundation. **221**. John Wiley & Sons, Chichester, England.

Frølund, B., R. Palmgren, K. Keiding, P.H. Nielson. 1996. Extraction of extracellular polymers from an activated sludge using a cation exchange resin. Water Research. **30**(8):1749-1758.

Gillam, D. 2003. Adaptation of subsurface microbial biofilm communities in response to chemical stressors. MS thesis. University of Cincinnati, Cincinnati, OH.

Gudapaty, S. K. Suzuki, X. Wang, P. Babitzke, and T. Romeo. 2001. Regulatory interactions of Csr components: the RNA binding protein CsrA activates *csrB* transcription in *Escherichia coli.* Journal of Bacteriology. **183**(20):6017-6027.

Hickman, G. T., and J. T. Novak. 1984. Acclimation of activated sludge to pentachlorophenol. Journal of the Water Pollution Control Federation. **56**(4):364-368.

Hutchins, S. R. 1991. Optimizing BTEX biodegradation under denitrifying conditions. Environmental Toxicology and Chemistry. **10**(11):1437-1448.

Karthikeyan, S., G. M. Wolfaardt, D. R. Korber, and D. E. Caldwell. 1999. Functional and structural responses of a degradative microbial community to substrates with varying degrees of complexity in chemical structure. Microbial Ecology. **38**:215-224.

Love, N. G., and C. B. Bott. 2002. Evaluating the role of microbial stress response mechanisms in causing biological treatment upset. Water Science and Technology. **46**(1-2):11-18.

Lovley, D. R., J. D. Coates, J. C. Woodward, and E. J. P. Phillips. 1995. Benzene oxidation coupled to sulfate reduction. Applied and Environmental Microbiology. **61**(3):953-958.

Madigan, M. T., J. M. Martinko, and J. Parker. 2003. Brock Biology of Microorganisms, 10th ed. Pearson Education, Inc., Upper Saddle River, NJ.

Mäkinen, P. M., T. J. Theno, J. F. Ferguson, J. E. Ongerth, and J. A. Puhakka. 1993. Chlorophenol toxicity removal and monitoring in aerobic treatment: Recovery from process upset. Environmental Science and Technology. **27**(7):1434-1439.

Meury, J., S. Lebail, and A. Kepes. 1980. Opening of potassium channels in *Escherichia coli* membranes by thiol reagents and recovery of potassium tightness. European Journal of Biochemistry. **113**:33-38.

Neilson, P.H., A. Jahn, and R. Palmgren. 1997. Conceptual model for production and composition of exopolymers in biofilms. Water Science and Technology. **36**(1):11-19.

Ness, L. S., G. P. Ferguson, Y. Nikolaev, and I. R. Booth. 1997. Survival of *Escherichia coli* cells exposed to iodoacetate and chlorodinitrobenzene is independent of glutathione-gated K^+ efflux systems KefB and KefC. Applied and Environmental Microbiology. **63**(10):4083-4086.

Phelps, C. D., J. Kazumi, and L. Y. Young. 1996. Anaerobic degradation of benzene in BTX mixtures dependent on sulfate reduction. FEMS Microbiology Letters. **145**:433-437.

Teitzel, G. M., and M. R. Parsek. 2003. Heavy metal resistance of biofilm and planktonic *Pseudomonas aeruginosa*. Applied and Environmental Microbiology. **69**(4):2313-2320.

Wang, C. L., D. S. Clark, J. D. Keasling. 2001. Analysis of an engineered sulfate reduction pathway and cadmium precipitation on the cell surface. Biotechnology and Bioengineering. **75**(3):285-291.

White, C., and G. M. Gadd. 1998. Accumulation and effects of cadmium on sulphate-reducing bacterial biofilms. Microbiology. **144**:1407-1415.

Zhang, T.C., and P. L. Bishop. 1994a. Structure, activity, and composition of biofilms. Water Science and Technology. **29**(7):335-344.

Zhang, T. C., and P. L. Bishop. 1994b. Competition in biofilms. Water Science and Technology. **29**(10-11):263-270.

Zhang, T. C., and P. L. Bishop. 1994c. Density, porosity, and pore structure of biofilms. Water Research. **28**(11):2267-2277.

Chapter 7: Conclusions

The objectives of this research were to determine the acute and chronic effect of a matrix of contaminants exhibiting biodegradability and/or electrophilicity on a subsurface microbial community, with specific attention paid to a known stress response, GGKE.

1. Benzene was a model biodegradable contaminant throughout the study and was aerobically biodegraded whereas there was no evidence in support of GGKE activation. This result is consistent with the original hypothesis.
2. PCP, a biodegradable electrophile, was not biodegraded. The data suggest that two metabolic responses may have been activated: oxidative phosphorylation uncoupling and the GGKE stress response. Oxidative phosphorylation uncoupling is believed to occur up to 10 mg/L, with GGKE activation occurring near 20 mg/L**.**
3. The effect of a biodegradable electrophile on GGKE activation with possible biomass detachment could not be determined.
4. Cadmium, a non-biodegradable electrophile, appears to have caused a K^+ efflux response resulting in biomass detachment during acute tests, but did exhibit chronic biomass loss due to possible complexation with EPS. K^+ efflux due to physical/chemical means could not be ruled out.
5. K^+ efflux detection was likely affected by pore water dilution during large scale experiments on the Cd sand column at Virginia Tech; while small-scale flowcell experiments at the University of Cincinnati by Gillam (2003) using a K^+ microelectrode showed biologically mediated K^+ efflux from Cd treated biofilm bacteria.

Literature Cited:

Gillam, D. 2003. Adaptation of subsurface microbial biofilm communities in response to chemical stressors. MS thesis. University of Cincinnati, Cincinnati, OH.

Engineering Significance

The information obtained from this work can be applied to subsurface contaminant biodegradation modeling software such as SEAM3D, substrate enhanced subsurface remediation decisions, and the expected bacterial community response to differing classes of xenobiotic influx. This research also reiterates oxygenation problems seen in subsurface environments with xenobiotic influences. The information gained from this research has provided valuable information on the functional responses of subsurface microbial communities with respect to biodegradable and/or electrophilic compounds, stress response activation, and biomass production.

Subsurface modeling software packages will benefit from the benzene biodegradation data obtained during Phase I, as it provides data that respond to variations in availability of electron acceptor. Simulation packages, specifically the Sequential Electron Acceptor Model – 3 Dimensional (SEAM3D) by Mark Widdowson, utilizes the availability of terminal electron acceptors to determine biodegradation of hydrocarbons via natural attenuation. There are important environmental implications pertaining to the ability of subsurface bacterial communities to anaerobically degrade hydrocarbons, and a possible lag-time in anaerobic biodegradation is likely to negatively effect remediation expectations.

The lack of anaerobic benzene biodegradation evidence can also contribute to the expected biodegradation processes of subsurface bacterial communities. The column inoculum was representative of soil and activated sludge microbial communities; therefore, is it likely to be representative of aerobic/anaerobic biodegradation responses. The lack of anaerobic benzene biodegradation in the columns may have implications for remediation projects, showing that subsurface air/oxygen sparging, addition of oxygen-release compounds (ORC), or addition of terminal electron acceptors (sulfate, Fe (III), CO_2) may be necessity for rapid benzene biodegradation.

The sand associated biomass information provided showed that bacterial communities can be sustained in the subsurface environment when in the presence of xenobiotic compounds. Remediation technologies that utilize complexation or sorption to biofilms to enhance removal, such as in reactive barrier walls, could assume that biomass contained within the barrier will not detach, making it an applicable technology for slowly biodegradable or non-biodegradable contaminants. In terms of benzene, complications from biomass concentration increases due to aerobic growth are to be considered so that the proper technology is applied to prevent pore clogging.

Functional responses of bacterial communities in the subsurface have far reaching effects in terms of biodegradation and oxygen availability. Aerobic biodegradation will negatively impact oxygen availability, which in return affects biodegradability. Fundamentally, aerobic biodegradation is the most desirable remediation strategy because it allows the fastest metabolism of many biodegradable xenobiotics. Although biodegradation product inhibition was not explicitly observed during this work, it is an important aspect to consider when studying remediation of xenobiotic chemicals. The

competitive metabolic responses observed during the PCP studies showed that oxygen is an important reactant in non-biodegradable, uncoupling-causing contaminant subsurface bioremediation.